

# Quantum Theoretical Methods in Application to Classical Systems

Dissertation

zur Erlangung des akademischen Grades  
doctor rerum naturalium (Dr. rer. nat.)

vorgelegt der

Mathematisch-Naturwissenschaftlich-Technischen Fakultät  
(mathematisch-naturwissenschaftlicher Bereich)  
der Martin-Luther-Universität Halle-Wittenberg

von Herrn *Christian Pigorsch*

geb. am 21. November 1971 in Lutherstadt Eisleben

## **Gutachter:**

1. PD Dr. M. Schulz (MLU Halle-Wittenberg)
2. Prof. Dr. I. Peschel (FU Berlin)
3. Prof. Dr. K. Handrich (TU Ilmenau)

Halle (Saale), dem 2. März 2001



# Contents

<b>1</b>	<b>Introduction</b>	<b>1</b>
<b>2</b>	<b>Master Equation and Fock Space</b>	<b>6</b>
2.1	Master Equation . . . . .	6
2.2	Operators of the Second Quantization . . . . .	8
2.2.1	$Q$ -Statistics . . . . .	8
2.2.2	Deformed Commutation Relation and Different Kinds of Number Operator . . . . .	10
2.2.3	Para-Statistics . . . . .	12
2.2.4	Generalized Operators . . . . .	13
2.2.5	Master Equation in Second Quantized Form (Fock-Space Formalism) . . . . .	14
2.2.6	Some Notes about Reference States . . . . .	19
2.2.7	Computation Rules of Expectation Values . . . . .	20
2.2.8	Elementary Reactions . . . . .	21
<b>3</b>	<b>Examples</b>	<b>28</b>
3.1	Fredrickson-Andersen Model . . . . .	28
3.1.1	The Ordinary Fredrickson-Andersen Model . . . . .	30
3.1.2	Mean-Field Theory of the Ordinary Model . . . . .	32
3.1.3	Modified Fredrickson-Andersen Model . . . . .	33
3.1.4	One-dimensional Study of the Modified Model . . . . .	33
3.1.5	Generalization from the Modified Model . . . . .	39
3.1.6	Lattice Formulation of the Extended Model . . . . .	39
3.1.7	Second Quantized Master Equation . . . . .	41
3.1.8	Mean-Field Approximation . . . . .	43
3.1.9	Interpretation . . . . .	48
3.2	Shocks in an Asymmetric Exclusion Model . . . . .	51
3.2.1	Shock Distribution in ASEP . . . . .	52
3.2.2	Drift Velocity and Diffusion Coefficient for the One Particle Random Walk . . . . .	61
3.2.3	Conclusions . . . . .	64

3.3	$Q$ -deformed Models . . . . .	67
3.3.1	The Surface Growth . . . . .	67
3.3.2	The Parking Lot Problem . . . . .	69
3.3.3	A $q$ -deformed Evolution Process . . . . .	70
3.3.4	The Equation of Evolution of the Number Operator . . . . .	74
3.3.5	The Decomposition of Projectors and Number Operators . . . . .	78
3.3.6	The $q$ -deformed Evolution Process for $s = 2$ . . . . .	79
3.3.7	Conclusions . . . . .	82
3.4	Functional Integral of a $q$ -deformed Object . . . . .	85
3.4.1	Introduction . . . . .	85
3.4.2	The $q$ -Deformed Free Particle . . . . .	86
3.4.3	The Pulsed Oscillator . . . . .	89
3.4.4	$Q$ -Objects . . . . .	90
3.4.5	The Propagator for the Chebyshev Process . . . . .	91
3.4.6	Special Cases . . . . .	95
3.4.7	Conclusions . . . . .	98
<b>4</b>	<b>Summary</b>	<b>99</b>
<b>A</b>	<b>Index of all applied symbols</b>	<b>102</b>
A.1	Latin Constants . . . . .	102
A.2	Index of all applied symbols . . . . .	103
A.3	Greek Constant and State dependent Quantities . . . . .	104
	<b>Bibliography</b>	<b>105</b>
	<b>Acknowledgment</b>	<b>111</b>
	<b>German Summary</b>	<b>113</b>
	<b>Curriculum Vitae</b>	<b>117</b>
	<b>Statement</b>	<b>119</b>

# Chapter 1

## Introduction

*Etwas Ungeheures entsteht da vor uns und mit uns - eine geistige Gebirgslandschaft, die man ein Leben lang nicht zu Ende ergründen und auslernen kann. [1]*

An important part of physical research forms the examination of temporal and spatial structures of classical complex systems. There were a remarkable progress in the theoretical treatment of such objects during the last years. New methods had been established to describe non-equilibrium processes, such as motion, diffusion, aggregation, recombination and other dynamical processes, but a general theory is still lacking (see e.g. [2–8] and citations therein). Systems far from the equilibrium as the most things around us are non-closed, but are characterized by a driven energy, particle or information exchange so that they cannot reach the equilibrium. They usually behave in a complex manner and reveal a rich spectrum of structures (think of glasses, the crystal growth and the pattern formation but also plants, animals, traffics, weather, stocks...). A theoretical exploration of out-of-equilibrium phenomena often yields only non-generalized results strongly depended on details in contrast to the general equilibrium physics of gases, liquids or solids which have been known since Boltzmann, Maxwell and Gibbs. The deeper reason bases on the difficulty to deal with the complex interaction with the environment as well as the huge number of degrees of freedom for such systems. Therefore, in moment we possess accumulated knowledge about these phenomena instead of a profound understanding. But because both, equilibrium and non-equilibrium systems, can show similar phenomenological effects like phase transition or critical processes one intensively searches for universal properties also in case of non-equilibrium systems. Remembering equilibrium systems there is a clear relation between the microstates and the macroscopic observed quantities (by the partition function). Starting from the partition function (the sum over all microstates) one may compute the probability for a macrostate, the inner energy, the free energy as well as their derivatives. Unfortunately, this approach is not applicable far away from the equilibrium. A possible way out is to treat non-equilibrium systems in a linear approximation of the perturbation but this is restricted to processes near the equilibrium. Hence, it

remains an important task to create a generalized formalism and an established universal theory which comprehends all these different complex systems and enables us to understand the rich variety of their structures.

Further, the treatments of the many-body systems have to adapt to the classical reality. Thus, important principles of the quantum mechanics like the Heisenberg's uncertainty relation and phase coherence do not play any significant rôle. But it will be demonstrated in this present work how one can apply quantum field theoretical knowledge in a formalism to overcome the above mentioned problem and thus to make a step forward to a universal theory for complex systems. This approach established by Doi [9, 10] lets us achieve exact results in low dimensions and mean-field information in higher ( $d$ ) dimensions about the behavior of many particles on a lattice [6, 7] (both one can find in the present work). Facts about the continuum world can be gained if one carries out the limit process for the lattice constant  $a \rightarrow 0$ .

The study of complex many-body systems shows that the quantum mechanical solution of their equations of motion is generally impossible and is also not necessary for the determination of relevant quantities. With other words expressed, the most classical systems are non-integrable due to the mutual interactions of many particles of which equations of motion are not integrable. Nevertheless, these systems could show ergodic or quasi-ergodic behavior. A possible exit from this dilemma could be the coarse graining of the temporal and spatial scales and separation of the relevant degrees of freedom from the irrelevant ones. Therefore, one may go on to mesoscopic time and length scales without loss of important information. One can suppose a leading mechanism on this scale and compute relevant quantities like density or magnetization. This is justified if the calculation agrees with experimental results. Thus, one is able to reveal the leading mechanism and can refine this procedure by adding further processes. If these latter disturb the dominant behavior of the former the additional processes can not be considered to be irrelevant, there is a misconception in the assumption of the leading mechanism. On the other hand, the concept is in general right if the correction by the latter is only small. Therefore, one can approximate the reality step by step and may obtain essential features of the system. For some findings, like critical exponents, the corrections are may be irrelevant at all, so that one can concentrate on the dominating process [7]. E.g. this approach is a gaining ansatz using a stochastic treatment to solve equations of motion of many-body systems undergoing Brownian motion. The neglected degrees of freedom can be interpreted as a perturbation, the relevant quantities become stochastic variables. Reviews about different methods are given by e.g. Gardiner [2], Honerkamp [3] and van Kampen [4]. The broad spectrum of methods includes Langevin and Fokker-Planck equation, master equation as well as functional integrals.

The temporal evolution of probabilities can be described by the master equation (usually on a lattice). The master equation is a time-dependent, homogeneous and linear differential equation. The Schrödinger equation belongs to the same type of

differential equations and takes its form if  $i\hbar$  is replaced by a characteristic time  $\tau^{-1}$ , the wave function is replaced by the probability amplitude and the Hamiltonian is replaced by the time evolution operator. The dynamics of the considered many-body systems bases on elementary steps of which velocities are given by (relaxation, diffusion etc.) rates occurring in the master equation. Processes taking place on a mesoscopic scale can often sufficiently modeled (e.g. diffusion) by this approach.

The Schrödinger equation may be expressed in terms of second quantized operators in order to compute the temporal development of the wave function. Hence, it is natural to transform this method on the evolution of "classical" probabilities. E.g. one can use the "classical" probabilities to express how many particles are situated in determined state and consequently to calculate the occupation number of a state. Then, one exploits second quantized operators to describe the change of the occupation number. But one should notice, whereas the expectation values in the quantum mechanics are bilinear the expectation values for "classical" probabilities are only linear.

Firstly, quantum methods were adjusted to classical objects by Doi [9, 10] today known as Quantum-Hamilton or Fock-space formalism. In this connection, Doi utilized operator representations as well as propagators and diagram technique to depict stochastic processes. Unfortunately, his thoughts were hesitated taken during the subsequent time. The next people exploring these field theoretical methods were Grassberger, Scheunert [11] and Peliti [12] at the beginning of the 80's. Sandow, Trimper and Schütz [13–15] gave an extension to systems undergoing the classical equivalence to the Pauli principle (for a comprehensive review see [6]). In the meanwhile, the usage of the whole palette of quantum methods is stretched from the exploration of aggregations, diffusion (DLA and RLA), glasses, pattern formation and chemical reactions [6, 7, 13, 14, 16–21].

Whereas Doi exploited "classical" objects being subject to a boson commutation relation at one lattice site, Trimper and Sandow extended the formalism using fermion commutation relation at one site (so-called Paulion). The last progress is the application of para-fermion description [19–23] as well as the use of the  $q$ -statistics [24]. In this connection, one takes into account the fact that the existence of one kind of particles or states at one site excludes the existence of a further one in determined systems (Pauli principle). Hence, it is very natural to extend this approach to systems in which only one of a finite number of possible states may exist at the same time. This modified Pauli principle is automatically realized by a Para-Fermi statistics. The research of such kind of statistics began in the mid of the century [25, 26] and has got a strong increase in attention recently [27]; so e.g. the possible study of the fractional quantum Hall effect [28, 29], the exploration of random sets [30, 31] and the possible application to anyons for description of superconductivity [32].

Only, if one takes the low density limit in high dimensions this hard-core like behavior of all (para-)fermion statistics is realized to be insignificant. Therefore, all

operators can be replaced by their boson counterparts. This cannot do be done in low dimensions [7].

Other stochastic methods like Fokker-Planck equation reveal a partially conform or similar approach comparing to the Fock-space formalism [2, 4].

When one models physical processes problems often occur if spatial and temporal dependent quantities interfere. The advantage of this quantum theoretical approach bases on the fact that one is capable to solve (at least theoretically) the resulting hierarchy equations. On the other hand, one has the possibility to break up higher correlations so that one can derive equations in lowest order already known from the mean-field approximation. But this approach is sometimes limited, especially in low dimensions, due to the spatial restrictions. A further benefit of this approach is the conceptional agreement with Monte-Carlo simulation.

The first part of this work is dominated by a methodical introduction of the master equation and its relation to second quantized operators. Basic dynamical mechanisms will be expressed in terms of these operators to create a powerful mathematical method for the treatment of complex systems. After the establishment of the mathematical formalism the approach will be demonstrated in a variety of examples.

Nowadays, one of the not well-understood phenomenon is the glass transition. To gain more understanding of relevant mechanisms Fredrickson and Andersen [33–36] established a kinetic model which maps density (mobility) states onto spin states with relatively simple rules. This lattice model will be extended by the introduction of an additional component leading to new insights into a possible scenario of the glass transition and the interaction of dynamical processes on different time scales. The model gives ideas how a more collective ( $\alpha$ -)process and a more local ( $\beta$ -)process emerge from a single process at a determined temperature. Hence, this extended facilitated kinetic Ising model (nSFM or resp. Fredrickson-Andersen model) is able to describe qualitatively supercooled liquids near the glass transition temperature. However, this kinetic systems with some restrictions concerning the dynamics proves itself also useful for the exact description of equilibrium properties of other complex systems with sharp transition temperature.

Another contemporary subject of exploration with a broad field of applications, like traffic [37], diffusion in zeolites [38] or the motion of bioparticles [39], is the Asymmetric Simple Exclusion Process (ASEP). Especially in the one-dimensional case, exact results with different mathematical tools such as Bethe ansatz and matrix product ansatz could be achieved [7, 40]. Moreover, many particles undergoing an ASEP can show a collective behavior and can be described by only a few variables. Such a phenomenon is a shock appearing as a sharp increase or decrease in the density, very known from the everyday collapse of the traffic on highways (jams). Here, I will exactly compute a time evolution of such a shock, which can be indicated by only one parameter, its position. I will show later that the many-body motion of the shock can be associated to a single random walk by means of this index. Using



this relation allows us to compute shock velocity and diffusion coefficient.

A further example is a  $q$ -deformed (birth and death) model or deposition-desorption process which could find possible applications in description of molecular beam epitaxy or servicing and waiting phenomena (e.g. filling factor of parking lots) [41, 42]. Computations can reveal the temporal evolution of covering and the average filling grade of the layer or parking lot. The here considered systems are running in their stationary state which depends on the ratio of their parameters. As shown below this stationary state may be regarded as an extended Poisson distribution. Interestingly, the systems switch from a more boson-like behavior at low filling to a more fermion-like behavior at sufficiently high occupation, the "atoms" (particles, cars etc.) gradually feel the hard-core interaction. The temporal evolution of expectation values can be obtained by rules derived in the chapter about the mathematical methods and includes the already known fermion and boson cases.

A further powerful method is the application of functional integral (path integral) to quantum and classical systems [43, 44]. Functional integrals enable to calculate e.g. the transition probabilities between two states (propagators). This allows us to ask for the propagator of the  $q$ -deformed motion of particles. Ordinary particles obeying the Newtonian equation of motion can be transformed to the harmonic oscillator by the Alfaro-Fubini-Furlan-Jackiw transformation [45–47]. However, it seems surprising that the motion of a particle undergoing the force-free  $q$ -deformed equation of motion can be related to a pulsed oscillator. These both (at first sight) different processes can be combined to one  $q$ -deformed object of which the propagator can be computed. I will demonstrate below that the special cases of the general propagator cover not only the  $q$ -objects but also the propagator of the ordinary free particle and of the harmonic oscillator.

After a short repetition of the general master equation I will introduce the parafermion as well as the  $q$ -deformed operators in the second chapter. After generalizing both together I will apply the operators to the master equation reformulated in an equivalent Fock-space representation. I will also discuss the important rôle of number operators, reference states as well as the computation of expectation values in this context. Some basic dynamics (elementary processes) will be introduced and represented in terms of the newly introduced second quantized operators. The relevance of this approach will be shown in some examples, such as the Fredrickson-Andersen model, the asymmetric simple exclusion model and the  $q$ -deformed model within the third chapter. The last section of the third chapter is dedicated to the functional integral of a  $q$ -deformed object. The achieved results will be summarized in the last chapter. In the appendix one can find the most used abbreviations and symbols as well as all references.

# Chapter 2

## Master Equation and Fock Space

*One standard exercise proposed here is to rederive all results, fixing the signs and factors in the process. [27]*

Throughout this work we will try to model physical reality and to find an analytical treatment for these obtained models of which results can be verified by experiments again. Such a mathematical tool is the master equation which yields in general a coarse grained view; instead of using a continuous description one assumes that particles are located on a lattice where they can move and interact with each other. These motions and interactions can be considered as elementary steps. One will recover how one can handle them by means of the master equation.

Starting with a short general discussion of the master equation the subsequent step is the more formal introduction of the  $q$ -deformed and para-algebra to describe systems undergoing some exclusion rules. To reduce the complexity in the following computation these both statistics are merged in one description. Together with the first step one is capable to formulate the master equation in the second quantized form. Some facts about reference states, a special kind of coherent states are given, before I will establish the general rules of some elementary steps, namely of the Glauber (spin-flip, spontaneous reaction) and of the Kawasaki (exchange, interchange or diffusion) dynamics.

### 2.1 Master Equation

Let me start with some general notes about a balance equation which connects the probabilities  $P(n, t)$  of macroscopic or mesoscopic states  $n$  at time  $t$ . Formally, it can be written in the following discrete manner

$$P(n, t + \Delta t) = \sum_m p_m^n P(m, t) =: T' P(n, t). \quad (2.1)$$

The system evolves from a set of states  $m$  (including  $n$ , then the system remains in the state) with the transition probabilities  $p_m^n \in [0, 1]$  to the unique state  $n$  during

one time step  $\Delta t$ . Generally,  $m$  and  $n$  are discrete variables. In case of studying continuum systems like in the classical mechanics one must carry out a coarse graining procedure to transform a continuous set to a discrete set of states. Taking up these transition probabilities  $p_m^n$  per time unit  $\Delta t$  one may derive transition rates

$$w_m^n = \frac{p_m^n}{\Delta t} \in [0, \infty) \quad (2.2)$$

with which physical, chemical or other processes run in order to gain a continuous description. Inserting the rates in the master equation yields

$$P(n, t + \Delta t) = \sum_m w_m^n \Delta t P(m, t). \quad (2.3)$$

Making this transition in a infinitesimal time step  $\Delta t \rightarrow 0$  it follows the continuous form of the master equation

$$\partial_t P(n, t) = \sum_m M_m^n P(m, t) =: L' P(n, t) \quad (2.4)$$

with  $(M_m^n)$  as the dynamical matrix. The elements of  $(M_m^n)$  guarantee that the sum of the probabilities remains always normalized in the temporal development, i.e.

$$\sum_m P(m, t) = 1 \quad \forall t \quad (2.5)$$

and

$$P(m, t) \in [0, 1]. \quad (2.6)$$

The diagonal elements of  $(M_m^n)$  are always non-positive and define a life time of a state  $n$  with  $\tau_n^{-1} = \sum_{m \neq n} w_m^n$ , the sum of all outgoing rates. On the other hand, all off-diagonal elements are non-negative giving the probability per time unit (or rate) for transition from  $m$  to  $n$ . Hence, it is obvious that the sum of each column of  $(M_m^n)$  is equal to zero representing the conservation of the total probability. All rates include the elementary rules to come from one state to another. Sometimes it is possible to solve the master equation (2.4) directly. The present approach (next sections) shows a more elegant and simpler way. In some examples the master equation will be given to compare the results gained by different methods. In this framework I shall consider only processes which have no memory in their history, i.e. the investigation takes into account only probabilities of the momentous state but not explicitly probabilities of the previous step. These processes are called Markovian and approximate the most systems in a good fashion. To transform the master equation in second quantized form one has to introduce the appropriate operators which can express the dynamics and guarantee the exclusion principle.

## 2.2 Operators of the Second Quantization

### 2.2.1 $Q$ -Statistics

It is advantageous for the convenience to introduce a  $(s + 1)$  dimensional vector space (Fock space) spanned by base states  $|n\rangle$  with  $n = 0..s \in \mathbf{N}$ . These states form a complete finite orthonormal set, i.e.

$$\langle m|n\rangle = \delta_{m,n} \quad (2.7)$$

and

$$\sum_{n=0}^s |n\rangle\langle n| = 1. \quad (2.8)$$

Now one is able to add operators appropriate to the physical system. One possible choice is to apply the  $q$ -statistics. Let me define the  $q$ -deformed raising operator  $\hat{b}_+$  and lowering operator  $\hat{b}_-$  as well as their adjoint operators (for more information, see e.g. [48] or [49]) acting on the Fock space by the following rules

$$\hat{b}_+|n\rangle = \sqrt{[n+1]_q}|n+1\rangle, \hat{b}_+|s\rangle = 0 \quad (2.9)$$

$$\hat{b}_+^\dagger|n\rangle = \sqrt{[n]_{q^{-1}}}|n-1\rangle, \hat{b}_+^\dagger|0\rangle = 0 \quad (2.10)$$

and

$$\hat{b}_-|n\rangle = \sqrt{[n]_q}|n-1\rangle, \hat{b}_-|0\rangle = 0 \quad (2.11)$$

$$\hat{b}_-^\dagger|n\rangle = \sqrt{[n+1]_{q^{-1}}}|n+1\rangle, \hat{b}_-^\dagger|s\rangle = 0. \quad (2.12)$$

Sometimes, especially for more practical calculation and for verifying relationships, one might prefer the matrix representation as  $(s + 1) \times (s + 1)$  matrices with rules for the matrix elements are written as

$$\hat{b}_{+m,n} = \langle m|b_+|n\rangle = \sqrt{[n+1]_q}\delta_{m,n+1} \quad (2.13)$$

$$\hat{b}_{+m,n}^\dagger = \langle m|b_+^\dagger|n\rangle = \sqrt{[n]_{q^{-1}}}\delta_{m,n-1} \quad (2.14)$$

and

$$\hat{b}_{-m,n} = \langle m|b_-|n\rangle = \sqrt{[n]_q}\delta_{m,n-1} \quad (2.15)$$

$$\hat{b}_{-m,n}^\dagger = \langle m|b_-^\dagger|n\rangle = \sqrt{[n+1]_{q^{-1}}}\delta_{m,n+1}. \quad (2.16)$$

The pre-factor are given by the  $q$ -deformed number

$$[n]_q = 1 + q^1 + \dots + q^{n-1} = \frac{1 - q^n}{1 - q} \quad (2.17)$$

with  $q \in \mathbf{C}$  as the deformation parameter. If  $q \rightarrow 1$  the  $q$ -deformed number  $[n]$  goes into  $n$ . The operators and their adjoint operators are connected by the relations (comp. e.g. [48])

$$\begin{aligned}\hat{b}_- &= q^{\frac{1}{2}\hat{N}}\hat{b}_+^\dagger \\ \hat{b}_+ &= \hat{b}_-^\dagger q^{\frac{1}{2}\hat{N}}\end{aligned}\quad (2.18)$$

using  $\hat{N}$ , the ordinary *number operator* (NO), with its eigenvalue relation

$$\hat{N}|n\rangle = n|n\rangle. \quad (2.19)$$

Before I shall continue I shortly want to consider a special, but important, case for the deformation parameter  $q$ . If one demands that the operator algebra should automatically include the restriction to the maximum number of states,  $s$ , then immediately follows from  $\hat{b}_+|s\rangle = \sqrt{[s+1]_q}|s\rangle \stackrel{!}{=} 0$  that  $[s+1]_q = 0$ . The consequence is, providing  $[s+1]_q = 0$  and  $q \neq 1$ , that  $q$  can be chosen as the  $(s+1)$ th simple root of unity, i.e.

$$q = j_{s+1} = \exp\left(\frac{2\pi i}{s+1}\right). \quad (2.20)$$

Another possible choice is to take positive or negative integer powers of this simple root.

Two certain simple roots of unity are from special point of interest. Firstly, if one chooses  $s = 1$  then  $j_{s+1} = -1$ . Then the square root of the deformation parameter to the power of the number operator can equivalently transform to

$$j_2^{\frac{1}{2}\hat{N}} = \exp\left(\frac{i\pi\hat{N}}{2}\right) \equiv 1 - (1-i)\hat{N}. \quad (2.21)$$

By means of this simplification and Eq.(2.18) one may conclude that  $\hat{b}_- = \hat{b}_+^\dagger$  and  $\hat{b}_+ = \hat{b}_-^\dagger$  bearing in mind  $\hat{b}_+|0\rangle = 0$  and  $\hat{b}_-|1\rangle = 0$ . This choice of  $j_{s+1}$  correspond to the *fermion limit* of the  $q$ -statistics.

The second special case is given if  $s \rightarrow \infty$  and  $j_{s+1} = 1$ . Hence, it is obvious that  $\hat{b}_- = \hat{b}_+^\dagger$  and  $\hat{b}_+ = \hat{b}_-^\dagger$  (from Eq.(2.18)). The limit process must be understood in this sense that

$$\lim_{s \rightarrow \infty} j_{s+1}^{\frac{1}{2}\hat{N}} = \lim_{s \rightarrow \infty} \exp\left(\frac{i\pi\hat{N}}{s+1}\right) = 1. \quad (2.22)$$

This case is the *boson limit* of the  $q$ -statistics. Only if  $j_{s+1}$  is real, like in fermion or boson case, the raising and the lowering operator are adjoint operators to each other.

Another choice is to declare  $\hat{b}_+$  and  $\hat{b}_-$  ad hoc in the  $(s+1)$ th power equal to zero similar to the Para-Grassmann operators. For the further calculation I will utilize  $q$  if the deformation parameter is general and  $j_{s+1}$  if the deformation parameter is a simple root of unity.

### 2.2.2 Deformed Commutation Relation and Different Kinds of Number Operator

By means of the rules for the application of the  $q$ -deformed operators Eqs.(2.9)-(2.12) the quon (called by Greenberg [51]) commutator rule

$$\left[ \hat{b}_-, \hat{b}_+ \right]_q := \hat{b}_- \hat{b}_+ - q \hat{b}_+ \hat{b}_- = 1 \quad (2.23)$$

can be verified. This relation is often denoted by *quon-commutation relation* ( $q$ -commutator) as well. The relation is discussed in connection with different kind of deformed oscillators (Weyl-Heisenberg, Fibonacci, Macfarlane oscillators [49–55]). The ordinary harmonic (Weyl-Heisenberg) oscillator is obtained in the limit  $q \rightarrow 1$  (boson case). Then the Eq.(2.23) reads

$$\left[ \hat{b}_-, \hat{b}_+ \right]_1 = \hat{b}_- \hat{b}_+ - \hat{b}_+ \hat{b}_- = \hat{b}_- \hat{b}_-^\dagger - \hat{b}_-^\dagger \hat{b}_- = 1. \quad (2.24)$$

A further interesting and later exploited limit is  $q \rightarrow -1$  (fermion case). Then the commutation relationship turns into

$$\left[ \hat{b}_-, \hat{b}_+ \right]_{-1} = \hat{b}_- \hat{b}_+ + \hat{b}_+ \hat{b}_- = \hat{b}_- \hat{b}_-^\dagger + \hat{b}_-^\dagger \hat{b}_- = 1. \quad (2.25)$$

It is possible to consider the general commutation relationship in a little bit other fashion. The two terms  $\hat{b}_- \hat{b}_+$  and  $\hat{b}_+ \hat{b}_-$  are equivalent to  $[\hat{N}+1]$  and  $[\hat{N}]$ , respectively using Eqs.(2.9)-(2.12) and  $[\hat{N}]$  being the *deformed number operator* (DNO) with

$$[\hat{N}]|n\rangle = [n]|n\rangle. \quad (2.26)$$

This choice (the number operator of the  $q$ -deformed oscillator) is still a special form of a more general case

$$\hat{b}_- \hat{b}_+ = f(\hat{N} + 1) \text{ and } \hat{b}_+ \hat{b}_- = f(\hat{N}) \quad (2.27)$$

where  $f(\hat{N})$  could be understood as a general number operator. As seen in the last section, generally  $b_-$  and  $b_+$  are not adjoint to each other if  $q \notin \mathbf{R}$ . But, one can transform (2.23) by means of Eqs.(2.18) to another deformed relation

$$\left[ \hat{b}_-, \hat{b}_-^\dagger \right]_{q^{\frac{1}{2}}} = \hat{b}_- \hat{b}_-^\dagger - q^{\frac{1}{2}} \hat{b}_-^\dagger \hat{b}_- = q^{-\frac{\hat{N}}{2}}. \quad (2.28)$$

This is the commutation relation for the *Biedenharn-Macfarlane oscillator* [55, 56]. In this connection, one may introduce a third kind of number operators, the *symmetric-deformed number operator* (SDNO), with

$$\hat{b}_- \hat{b}_-^\dagger = |[\hat{N} + 1]| \text{ and } \hat{b}_-^\dagger \hat{b}_- = |[\hat{N}]|, \quad (2.29)$$

the eigenvalue relation

$$|[\hat{N}]|n\rangle = |[n]|n\rangle \quad (2.30)$$

and their eigenvalues

$$|[n]| = \frac{q^{\frac{n}{2}} - q^{-\frac{n}{2}}}{q^{\frac{1}{2}} - q^{-\frac{1}{2}}}. \quad (2.31)$$

$|[n]|$  is always a real number if  $q$  is  $\in \mathbf{S}^1$  or  $q$  is  $\in \mathbf{R}$ . If  $q$  is chosen to be an element of  $\mathbf{S}^1$  only for the two real limits of  $q$ ,  $\hat{b}_-$  and  $\hat{b}_+$  are adjoint to each other [49]. The reality of  $q$  ensures this. For the choice  $q \in \mathbf{R}$  one may always find adjoint operators to each other. Due to the diagonal form of all kind of number operators,  $\hat{N}$ ,  $[\hat{N}]$  and  $|[\hat{N}]|$ , the commutation rules with the raising and lowering operators show similar forms, e.g.

$$\begin{aligned} [\hat{N}, \hat{b}_\pm]_1 &= \pm \hat{b}_\pm, \\ [[\hat{N}], \hat{b}_+]_q &= \hat{b}_+, \\ [\hat{b}_-, [\hat{N}]]_q &= \hat{b}_-, \\ [[[\hat{N}]], \hat{b}_+]_{q^{\frac{1}{2}}} &= \hat{b}_+ q^{-\frac{\hat{N}}{2}}, \\ [\hat{b}_-, |[\hat{N}]|]_{q^{\frac{1}{2}}} &= q^{-\frac{\hat{N}}{2}} \hat{b}_-. \end{aligned} \quad (2.32)$$

Moreover, the elements  $\hat{b}_-$ ,  $b_+$ , and  $\hat{N}$  constitute the quon algebra. For the two limit case  $s = 1$  ( $q = -1$ ) and  $s = \infty$  ( $q = 1$ ) the three number operators coincide. In some computation it is convenient that the ordinary number operator can be decomposed in terms of DNO's and more elementary in terms of raising and lowering operators

$$\hat{N} = \sum_{m=1}^s (1-q)^{m-1} [m-1]! \frac{[\hat{N}]!}{[m]![\hat{N}-m]!} = \sum_{m=1}^s \frac{(1-q)^m}{1-q^m} \hat{b}_+^m \hat{b}_-^m. \quad (2.33)$$

The  $q$ -deformed exponential function  $\exp_q(x)$  is explained as

$$\sum_n \frac{x^n}{[n]!}. \quad (2.34)$$

Notice,  $\exp(x)$  denotes the ordinary exponential function in the subsequent sections. The symbol  $[n]_q!$  abbreviates the  $q$ -deformed factorial with

$$[n]_q! := [1]_q \cdots [n]_q, \quad [0]_q! := 1. \quad (2.35)$$

More information about  $q$ -deformed functions can be found in [57]. To these relations one may add the rescaling transformation

$$\langle 0|f_1(\hat{b}_-)f_2(\hat{b}_+)|0\rangle = \langle 0|f_1(B\hat{b}_-)f_2(\hat{b}_+B^{-1})|0\rangle. \quad (2.36)$$

with  $B$  as a complex number. The importance of all relationships will be revealed in the calculation of the time evolution of relevant quantities which one will see more convincingly in practical examples.

### 2.2.3 Para-Statistics

Another possibility to include an exclusion principle is to exploit a para-statistics. It has been being a current field of research since mid of this century. More recent results show its relevance for the description to anyons and probably for high temperature superconductivity [26, 32, 51, 58–61]. The commutation rules between the (ordinary) number operator  $\hat{N}$  (the same defined in Eq.(2.19)) and the raising operator  $\hat{a}^\dagger$  are the same for all kinds of para-statistics [26]

$$[\hat{N}_k, \hat{a}_l^\dagger]_- = \hat{a}_k^\dagger \delta_{k,l}. \quad (2.37)$$

Then the (ordinary) number operator can be represented by

$$\hat{N}_k = \frac{1}{2}[\hat{a}_k^\dagger, \hat{a}_k]_\pm + \text{const.} \quad (2.38)$$

The upper index is valid for boson-type statistics whereas the lower index is applicable for fermion-type statistics. If one replaces  $\hat{N}_k$  by the transition operator  $\hat{N}_{k,l}$  which annihilates the state  $k$  and creates the state  $l$  one obtains a tri-commutation relation by noting (2.37)

$$[[\hat{a}_k^\dagger, \hat{a}_l]_\pm, \hat{a}_m^\dagger]_- = 2\hat{a}_k^\dagger \delta_{k,m}. \quad (2.39)$$

The vacuum relation

$$\hat{a}_k|0\rangle = 0 \quad (2.40)$$

is not sufficient and must be extended by

$$\hat{a}_l \hat{a}_k^\dagger |0\rangle = s \delta_{k,l} |0\rangle. \quad (2.41)$$

Using a special expansion (see [61])

$$\hat{a}_k^\dagger = \sum_{m=1}^s \hat{\alpha}_k^\dagger(m) \quad \text{and} \quad \hat{a}_k = \sum_{m=1}^s \hat{\alpha}_k(m) \quad (2.42)$$

where  $\hat{\alpha}_k^\dagger(m)$  and  $\hat{\alpha}_k(n)$  are ordinary Fermi (Bose) operators for  $m = n$ , but anti-commuting (commuting) for  $m \neq n$ , Green could show, that the tri-commutation relation (2.39) is fulfilled under these assumptions [26].  $s$  is the order of the para-statistics and gives the maximum number of particles being in a antisymmetric state in the boson-type case at the same time. In contrast, the number gives the particles occupying a symmetric state in the fermion-type case at the same time, or more



easily how many particles can be in one state at the same time. If one chooses  $s = 1$  the ordinary Bose and Fermi statistics emerge. For the same site the commutator and the anticommutator of the operators are equivalent to the interrelation (2.24) and (2.25), respectively. Due to the equivalence I shall always apply  $\hat{a}$  operators instead of the  $\hat{b}$  operators if I explore dynamics in these limit cases. In all other cases  $\hat{a}$  and  $\hat{b}$  operators are used separately.

By means of underlying rules one is able to compute the pre-factors in the action to states for the Para-Fermi statistics [19, 20]

$$\hat{a}_k^\dagger |n_k\rangle = \sqrt{(n_k + 1)(s - n_k)} |n_k + 1\rangle, \quad (2.43)$$

$$\hat{a}_k |n_k\rangle = \sqrt{n_k(s + 1 - n_k)} |n_k - 1\rangle. \quad (2.44)$$

Because of the classical properties of the focused systems operators at different lattice sites commute with each other. Therefore the here applied tri-commutator relation (2.39) changes slightly to

$$[[\hat{a}_k^\dagger, \hat{a}_l]_\pm, \hat{a}_m^\dagger]_- = 2\hat{a}_k^\dagger \delta_{k,l} \delta_{k,m}. \quad (2.45)$$

Only the Para-Fermi statistics will be appeared during this work.

## 2.2.4 Generalized Operators

Different kinds of operators are potentially useful describing the same physical background as shown in the last section. To simplify as well as clarify the derivation of the formalism in the next sections it is preferable to introduce some generalized operators to unite operators of different kinds of statistics.

Let me start with the general raising operator symbolized by  $\hat{c}_+$ . It includes operators like e.g.  $\hat{b}_+$ . The action to a Fock state  $|n\rangle$  is then given by

$$\hat{c}_+ |n\rangle = \sqrt{z_{n+1}} |n + 1\rangle \quad (2.46)$$

where  $z_n$  is the eigenvalue of the later introduced general number operator  $\hat{Z}_n$ . The adjoint operators like  $\hat{b}_-$  and  $\hat{a}^\dagger$  are summarized by  $\hat{c}_-^\dagger$  with its action on a Fock state

$$\hat{c}_-^\dagger |n\rangle = \sqrt{\bar{z}_{n+1}} |n + 1\rangle. \quad (2.47)$$

Further, a general lowering operator  $\hat{c}_-$  includes operators like  $\hat{a}, \hat{b}_-$  and so on. Its function is to decrease a Fock state, i.e.

$$\hat{c}_- |n\rangle = \sqrt{z_n} |n - 1\rangle. \quad (2.48)$$

The adjoint operators like  $\hat{b}_+^\dagger$  are abbreviated by  $\hat{c}_+^\dagger$  with the action on a Fock space

$$\hat{c}_+^\dagger |n\rangle = \sqrt{\bar{z}_n} |n - 1\rangle. \quad (2.49)$$

Last, but not least I will complete this summary with the general number operator. It represents number operators like  $\hat{N}$  and  $[\hat{N}]$ . The eigenvalue equation is given by  $\hat{Z}_n |n\rangle = z_n |n\rangle$ .  $\hat{Z}_n$  is to understand in this sense that  $\hat{Z}_n = \hat{c}_+ \hat{c}_-$ . In the same manner the symmetric form  $|\hat{Z}_n| = \hat{c}_-^\dagger \hat{c}_-$  is related to its eigenvalue relation  $|\hat{Z}_n| |n\rangle = |z_n| |n\rangle$ . Notice, that  $\hat{c}_-^\dagger = \hat{c}_+$  and  $\hat{c}_+^\dagger = \hat{c}_-$  apply to the Para-Fermi statistics. Further, the difference between  $\hat{Z}_n$  and  $|\hat{Z}_n|$  occurs only in case of the  $q$ -statistics but not in case of the Para-Fermi statistics due to its real  $z_n$ . E.g.

$$z_n = \frac{1 - q^n}{1 - q} \text{ and } |z_n| = \frac{q^{\frac{n}{2}} - q^{-\frac{n}{2}}}{q^{\frac{1}{2}} - q^{-\frac{1}{2}}} \quad (2.50)$$

for the  $q$ -statistics and  $z_n = |z_n| = n(s + 1 - n)$  for the Para-Fermi statistics. If the statistics has a lower bound 0 then it is one probable solution to set  $z_0 = 0$ . On the other hand, if the statistics possesses an upper bound  $s$  then one can fix  $z_{s+1} = 0$  [62].

### 2.2.5 Master Equation in Second Quantized Form (Fock-Space Formalism)

After the introduction of the operators, the next step is to relate them to the master equation (2.1) and (2.4). One will obtain an equivalent formulation in second quantization. By means of Doi's [9,10] established algorithm the discrete version of the master equation (2.1) can be transformed to a Fock space ( $T'$  is substituted by  $\hat{T}$ , the stochastic transfer matrix, and the probability  $P(n, t)$  is formally replaced by the state vector  $|\Pi(t)\rangle$ )

$$|\Pi(t + \Delta t)\rangle = \hat{T} |\Pi(t)\rangle. \quad (2.51)$$

The relationship to the probabilities in (2.1) is given by the matrix elements of  $\hat{T}$

$$\langle n | \hat{T} | m \rangle = p_m^n \text{ for } m \neq n \text{ and } \langle n | \hat{T} | n \rangle = 1 - \sum_{m \neq n} p_m^n. \quad (2.52)$$

If the transition probabilities are temporal independent the formal solution of this equation is

$$|\Pi(t)\rangle = |\Pi(n\Delta t)\rangle = \hat{T}^n |\Pi(0)\rangle \quad (2.53)$$

with  $|\Pi(0)\rangle$  as initial distribution and  $t = n\Delta t$ . To achieve the continuous Fock space form of the master equation one may use

$$\hat{T} = 1 + \hat{L}\Delta t \quad (2.54)$$

in agreement with the introduction of the master equation above. Or equivalently one repeats the replacement in Eq.(2.4) ( $L'$  is substituted by  $\hat{L}$  and the probability  $P(n, t)$  is formally replaced by the state vector  $|\Pi(t)\rangle$ ) resulting in

$$\partial_t |\Pi(t)\rangle = \hat{L} |\Pi(t)\rangle. \quad (2.55)$$

The formal solution of this equation is given by

$$|\Pi(t)\rangle = U(t) |\Pi(0)\rangle \text{ with } U(t) = \exp(\hat{L}t). \quad (2.56)$$

$\hat{L}$  is known in the literature as "quantum Hamiltonian" or time evolution operator. The often used notation "quantum Hamiltonian" is misleading because this approach is usually applied to a description of stochastic variables but not to quantum observables. Their expectation values differ from the expectation values of the former one. Besides  $\hat{L}$  is in general not (anti-) Hermitian and hence may have complex eigenvalues. Thus, I shall prefer to call it time evolution operator.  $\hat{L}$  can be expressed by means of the introduced raising and lowering operators. The structure of  $\hat{L}$ , originated by the algebraic properties of operators as well as by the Fock-space base, determines the dynamics of the system.

Before I continue I want to make some extensions. Up to here, systems are zero dimensional (apart from the introduction of the para-statistics), i.e. the dynamics would be fixed on one single site. But in the most cases, particles interact from different (lattice-) sites. Thus, one must add a site index to denote the local dependence. E.g. the vector  $\vec{n}$  should be understood as a set of single (occupation) numbers for every point,

$$\vec{n} = \{n_1, \dots, n_i, \dots, n_n\} \quad (2.57)$$

where  $i$  counts the sites from 1 to  $n$ . The equivalent description in the Fock space is a tensor product of single sites states, that means

$$|\vec{n}\rangle = |n_1\rangle \otimes \dots \otimes |n_i\rangle \otimes \dots \otimes |n_n\rangle.$$

The total dimension of the vector space is  $n \times n \times (s+1) \times (s+1)$  if one chooses the representation of the operators as  $(s+1) \times (s+1)$  matrices.

The picture behind the present lattice description can be easily explained: one separates the macroscopic system in mesoscopic cells of the length  $l$ . These cells can be occupied by  $n$  particles and contain all (for the statistical purpose) physically relevant information. One may include the rest of the neglected quantities (like momentum of the atoms) into the noise term. Therefore, all variables become stochastic variables.

The relationship

$$|\Pi(t)\rangle = \sum_{\{\vec{n}\}} P(\vec{n}, t) (\langle \vec{r} | \vec{n} \rangle)^{-1} |\vec{n}\rangle \quad (2.58)$$

or equivalently

$$P(\vec{n}, t) = \langle \vec{r} | \vec{n} \rangle \langle \vec{n} | \Pi(t) \rangle \quad (2.59)$$

assign the state vector  $|\Pi(t)\rangle$ , base vectors  $|\vec{n}\rangle$  and the probability  $P(\vec{n}, t)$ . In this connection, the configuration  $|\vec{n}\rangle$  is given by  $\vec{n}$  as a tensor product of stochastic variables. The bra-vector is formed by the reference state vector

$$\langle \vec{r} | = \langle r_1 | \otimes \dots \otimes \langle r_i | \otimes \dots \otimes \langle r_n | .$$

The Eq.(2.58) is compatible with the conservation of the probability as we will see below. To guarantee a proper definition of (2.58) one must require that the scalar product  $\langle \vec{r} | \vec{n} \rangle \neq 0$ . Thus, one has to find an appropriate representation of the reference vector which includes all possible base vectors of the system. As we will recover within the next section, this special state vector can be expanded in base vectors

$$\langle \vec{r} | = \bigotimes_i \sum_n \langle n_i | \frac{\bar{r}_i^{n_i}}{\sqrt{\bar{z}_{n_i}!}} \quad (2.60)$$

with non-zero  $\bar{r}_i$ .  $\bar{z}_n! \in \mathbf{C}$  is the complex conjugated generalized factorial of the eigenvalues of the general number operator. The general factorial is defined as

$$z_n! := z_1 \dots z_n, z_0! := 1, \forall z_n \in \mathbf{C}. \quad (2.61)$$

The product between the reference state and the base vector (or occupation number vector) can be easily computed to

$$\langle \vec{r} | \vec{n} \rangle = \prod_i \frac{\bar{r}_i^{n_i}}{\sqrt{\bar{z}_{n_i}!}}. \quad (2.62)$$

A more detailed discussion about the reference state follows in the subsequent subsection. The scalar product between two base vectors is given by

$$\langle \vec{m} | \vec{n} \rangle = \prod_i \langle m_i | n_i \rangle. \quad (2.63)$$

An arbitrary base vector of the system  $|\vec{n}\rangle$  can be created from the vacuum state by

$$|\vec{n}\rangle = \bigotimes_i \frac{(\hat{c}_-^\dagger)_i^{n_i}}{\sqrt{\bar{z}_{n_i}!}} |0_i\rangle. \quad (2.64)$$

The index  $i$  runs over all lattice sites and  $(\hat{c}_-^\dagger)_i$  raises the vacuum state  $|0_i\rangle$ . To lowering a state one can use  $(\hat{c}_-)_i$  which is only the adjoint operator to  $(\hat{c}_+)_i$  in some special cases. E.g. the commutation relation between  $\hat{c}_-^\dagger$  and  $\hat{c}_+$  are the same like for bosons in case of non-interacting classical particles. It is very important to stress that all operators of different spatial indices always commute due to classical properties of the regarded objects in contrast to the quantum mechanics.

In the statistical physics as well as in the quantum mechanics expectation values are quantities of interest which give averages of series of identical measurements (ensemble average). An arbitrary observable,  $G$ , may be represented in a diagonal form by

$$\hat{G} = \sum_{\{n_i\}} \hat{G}(\vec{n}) |\vec{n}\rangle \langle \vec{n}|. \quad (2.65)$$

Then one transforms the time dependent operator  $G(t)$  in a Heisenberg picture

$$\hat{G}(t) = \exp(-\hat{L}t)\hat{G}\exp(\hat{L}t). \quad (2.66)$$

Similar to the quantum mechanics, the expectation value of a physical quantity  $G(\vec{n})$  is given by the trace of the operator  $\hat{G}$  :

$$\begin{aligned} \langle \hat{G}(t) \rangle &= \sum_{\{n_i\}} P(\vec{n}, t)G(\vec{n}) = \langle \vec{r} | \hat{G}(t) | \Pi(0) \rangle \\ &= \langle \vec{r} | \hat{G}\exp(\hat{L}t) | \Pi(0) \rangle. \end{aligned} \quad (2.67)$$

In this connection,  $\langle \vec{r} | \hat{L} = 0$  (or equivalently  $\langle \vec{r} | \exp(\hat{L}t) = \langle \vec{r} |$ ) was applied which manifests the conservation of the total probability to 1. In contrast to the quantum mechanics, the function  $\Pi(t)$  influences only linear the expectation value because  $\Pi(t)$  is a non-complex but real function. Then the temporal evolution of the operator  $\hat{G}$  may be written

$$\partial_t \langle \hat{G}(t) \rangle = \langle \vec{r} | \hat{G}\hat{L} | \Pi(t) \rangle = \langle \vec{r} | [\hat{G}, \hat{L}]_- | \Pi(t) \rangle \quad (2.68)$$

putting Eq.(2.67) in Eq.(2.55). Obviously, if an arbitrary quantity  $\hat{G}$  commutes with  $\hat{L}$  then  $\hat{G}$  is a conserved quantity with no temporal dependency. For the discrete temporal evolution of the expectation value

$$\langle \hat{G}(t) \rangle = \langle \hat{G}(n\Delta t) \rangle = \langle \vec{r} | \hat{G}\hat{T}^n | \Pi(0) \rangle \quad (2.69)$$

one accordingly obtains

$$\langle \hat{G}(t + \Delta t) \rangle = \langle \vec{r} | \hat{G}\hat{T} | \Pi(t) \rangle. \quad (2.70)$$

The last formula implies the probability conservation with  $\langle \vec{r} | \hat{T} = \langle \vec{r} |$ .

These equations of motion can be solved in different ways, for instance by hierarchy equations broken up at determined level. Generally, an exact solution cannot be obtained because the equations of motion usually produce higher order terms of the derived quantity.

If one favors the master equation for the probabilities  $P(\vec{n}, t)$  instead of the operator approach then the expression (in the continuous form) is given by

$$\begin{aligned} \partial_t P(\vec{n}, t) &= \langle \vec{r} | \vec{n} \rangle \langle \vec{n} | \hat{L} | \Pi(t) \rangle \\ &= \langle \vec{r} | \vec{n} \rangle \sum_{\vec{m}} \langle \vec{n} | \hat{L} | \vec{m} \rangle \langle \vec{m} | \Pi(t) \rangle \\ &= \sum_{\vec{m}} \left( \frac{\langle \vec{r} | \vec{n} \rangle}{\langle \vec{r} | \vec{m} \rangle} \langle \vec{n} | \hat{L} | \vec{m} \rangle \right) P(\vec{m}, t) \\ &= \sum_{\vec{m}} M_m^n P(\vec{m}, t) \end{aligned} \quad (2.71)$$

using the expansion (2.59), completeness relation (2.8) and the master equation (2.4). Hence, one can compute the elements of the dynamical matrix by means of the scalar product between the reference vector and the base vectors as well as the matrix elements of  $\hat{L}$ . Further, one obtains the correlation function by means of

$$\langle \hat{A}(t)\hat{B}(0) \rangle = \langle \vec{r} | \hat{A}U(t)\hat{B} | \Pi(0) \rangle. \quad (2.72)$$

This can be generalized for the  $n$ -point function as a correlation function of different states  $A, B, C \dots$  at different time points  $t_1 > t_2 > t_3 \dots$  to

$$\langle \hat{A}(t_1)\hat{B}(t_2)C(t_3) \dots \rangle = \langle \vec{r} | \hat{A}U(t_1 - t_2)\hat{B}U(t_2 - t_3)\hat{C} \dots | \Pi(0) \rangle. \quad (2.73)$$

Starting from a pure state, say  $\vec{m}$ , the initial condition is given by  $P(\vec{n}, 0) = \delta_{\vec{n}, \vec{m}}$ . Hence, the state vector for this initial state can be expressed as

$$| \Pi(0) \rangle = \bigotimes_i \frac{(\hat{c}_-^\dagger)_i^{m_i}}{\bar{r}^{m_i}} | 0_i \rangle. \quad (2.74)$$

The reference state has to fulfil the normalization  $\langle \vec{r} | \Pi(t) \rangle = 1$ . This seems reasonable: the expectation value (2.67) of the identity operator  $\hat{i}$  should be one. If one assumes that the reference state is the eigenstate of a raising-type operator  $\hat{C}_+$  with

$$\bigotimes_i \langle r_i | \left( \hat{C}_+ \right)_i^{m_i} = \bigotimes_i \langle r_i | \bar{r}^{m_i} \quad (2.75)$$

then one can show that all initial states are normalized. (Notice, that  $\hat{C}_+$  is not necessary identical with  $\hat{c}_+$  or  $\hat{c}_-^\dagger$ - this will be discussed in the subsequent section about the reference state.) It can be realized if one considers (applying Eq.(2.74))

$$\langle \vec{r} | \Pi(0) \rangle = \prod_i \langle r_i | \frac{(\hat{c}_-^\dagger)_i^{m_i}}{\bar{r}^{m_i}} | 0_i \rangle = \prod_i \langle r_i | \frac{(\hat{C}_+)_i^{m_i}}{\bar{r}^{m_i}} | 0_i \rangle = 1 \quad (2.76)$$

providing  $(\hat{C}_+)_i^{m_i}$  and  $(\hat{c}_-^\dagger)_i^{m_i}$  have the identical action on the right hand side for  $m_i \leq s$ . It is indeed valid for the below derived realization of  $\hat{C}_+$ . Further, this product remains always normalized during the subsequent temporal evolution

$$\langle \vec{r} | \Pi(t) \rangle = \sum_{\{n_i\}} P(\vec{n}, t) (\langle \vec{r} | \vec{n} \rangle)^{-1} \langle \vec{r} | \vec{n} \rangle = \sum_{\{n_i\}} P(\vec{n}, t) = 1. \quad (2.77)$$

If one is not situated near a critical point and the system is ergodic the initial condition does not play a significant rôle for the time evolution. The only conditions for the  $P(\vec{n}, t)$  are that they have to be normalized and non-negative at the beginning. Then they satisfy both conditions for the whole temporal evolution.

If there is a distribution of probabilities  $|\Pi(t)\rangle$  vanishing under continuous-time translation or remaining invariant under discrete-time translation  $\hat{T}$  then I call it *stationary* and denote it  $|\Pi^*\rangle$ , i.e.

$$\hat{L}|\Pi^*\rangle \equiv \hat{L}\Pi^*|\vec{r}\rangle = 0 \quad (2.78)$$

or

$$\hat{T}|\Pi^*\rangle \equiv \hat{T}\Pi^*|\vec{r}\rangle = |\Pi^*\rangle. \quad (2.79)$$

As shown the stationary state  $|\Pi^*\rangle$  is not identical with  $|\vec{r}\rangle$  but a more complex object.

### 2.2.6 Some Notes about Reference States

Like mentioned in the last section, the total probability is only conserved if

$$\langle r | \hat{L} = 0. \quad (2.80)$$

Here, I want to regard only one lattice point the extension to all lattice sites is easily made. It is advantageous for the calculation to split the time evolution operator in two parts

$$\hat{L} = \hat{L}_r \hat{L}_c. \quad (2.81)$$

If  $\hat{L}_r$  fulfils the conservation (2.80) then  $\hat{L}$  does it as well. Hence,  $\hat{L}_c$  is free to include further dynamics and restrictions to the states. Let me firstly concentrate on  $\hat{L}_r$ . In the boson limit the reference state is the coherent state to the raising operator

$$\langle r | (\hat{a}^\dagger - \bar{r}) = 0. \quad (2.82)$$

where  $\bar{r}$  is its eigenvalue. Now one can transfer this relationship to finite systems and gets

$$\langle r | (\hat{C}_+ - \bar{r}) = 0. \quad (2.83)$$

Therefore, the  $(s+1)$ th power of the eigenvalues  $\bar{r}$  has to satisfy

$$\langle r | (\hat{C}_+^{s+1} - \bar{r}^{s+1}) = 0. \quad (2.84)$$

Assuming  $\hat{C}_+$  is identical with  $\hat{c}_-^\dagger$  then  $\bar{r}$  is a Para-Grassmann number vanishing in the  $(s+1)$ th power because the action of  $(\hat{c}_-^\dagger)^{s+1}$  vanishes as well. The Para-Grassmann number can be seen as the solution of  $\bar{r}^{s+1} = 0$  [63]. The eigenvector equation

$$\langle r | \hat{c}_-^\dagger = \langle r | \bar{r} \quad (2.85)$$

yields the expression for the coherent state

$$\langle r | = \sum_{n=0}^s \langle n | \frac{\bar{r}^n}{\sqrt{\bar{z}_n!}}. \quad (2.86)$$

On the other hand, if one prefers that  $\bar{r}$  is a complex number then it should  $\hat{C}_+ \neq \hat{c}_-^\dagger$ . In order to compensate the missing highest state after the application  $\hat{c}_-^\dagger$  to  $\langle r |$  one can add a counterterm. As the only possibility it remains

$$\hat{C}_+ = \hat{c}_-^\dagger \rightarrow \hat{c}_-^\dagger + \frac{\bar{r} (\bar{r} \hat{c}_-)^s}{|\bar{z}_s|!}. \quad (2.87)$$

The states  $\langle 0 |$  to  $\langle s-1 |$  are created by the application of the raising operator to the single states  $\langle 1 | \dots \langle s |$  of the reference state whereas the counterterm operator  $\frac{\bar{r} (\bar{r} \hat{c}_-)^s}{|\bar{z}_s|!}$  creates the state  $\langle s |$  by applying to  $\langle 0 |$ . The reference state is identical with that in Eq.(2.86), but  $\bar{r} \in \mathbf{C}$  now.

I want to reduce the effort for further steps and set  $\hat{C}_+^{new}$  equal to  $\bar{r}^{-1} \hat{C}_+$ . Hence, the eigenvalue of the new operator

$$\hat{C}_+^{new} = \frac{\hat{c}_-^\dagger}{\bar{r}} + \frac{(\bar{r} \hat{c}_-)^s}{|\bar{z}_s|!} \quad (2.88)$$

is 1. In the future, I will neglect the index "new" again.

Consequently, following the rules of the action for operators applied to the reference state, one obtains the identity relations

$$\begin{aligned} \langle r | \hat{C}_+ &\equiv \langle r | \text{ and } \langle r | \hat{C}_+^{-1} \equiv \langle r |, \\ \bar{r} \langle r | \hat{C}_+ \hat{c}_- &\equiv \langle r | \hat{c}_-^\dagger \hat{c}_- \equiv \langle r | |\hat{Z}_n\rangle = \bar{r} \langle r | \hat{c}_-. \end{aligned} \quad (2.89)$$

These relationships prove very useful in derivation of the second quantized representation of the elementary reactions.

### 2.2.7 Computation Rules of Expectation Values

Different studies show that it is preferable to apply the ordinary number operator despite its complicate representation (2.33). Therefore, I will take the conclusion from the formalism of the last sections and gain some simplifications for the practical calculation of the expectation values. I want to concentrate on the  $q$ -statistics in this section but the derivation for the Para-Fermi statistics might be done in the same manner leading to similar results.

If one assumes an arbitrary operator  $\hat{G}$  has the diagonal form of (2.65) then it can be expanded in terms of the ordinary number operator

$$\hat{G}\{\hat{N}\} = \sum_{m=0}^s g_m \hat{N}^m. \quad (2.90)$$

Firstly, one should remember the definition of the evolution of the expectation value  $\partial_t \langle \hat{G} \rangle = \langle \vec{r} | \hat{G} \hat{L} | \Pi(t) \rangle$ . Often, one has to evaluate terms of  $\hat{L}$  such as  $\hat{b}_-^\dagger, \hat{b}_-$



and  $[[\hat{N}]]$ . Hence, I will demonstrate the simplification of the average terms with  $\langle \hat{G}\{\hat{N}\}\hat{b}_-^\dagger \rangle$  as one example using the commutation relationship (2.32), the raising-type operator  $\hat{C}_+$  (2.88) and the identity relations (2.89)

$$\begin{aligned}
\langle \hat{G}\{\hat{N}\}\hat{b}_-^\dagger \rangle &= \langle r | \hat{G}\{\hat{N}\}\hat{b}_-^\dagger | \Pi(t) \rangle \\
&= \sum_m g_m \langle r | \hat{N}^m \hat{b}_-^\dagger | \Pi(t) \rangle \\
&= \sum_m g_m \langle r | \hat{N}^{m-1} \hat{b}_-^\dagger (\hat{N} + 1) | \Pi(t) \rangle \\
&= \sum_m g_m \langle r | \hat{b}_-^\dagger (\hat{N} + 1)^m | \Pi(t) \rangle \\
&= \sum_m g_m \bar{r} \langle r | (\hat{i} - \hat{S})(\hat{N} + 1)^m | \Pi(t) \rangle.
\end{aligned} \tag{2.91}$$

$\hat{i}$  is the identical operator and  $\hat{S}$  is defined as the projector on the state  $s$ , i.e.

$$\langle n | \hat{S} = \langle n | \delta_{n,s}. \tag{2.92}$$

Thus, one can derive all other equalities of frequent terms in the same manner. This leads to the following results of the expectation values

Expectation value	Evaluated general result	
$\langle \hat{G}\{\hat{N}\}\hat{b}_-^\dagger \rangle$	$\langle \hat{G}\{\hat{N} + 1\}(\hat{i} - \hat{S})\bar{r} \rangle$	
$\langle \hat{G}\{\hat{N}\}[[\hat{N}]] \rangle$	$\langle \hat{G}\{\hat{N}\}[[\hat{N}]] \rangle$	(2.93)
$\langle \hat{G}\{\hat{N}\}\hat{b}_- \rangle$	$\langle \hat{G}\{\hat{N} - 1\}[[\hat{N}]]\bar{r}^{-1} \rangle$	
$\langle \hat{G}\{\hat{N}\}\hat{B}_+ \rangle$	$\langle \hat{G}\{\hat{N} + 1\}(\hat{i} - \hat{S}) + g_0\hat{S} \rangle$	

where  $\hat{B}_+$  is  $\hat{C}_+$  specified for the  $q$ -statistics. Finally, it remains interesting to explore the special limits, the boson and fermion case. Realizing the limit for  $q$  the formulae transform to

Expectation value	Fermion case	Boson case	
$\langle \hat{G}\{\hat{N}\}\hat{b}_-^\dagger \rangle$	$\langle \hat{G}\{1 - \hat{N}\}(1 - \hat{N})\bar{r} \rangle$	$\langle \hat{G}\{\hat{N} + 1\}\bar{r} \rangle$	
$\langle \hat{G}\{\hat{N}\}[[\hat{N}]] \rangle$	$\langle \hat{G}\{\hat{N}\}\hat{N} \rangle$	$\langle \hat{G}\{\hat{N}\}\hat{N} \rangle$	(2.94)
$\langle \hat{G}\{\hat{N}\}\hat{b}_- \rangle$	$\langle \hat{G}\{\hat{N} - 1\}\hat{N}\bar{r}^{-1} \rangle$	$\langle \hat{G}\{\hat{N} - 1\}\hat{N}\bar{r}^{-1} \rangle$	
$\langle \hat{G}\{\hat{N}\}\hat{B}_+ \rangle$	$\langle \hat{G}\{1 - \hat{N}\}(1 - \hat{N}) + g_0\hat{N} \rangle$	$\langle \hat{G}\{\hat{N} + 1\} \rangle$	

which allows to study the equations at the boundary of the spectrum of  $q$  values. Here, I applied the identity  $1 - \hat{N}^2 = 1 - \hat{N}$  for the fermion result.

## 2.2.8 Elementary Reactions

The dynamics of many (physical and non-physical) systems are modeled by two different kinds of "elementary" evolutions. The first is known as a spontaneous

reaction or flip process (Glauber dynamics) and will be considered here as a one-site action, but extensions should be easily made. Then it is possible to describe still more complicated phenomena. The second is a necessarily spatial process because it leads to an exchange of particles between two different places within a system. It is called diffusion or exchange process (Kawasaki dynamics).

### Glauber (Flip or Reaction) Processes

This process was firstly described when Glauber [64] was studying how a Ising-spin system reaches its equilibrium state. Originally, the model gives the flip rate of a single spin depending on the interaction energy and the temperature. It could be extended to a more-than-one site effect, but here, I will concentrate only on the one-site process, accordingly the lattice index is neglected. For this type of spontaneous reaction it is advantageous to distinguish further, i.e. in a generation process (if the Fock state raises to a higher number) and in an annihilation process (if a Fock state goes to a lower number).

Firstly, the generation process is given in an one-step raising form

$$\hat{L}_G^1 = \left( \hat{C}_+ - \hat{i} \right). \quad (2.95)$$

The term  $\hat{C}_+$  carries out the raising part whereas  $\hat{i}$  is necessary due to the normalization  $\langle r | \hat{L}_G^1 = 0$ .  $\hat{L}_G^1$  can be understood as a trial of the wished raising process. It should be only successful if the system is not in the highest possible state.  $\hat{C}_+$  is even chosen to fulfil this condition. In the boson case,  $s \rightarrow \infty$  ( $q = 1$ ), the operator takes the known form (see e.g. [6])

$$\hat{L}_G^1 = \left( \bar{r}^{-1} \hat{a}^\dagger - \hat{i} \right). \quad (2.96)$$

Then the corresponding master equation in the probability description reads

$$\partial_t P(n, t) = P(n-1, t) - P(n, t) \quad (2.97)$$

benefiting from the probability representation in (2.71). The probability to be in the state  $n$  increases proportional to the probability of the state  $(n-1)$  and decreases proportional to the probability of the state  $n$ .

If one increases the Fock state by  $n$  steps instead by one step then the relationship transforms to

$$\hat{L}_G^n = \left( \hat{C}_+^n - \hat{i} \right) \quad (2.98)$$

noting  $\hat{i}^n = \hat{i}$ .

Naturally, one considers reaction processes where one species spontaneously reacts to another. If one identifies this species with a fixed Fock state and the reactant with another, the  $n$ -step increase should only transform between these both states. Since  $(\hat{C}_+ - \hat{i})$  was even so introduced to fulfil the normalization (to the left hand

side) the unique possibility to imply restrictions is multiplying these at the right hand side of this operator. To arrive this aim one exploits the projectors  $\hat{O}$  assigned to every state with

$$\hat{O}|n\rangle = \delta_{o,n}|n\rangle \quad (2.99)$$

and uses their orthogonality to each other

$$\hat{O}_1\hat{O}_2 = \delta_{o_1,o_2}. \quad (2.100)$$

One explicit formulation of  $\hat{O}$  is given by

$$\hat{O} = \frac{1}{|z_s|!} \hat{c}_+^o \hat{c}_-^s (\hat{c}_+^\dagger)^s (\hat{c}_+^\dagger)^{-o}. \quad (2.101)$$

Therefore, one gets an  $n$ -step generating process starting from the state  $o$  by the operator

$$\hat{L}_{o;G}^n = \left( \hat{C}_+^n - \hat{i} \right) \hat{O}. \quad (2.102)$$

Further, one can particularize for a spin flip from  $|0\rangle \rightarrow |1\rangle$  of the fermion model ( $s = 1, q = -1$ ). The assigned generation operator in Eq.(2.102) results in

$$\hat{L}_{0;G}^1 = \left( \hat{C}_+ - \hat{i} \right) \hat{O} \quad (2.103)$$

or equivalently in detail

$$\begin{aligned} \hat{L}_{0;G}^1 &= (\bar{r}^{-1}\hat{a}^\dagger + \bar{r}\hat{a} - \hat{i}) \hat{a}\hat{a}^\dagger \\ &\equiv (\bar{r}^{-1}\hat{a}^\dagger - \hat{i}) \hat{a}\hat{a}^\dagger \equiv (\bar{r}^{-1} - \hat{a}) \hat{a}^\dagger. \end{aligned} \quad (2.104)$$

In this connection, I applied the ordinary commutation rules for fermions

$$\hat{a}\hat{a}^\dagger + \hat{a}^\dagger\hat{a} = 1 \quad (2.105)$$

for the last steps (see the comment in section about the para-statistics and Eq.(2.25)). The next example is a further flip process exploiting in the framework of the Fredrickson-Andersen model later. Choosing ( $s = 2$ ) and considering a flip  $|0\rangle \rightarrow |2\rangle$  the generation operator takes the form (specified for the para-fermions)

$$\begin{aligned} \hat{L}_{0;G}^2 &= \left( \hat{C}_+^2 - \hat{i} \right) \hat{O} \\ &= \left( \left( \frac{\hat{a}^\dagger}{\bar{r}} + \frac{(\bar{r}\hat{a})^2}{z_2!} \right)^2 - \hat{i} \right) \frac{\hat{a}^2 (\hat{a}^\dagger)^2}{z_2!}. \end{aligned} \quad (2.106)$$

By means of a detailed calculation this equation can be simplified to

$$\hat{L}_{0;G}^2 = \left( \bar{r}^{-2} - \frac{\hat{a}^2}{z_2!} \right) (\hat{a}^\dagger)^2. \quad (2.107)$$

Secondly, one may adopt the same procedure for the annihilation operator. Thus, one obtains the one-step form

$$\hat{L}_A^1 = - \left( \hat{C}_+ - \hat{i} \right) \left( \bar{r} |\hat{Z}_{n+1}|^{-1} \hat{c}_- \right). \quad (2.108)$$

The first part guarantees the normalization, the second part provides the decrease of the states and insures that  $|\hat{Z}_{n+1}|^{-1}$  remains always finite in application to the Fock states. Notice, that  $|\hat{Z}_{n+1}|^{-1}$  fulfils the equation

$$|\hat{Z}_{n+1}|^{-1} |n\rangle = |z_{n+1}|^{-1} |n\rangle. \quad (2.109)$$

Again, exploring the limit  $s \rightarrow \infty$  ( $q = 1$ ), the annihilation operator can be represented by

$$\hat{L}_A^1 = - \left( \hat{a}^\dagger - \bar{r} \right) \left( \left( \hat{N} + 1 \right)^{-1} \hat{a} \right). \quad (2.110)$$

Like in case of the generating operator, it seems interesting to study the probability representation

$$\partial_t P(n, t) = P(n+1, t) - P(n, t). \quad (2.111)$$

The interpretation is similar to the case of the generating process with the only difference that the states are decreased. Here, one would effortlessly recognize the distinction if one neglected the inverse of the number operator  $|\hat{Z}_{n+1}|$  in (2.108):

$$\partial_t P(n, t) = (n+1) P(n+1, t) - n P(n, t). \quad (2.112)$$

The resulting equilibrium (stationary state) is the Poisson distribution whereas the equilibrium of the former is an equidistribution. Later in the framework of a  $q$ -deformed model I will work out how this equation transforms if one exploits the probability representation for a finite Fock space. Comparing with the approach for the generating process, the next operator of interest, the  $n$ -step annihilation operator, can be derived in the same manner

$$\hat{L}_A^n = - \left( \hat{C}_+^n - \hat{i} \right) \left( \bar{r} |\hat{Z}_{n+1}|^{-1} \hat{c}_- \right)^n. \quad (2.113)$$

Due to the discussed reasons the restrictions must multiply at the right hand side of the annihilation operator. Then the  $n$ -step annihilation operator, starting from the state  $o$ , follows directly,

$$\hat{L}_{o;A}^n = - \left( \hat{C}_+^n - \hat{i} \right) \left( \bar{r} |\hat{Z}_{n+1}|^{-1} \hat{c}_- \right)^n \hat{O}. \quad (2.114)$$

Depicting it for the fermion model ( $s = 1, q = -1$ ) in detail one can study the reverse process to (2.104),  $|1\rangle \rightarrow |0\rangle$ . Specify the annihilation operator in Eq.(2.114) leads to

$$\hat{L}_{1;A}^1 = - \left( \hat{C}_+ - \hat{i} \right) \left( \bar{r} (\hat{N} + 1)^{-1} \hat{c}_- \right) \hat{N} \quad (2.115)$$

which boils down to

$$\begin{aligned}\hat{L}_{1;A}^1 &= -(\bar{r}^{-1}\hat{a}^\dagger + \bar{r}\hat{a} - \hat{i})\bar{r}\hat{a}\hat{a}^\dagger\hat{a} \\ &\equiv -(\hat{a}^\dagger - \bar{r})\hat{a}\hat{a}^\dagger\hat{a} \equiv -(\hat{a}^\dagger - \bar{r})\hat{a}.\end{aligned}\quad (2.116)$$

One has to use the commutation rules (2.105) for the last steps. Now I want to return to the Fredrickson-Andersen model ( $s = 2$ ) to examine the back process  $|2\rangle \rightarrow |0\rangle$ . The annihilation operator can be calculated to (specified again for the Para-Fermi statistics)

$$\begin{aligned}\hat{L}_{2;A}^2 &= -(\hat{C}_+^2 - \hat{i})\left(\bar{r}|\hat{Z}_{n+1}|^{-1}\hat{c}_-\right)^2\hat{a} \\ &= -\left(\left(\frac{\hat{a}^\dagger}{\bar{r}} + \frac{(\bar{r}\hat{a})^2}{z_2!}\right) - \hat{i}\right)\left(\bar{r}|\hat{Z}_{n+1}|^{-1}\hat{a}\right)^2\frac{(\hat{a}^\dagger)^2\hat{a}^2}{z_2!}.\end{aligned}\quad (2.117)$$

It is easy to prove that this operator is equivalent to

$$\hat{L}_{2;A}^2 = \left(\bar{r}^2 - \frac{(\hat{a}^\dagger)^2}{z_2!}\right)\hat{a}^2. \quad (2.118)$$

Here, these results are mentioned for the illustration of the mechanism. I will revert to this reference in this work later to compute relaxation phenomena in glasses by means of the Fredrickson-Andersen model.

### Kawasaki Dynamics or Diffusion (Exchange) Process

The diffusion is a necessarily spatial process due its main rôle to transport objects to the points "where the action is" [6]. Let me assume that  $\vec{R}$  is a lattice vector. The temporal change of the probability  $P(\vec{R}, t)$  to find a particle at a position  $\vec{R}$  jumping from another positions  $\vec{R} + \delta\vec{R}$  can be expressed by

$$\partial_t P(\vec{R}, t) = \frac{D}{l^2} \sum_{\delta\vec{R}} \left[ P(\vec{R} + \delta\vec{R}, t) - P(\vec{R}, t) \right] \quad (2.119)$$

where  $l$  is the lattice length. In a lattice picture, the diffusion can be approximated by a discrete hopping of particles between two lattice sites  $i$  and  $j$ . This hopping in kinetic Ising models was probably at first described by Kawasaki [65, 66]. The particles should diffuse throughout the media with the diffusion coefficient  $D$  which is assumed to be the same for all lattice points, hence to be space-independent. Supposing  $n_i(n_j) \leq s$  (the maximum number of particles which fit on one site) gives the number of particles at site  $i(j)$ . Then one can write down the temporal evolution of the probability if a particle jumps from  $i$  to  $j$  (for the reverse process the approach is the same)

$$\partial_t P(\vec{n}, t) = D \sum_j (n_i + 1) P(\dots, n_i + 1, \dots, n_j - 1, \dots, t) - (n_i) P(\vec{n}, t). \quad (2.120)$$

This formula can be interpreted as follow: There are two possibilities that the probability

$$P(\vec{n}, t) = P(\dots, n_i, \dots, n_j, \dots, t)$$

is altered during a time period. Firstly, there is a positive contribution when at a possible lattice site  $j$  one particle is still missing to have  $n_j$  particles and there is still one particle too much at site  $i$  which can jump to  $j$ . Since it can jump only one of  $(n_i + 1)$  particles at the same time the rate  $D(n_i + 1)$  expresses the equivalence of all jumps (This master equation takes only one-step processes into consideration.). On the other hand, the probability of finding  $P(\vec{n}, t)$  decreases with  $Dn_i$  due to a further jump of a particle away from  $i$  to all sites  $j$ . Neglecting the first term the solution would describe only a decay of this state.

The assigned time evolution operator is a compound of a generation and annihilation operator applied to Fock states at different lattice sites. Again like in case of zero-dimensional processes I start with the simplest form to lower one state at site  $i$  and to raise one state at site  $j$ ,

$$|n_i + 1, \dots, n_j - 1\rangle \rightarrow |n_i, \dots, n_j\rangle. \quad (2.121)$$

The one-step diffusion operator reads

$$\hat{L}_D^1 = \left( \hat{C}_{+j} - \hat{C}_{+i} \right) \left( \bar{r} (|\hat{Z}_{n+1}|)_i^{-1} \hat{c}_{-i} \right). \quad (2.122)$$

E.g. if one identifies  $n_i + 1$  with a particle,  $n_i$  with an empty place and sets  $n_j - 1 = n_i$  the process is nothing more than a jump of a particle from position  $i$  to  $j$ . If one ignores the term  $\hat{Z}_{n+1}^{-1}$  and sums up over all  $j$  the operator leads to the same master equation up to a constant like (2.120). The diffusion operator is written

$$\hat{L}_D^1 = \left( a_j^\dagger - a_i^\dagger \right) \left( \hat{N} + 1 \right)_i^{-1} a_i \quad (2.123)$$

in the boson limit ( $s \rightarrow \infty, q = 1$ ) and

$$\hat{L}_D^1 = \left( a_j^\dagger - a_i^\dagger \right) a_i + \bar{r}^2 a_j a_i \quad (2.124)$$

or in the more familiar form

$$\hat{L}_D^1 = a_j^\dagger a_i - (1 - \hat{N}_j) \hat{N}_i \quad (2.125)$$

in the fermion limit ( $s = 1, q = -1$ ). The next step is to model an exchange between two sites in the following manner

$$|n_i + n, \dots, n_j - n\rangle \rightarrow |n_i, \dots, n_j\rangle. \quad (2.126)$$

Remaining in a particle picture: a particle at  $i$  represented by the state number  $n_i + n$  changes its position with a particle at  $j$  represented by the state number

$n_j - n$ . Since it is wishful (and often convenient) that only particles with the state number  $n_i + n$  but not particles with  $n_i + \tilde{n}$  and  $\tilde{n} \neq n$  diffuse one must multiply the restriction on the right hand side. Assuming without the loss of generality that  $n$  is positive the restricted diffusion operator is supplied by

$$\hat{L}_{o_i, o_j; D}^n = \left( \hat{C}_{+j}^n - \hat{C}_{+i}^n \right) \left( \bar{r}(|\hat{Z}_{n+1}|)_i^{-1} \hat{c}_{-i} \right)^n \hat{O}_i \hat{O}_j. \quad (2.127)$$

Apart from the flip processes, an extended version of the Fredrickson-Andersen model ( $s = 2$ ) includes also a diffusion of a particle at site  $i$  (assigned to  $|2_i\rangle$ ) to an empty site  $j$  (assigned to  $|1_j\rangle$ ) how one will recover in the next section. Now one particularizes the operator and obtains

$$\hat{L}_{2,1; D}^1 = \left( \hat{C}_{+j} - \hat{C}_{+i} \right) \left( \bar{r}(|\hat{Z}_{n+1}|)_i^{-1} \hat{c}_{-i} \right) \hat{2}_i \hat{1}_j. \quad (2.128)$$

The computation of this expression shows that it can be written in a simpler manner

$$\hat{L}_{2,1; D}^1 = \frac{1}{(|z_2|!)^2} \left( \frac{1}{|z_2|!} a_j^\dagger a_i - \hat{i} \right) (a_i^\dagger)^2 (a_i)^2 a_j^\dagger (a_j)^2 a_j^\dagger. \quad (2.129)$$

Naturally, this Fredrickson-Andersen model should also comprehend the reverse process from an occupied site  $j$  to a vacant site  $i$

$$\hat{L}_{1,2; D}^1 = - \left( \hat{C}_{+j} - \hat{C}_{+i} \right) \left( \bar{r}(|\hat{Z}_{n+1}|)_j^{-1} \hat{c}_{-j} \right) \hat{1}_i \hat{2}_j. \quad (2.130)$$

After some steps of straight forward simplification the operator reads

$$\hat{L}_{1,2; D}^1 = \frac{1}{(|z_2|!)^2} \left( \frac{1}{|z_2|!} a_i^\dagger a_j - \hat{i} \right) (a_j^\dagger)^2 (a_j)^2 a_i^\dagger (a_i)^2 a_i^\dagger. \quad (2.131)$$

Summarizing these last both subsections every dynamical operator can be combined in the following abstract form

$$\hat{L} = \hat{L}_r \hat{L}_c = \text{Normalization term} \times \text{Additional dynamics} \times \text{Restrictions}. \quad (2.132)$$

In the next chapter we will see how one can relate and apply the more or less abstract operators to physical models.

# Chapter 3

## Examples

*Erkennen ist Anwendung. Nur der Wissende erkennt. [67]*

Nowadays reactions, aggregation, diffusion and other similar processes are strongly discussed fields of physical research [68]. As already mentioned, it proves very hard itself to find a unique mathematical formalism for their description, but in this section one will realize that the master equation can yield a sufficient description for at least some of these phenomena. The main reasons for differing of natural processes in their macroscopic pictures are the different underlying time scales and ratio to each other. Examples are the diffusion and reaction limited aggregations. Obviously, the longest time scale determines the long time behavior in the system. Another interesting example for competing time scales is the glass transition. Apart from the fast  $\gamma$ -relaxation time the  $\alpha$ -process and, in the most glasses,  $\beta$ -process, play the main roles [69]. We will see how the processes can emerge from the inherent cooperativity inside of glasses and how one can use lattice models to compute their behavior. In this connection, the mathematical formalism introduced in the last sections will be demonstrated in this chapter at some chosen examples, like a spin-flip system, a glassy system, shocks in an exclusion process and a  $q$ -deformed model. The usage of second quantized operators and of derived relations including the rules for the dynamics should emphasize the possible wide range of application of the Fock-space method.

### 3.1 Fredrickson-Andersen Model

In this section I want to outline the research to the  $n$ -spin facilitated kinetic Ising model (Fredrickson–Andersen model) and its extension with mobile vacancies (published in [21]). This model should be studied as an example for glass forming materials by means of the Fock-space representation for the master equation introduced in the previous section.

Despite of recent advances in the description of liquids near the glass transition using different approaches the phenomenon is not completely understood [70–73].



Glasses often reveal a non-Arrhenius behavior of characteristic relaxation times. In contrast to the conventional phase transitions, a long range order is not developed. Moreover, the dynamical glass transition is also characterized by an increasing cooperativity of local processes with decreasing temperature [74]. This cooperativity is the reason for the well-known slowing down occurring within the dynamical behavior. It is reflected by the strongly curved trajectory in the Arrhenius plot (logarithm of the relaxation time  $\ln \tau$  versus the inverse temperature  $T^{-1}$ ) which can be possibly fitted by the Williams-Landel-Ferry curve [75] with  $\ln \tau \propto (T - T_0)^{-1}$  and the Vogel temperature  $T_0$ .

Two relevant relaxation processes (besides of the much faster  $\gamma$ -process) should be incorporated in our model: the slower  $\alpha$ -process and the faster  $\beta$ -process. The former is a universal phenomenon of glasses and corresponds to the cooperative molecular diffusion. The latter stresses that most of glasses of complex fluids (e.g. polymer melts, gels, proteins and others) can show a more complicated behavior as simple liquids.

Various types of molecular motions [74] are expected in glass formers, such as intermolecular diffusion processes as well as intermolecular motions of subchains or rotational relaxations of monomer groups. Each of this 'secondary' [76] processes are manifested by relaxation times and usually denoted as  $\beta_{JG}$ -processes (Johari-Goldstein process). The  $\beta_{JG}$ -process is a simply activated one (straight line in the Arrhenius plot) and its fast relaxation time  $\tau_\beta$  expresses a more or less local character. The  $\alpha$ -process corresponds to non-local structural relaxations (caused by the intermolecular diffusion). For increasing temperatures both processes, the  $\alpha$ - and the  $\beta_{JG}$ -process, respectively are approaching each other. A rough extrapolation suggests a bifurcation of both processes at a finite temperature [77, 78].

The nowadays dominating theory for glasses, the mode coupling theories (MCT), [70, 76, 79] predicts the existence of both, a slow  $\alpha$ - and a fast  $\beta$ -process above a kinetic critical temperature  $T_c$  and a remaining non-ergodic  $\beta$ -process below  $T_c$  being in between the melting temperature  $T_m$  and the glass temperature  $T_G$ . At  $T_c$  the system undergoes a sharp phase transition to a state with frozen (density) fluctuations. The MCT interprets the  $\alpha$ -process as the slow structural relaxations of the supercooled liquid, whereas the  $\beta$ -process is often identified with a rearrangement of the neighbor environments breaking up the local cages. However, this  $\beta$ -process is not identical with the Johari-Goldstein process which appears at much longer relaxation times and at a temperature lower than  $T_c$ .

Hence, it remains the question of interaction between  $\beta_{JG}$ -process and phenomenon of cooperativity inherent to glasses. As suggested recently [80] the relaxation time of supercooled liquids should be independent of the microscopic dynamics, the unique atomic processes reveal as irrelevant. Thus, mesoscopic scales dominating the system are much larger than the atomic scale but smaller than the macroscopic scale. Therefore, our analysis will be based on a mesoscopic formulation which reduces the degrees of freedom and applies a smaller set of relevant

observables following the idea of Fredrickson's and Andersen's lattice model (also denoted as the  $n$ -spin facilitated Ising model, nSFM) [33–36]. The justification of this approach is then given by other observations in experiments, by comparison with similar phenomena or by agreement of the achieved results.

In the following rows I will shortly sketch the basic ideas of Fredrickson and Andersen and emphasis made extensions. Our many-body system may be treated on a virtual lattice with sufficiently small cells of mesoscopic size  $l$ , which does not influence the underlying dynamics of the supercooled liquid. The cell structure enables us to attach to each cell an observable  $\sigma_j = 2n_j - 1$  characterizing the actual state of particles inside the cell  $j$ . The usual realization is given by the local density  $\rho_j$  (particles per cell) with  $\sigma_j = -1$  if  $\rho_j > \bar{\rho}$  and  $\sigma_j = 1$  if  $\rho_j < \bar{\rho}$  where  $\bar{\rho}$  is the averaged density of the whole system. This mapping represents different mobilities of the particles inside such a cell;  $\sigma_j = -1$  corresponds to the immobile solid-like state and  $\sigma_j = 1$  to the mobile liquid-like state. The two density states per lattice cell could be only a rough approximation of supercooled liquids but allow us to concentrate on relevant processes. I will assume that the kinetics is a simple Glauber process  $\sigma_j = +1 \leftrightarrow \sigma_j = -1$  controlled by self-induced topological restrictions. These constraints reflect the relaxation behavior of a supercooled liquid. In particular, an elementary flip at a given cell should be allowed only if the number of nearest neighbor mobile cells ( $\sigma_j = +1$ ) is equal to or larger than a certain restrictive number  $n_R$  with  $0 \leq n_R \leq n_C$  ( $n_C$  is the coordination number of the lattice). The idea: elementary flip processes combined with the geometrical restrictions may lead to the cooperative rearrangements. As demonstrated, such a mesoscopic approach can model a supercooled liquid below  $T_c$ . Besides of Fredrickson and Andersen [33–36] this could be proved by numerical [81–85] and analytical studies [18, 86–88]. The nSFM can be classified as an Ising-like model the kinetics of which is confined by restrictions of the ordering of nearest neighbors to a given lattice cell. These self-adapting environments influence in particular the long time behavior of the spin-spin and therefore of the density-density correlation functions.

### 3.1.1 The Ordinary Fredrickson-Andersen Model

Before I will explore the extended Fredrickson-Andersen model I want to study the thermodynamical properties of the usual model for one dimensions, but often holding also in higher dimension. As mentioned above the Fredrickson-Andersen model associates each mesoscopic cell with a Ising spin on a lattice.

The thermal equilibrium probabilities for a site being spin-up (being liquid-like),

$$p_A = (1 - p_B) = \frac{\exp(-\beta h)}{2 \cosh(\beta h)} \quad (3.1)$$

where  $\beta$  is the inverse temperature and  $h$  and  $-h$  are the effective energies of the liquid-like and the solid-like cells. Remaining in the spin picture the thermal equi-

librium of this kinetic model is approached through individual spin flips. A spin-up site flips to a spin-down site at a rate  $\lambda_{AB} = \tilde{\lambda}_{AB} \exp[\beta h]$ . The spin-flip rate for the reverse process is  $\lambda_{BA} = \tilde{\lambda}_{BA} \exp[-\beta h]$ . The temperature dependent spin-flip rates satisfy the condition of detailed balance, so

$$p_B \lambda_{BA} = (1 - p_A) \lambda_{BA} = p_A \lambda_{AB}. \quad (3.2)$$

Thermal equilibrium will be achieved as long as the spin-flip rates ( $\lambda$ ) do not vanish. However, thermodynamic ambiguity of the Fredrickson-Andersen model is achieved by allowing some spin-flip rates to vanish. This slows (and perhaps stops) the approach to thermal equilibrium.

The core of the Fredrickson-Andersen model is the criterion which determines the non-zero spin-flip rates. Let us denote cells with mobile or immobile states at position  $i$  ( $\sigma_i = \pm 1$ ) as occupied cells. The flip process of the usual Fredrickson-Andersen model is

$$\sigma_i = -1 \rightleftharpoons \sigma_i = +1. \quad (3.3)$$

Further, I want to abbreviate the maximum number of nearest-neighbor sites (coordination number) by  $n_C$  and the number of sites of the nearest neighborhood having  $\sigma_i = 1$  by  $\nu_i$ , i.e.

$$\nu_i = \frac{1}{2} \sum_{j(i)} \sigma_j (1 + \sigma_j) \quad (3.4)$$

( $j(i)$  means all  $n_C$  nearest neighbors of the lattice point  $i$ ). Then, additionally to the thermodynamic flip rates  $\lambda$ , I include the topological restrictions for the flip. It is only possible, if at least  $n_R$  ( $0 \leq n_R \leq n_C$ ) nearest neighbors at site  $i$  have  $\sigma_i = 1$ ,

$$\nu_i \geq n_R \quad (3.5)$$

This restriction is the central idea of the nSFM and leads to the characteristic hindrance effects. If a spin-flip at site  $j$  changes  $\nu_i$  at all sites  $i$  neighboring site  $j$ , mobile spins can become immobile and immobile spins can become mobile.

The thermodynamic limitation of the Fredrickson-Andersen model should be illustrated for a square lattice where  $n_C$  is 4. For this case, if  $n_R$  is 3 or 4, rectangular spin-down regions of the lattice are permanent and cannot change at any temperature. This is not reasonable since initial conditions determine the possible configurations for all future times. (“Configuration” denotes the orientation of a set of spins). However, if  $n_R$  is 0, 1, or 2, the thermodynamic properties are those of a set of free spins. To prove this result, one can apply (with notational modifications) the theorem by van Enter [89] which describes accessible states in a related class of models called “bootstrap percolation” [90] (or “diffusion percolation” [91]). The van Enter theorem applied to the Fredrickson-Andersen square lattice for  $n_R = 2$  (the only interesting case) shows that sequences of spin flips at mobile sites connect essentially all possible spin configurations i.e. the system is ergodic. Furthermore,

one may generalize this theorem to show that the energy fluctuation needed to flip essentially any spin is finite. (Formally, given any small number  $\epsilon > 0$  and a random distribution of spins with spin-up probability  $p_A > 0$ , an arbitrary spin can be flipped with a probability greater than  $(1 - \epsilon)$  by a finite energy fluctuation  $\delta E(\epsilon, p)$ .) Thus, the partition function must include essentially all spin configurations, and the thermodynamics are unaffected by the spin-flip restriction when  $n_R = 2$ . Of course, when  $p_A$  is small, the energy fluctuation needed to flip spins can be so large that relaxation times would be too long to be observed. Generalizations of these comments apply to the Fredrickson-Andersen model on other lattices and for three dimensions.

### 3.1.2 Mean-Field Theory of the Ordinary Model

We apply the simplest possible version of a mean-field theory to the Fredrickson-Andersen model by replacing the number of spin-up neighbors of site  $i$  ( $\nu_i$  of Eq.(3.5)) by its average over all the sites, called  $\bar{\nu}$ . In thermal equilibrium

$$\bar{\nu} = n_C p_A \quad (3.6)$$

with  $p_A$  given by Eq.(3.1). Since every site is characterized by the same  $\bar{\nu}$ , a phase transition takes place at a critical spin-up probability

$$(p_A^c)_{MFA} = \frac{n_R}{n_C}. \quad (3.7)$$

Solving Eq.(3.1) for the temperature  $T$

$$T^{-1} = \beta = \frac{1}{2h} \ln \left( \frac{1 - p_A}{p_A} \right) \quad (3.8)$$

so if  $(p_A^c)_{MFA} < 1/2$  and  $h > 0$ , the mean field transition temperature is positive and finite. Above the mean-field transition temperature  $T_{MFA}^c$ , the system has the properties of a set of free spins, since every spin is flipable. However, cooling below  $T_{MFA}^c$  cannot lower the energy or the entropy because all spin-flip rates vanish for  $p_A < (p_A^c)_{MFA}$ .

This mean-field model restricts the spin configurations to those in which the fraction of spin-up sites is at least  $(p_A^c)_{MFA}$ . The thermodynamic properties of this (mean-field) model with a restricted configuration space are unusual in due to the highly degenerated ground state. This means there is a residual non-zero entropy even at zero temperature. Also, since the system's internal energy approaches the lowest allowed energy at  $T_{MFA}^c$ , the heat capacity vanishes at temperatures below  $T_{MFA}^c$ . But nevertheless, mean-field theory may become accurate in the limit of long-ranged interactions.

### 3.1.3 Modified Fredrickson-Andersen Model

In order to understand the Fredrickson-Andersen model more detailed we will regard it only as a combinatorial problem of spins with some modifications at first [92]. To overcome the inadequate approximation of the simple mean-field theory one has to properly describe effects associated with the dominant short-ranged interactions. This modified Fredrickson-Andersen model assumes both long-ranged and short-ranged effects control the spin-flip rates. The long-ranged interaction is treated in the spirit of mean-field theory, but the short-ranged part is included on the mesoscopic scale.

I modify the Fredrickson-Andersen model as follows:

1. Each spin is either “unflipable” or “flipable”. Unflipable spins can not flip, and the ratios of the spin-flip rates for the flipable spins are determined by the detailed balance.
2. As with the original Fredrickson-Andersen model, a spin is flipable if it is embedded in a sufficiently large concentration of spin-up sites. However, these spin-up sites can be either nearest neighbors or distant neighbors. Thus, a spin is flipable if *either*

A a spin is adjacent to at least  $n_R$  spin-up sites *or*

B the number-density of spin-up sites is greater than a fixed critical density  $p_A^c$ .

This extended Fredrickson-Andersen model has two parameters; the integer  $n_R$  for nearest neighbors and long-ranged criterion  $p_A^c$ . Unlike the mean-field treatment of the Fredrickson-Andersen model, these parameters are independent and they are not related by Eq.(3.7).

At temperatures such that  $p_A > p_A^c$ , there is no restriction of the dynamics. When  $p_A < p_A^c$  some of the spins will be fixed in due to the short-range condition (property 2A). If  $n_R$  is chosen to be sufficiently large, the restricted dynamics at low temperatures will restrict the number of possible configurations and will alter the thermodynamics.

### 3.1.4 One-dimensional Study of the Modified Model

Simple results can be obtained on a one-dimensional lattice. If  $n_R < 2$  the thermodynamics are the same as for free spins, so I will consider only the case  $n_R = 2$ . For  $T < T_c$  and  $n_R = 2$ , the one-dimensional chain of spins is separated into “static” and “alterable” segments, as is illustrated in Fig. 3.1.

These segments are determined by the configuration of the system as it cools through the transition temperature. Spins in the static segments are permanently

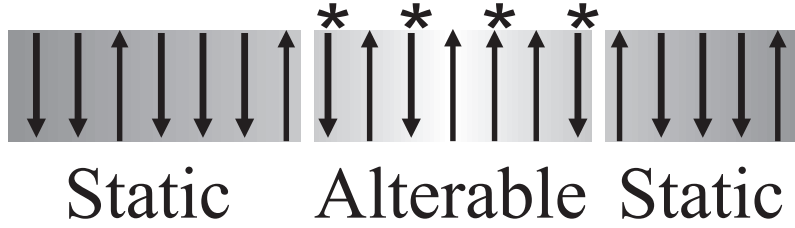


Figure 3.1: A spin chain with static and alterable parts. Flipable spins are highlighted with a (\*).

unflipable (as long as  $T < T_c$ ). The spins in the alterable segments may either flip or not flip. However, allowed spin flips can “free up” an unflipable spin, so no spin in an alterable segment is permanently unflipable. The flipable spins in the alterable segment are labeled with an asterisk in Fig. 3.1. Spin configurations in each alterable segment are restricted to a subset of all possible configurations. Within this subset, thermal equilibrium is obtained. Since static segments are permanent below  $T_c$ , temperature variations of the thermal properties are determined by the alterable segments.

An alterable segment is characterized by its length,  $n$ . Let  $n\pi_n$  be the probability that a random site will lie in an alterable segment of length  $n$ . For an one-spin alterable segment

$$\pi_1 = (p_A^c)^2 (p_B^c)^4. \quad (3.9)$$

In Eq.(3.9),  $(p_A^c)^2$  represents the probability that the single alterable spin is surrounded by two spin-up sites (as required by Property 2A when  $n_R = 2$ ). The  $(p_B^c)^4$  represents the probability that both of these neighboring spins are adjacent to a pair of down spins, which is required for them to be in static segments. Similarly, the probability of finding an alterable segment of length two is

$$\pi_2 = ((p_A^c)^2 + 2p_A^c p_B^c) \pi_1 \quad (3.10)$$

because the two mobile spins can only be in the configurations “up-up,” “up-down” or “down-up.”

To facilitate my calculation of the internal energy, I write

$$\pi_n = (p_A^c)^2 (p_B^c)^4 \psi_n(p_A^c, p_B^c) \quad (3.11)$$

and insist that  $\psi_n(p_A, p_B)$  be treated formally as a function of two independent variables,  $p_A$  and  $p_B$ , even though physically  $p_A + p_B = 1$ . For  $n = 1, 2$  I pick

$$\psi_1(p_A, p_B) = p_A + p_B \quad (3.12)$$

$$\psi_2(p_A, p_B) = p_A^2 + 2p_A p_B. \quad (3.13)$$

For longer segments, the  $\psi_n(p_A, p_B)$  are obtained from a recursion relation, which is a generalization of the recursion relation for the Fibonacci numbers;

$$\psi_{n+1}(p_A, p_B) = p_A \psi_n(p_A, p_B) + p_A p_B \psi_{n-1}(p_A, p_B). \quad (3.14)$$

This generates the  $\pi_n$  because for a portion of an alterable segment of length  $n$ , the  $(n+1)$  lattice site will also be in that alterable segment if it is spin up (probability  $p_A^c$ ). However, if the  $n+1$  site is spin-down (probability  $p_B^c$ ), it will be part of the alterable segment if a spin-up site and then a spin-down site is added to the segment of length  $n-1$ .

To obtain  $\psi_n(p_A, p_B)$  for any  $n$ , one can write the recursion relations in matrix form

$$\begin{pmatrix} \psi_{n+1} \\ \psi_n \end{pmatrix} = \begin{pmatrix} p_A & p_A p_B \\ 1 & 0 \end{pmatrix} \begin{pmatrix} \psi_n \\ \psi_{n-1} \end{pmatrix}. \quad (3.15)$$

Eigenvalues of the matrix are

$$\gamma_{\pm} = \frac{p_A}{2} \pm \sqrt{\left(\frac{p_A}{2}\right)^2 + p_A p_B}. \quad (3.16)$$

The  $\psi_n(p_A, p_B)$  must be a sum of powers of these eigenvalues

$$\psi_n(p_A, p_B) = a \gamma_+^{n-1} + b \gamma_-^{n-1}. \quad (3.17)$$

The coefficients  $a$  and  $b$  are obtained using Eqs.(3.12) and (3.13) yielding

$$\psi_n(p_A, p_B) = (p_A + p_B) \left( \frac{\gamma_+^{n-1} + \gamma_-^{n-1}}{2} \right) + \left( \frac{p_A^2 + 3p_A p_B}{2} \right) \left( \frac{\gamma_+^{n-1} - \gamma_-^{n-1}}{\gamma_+ - \gamma_-} \right). \quad (3.18)$$

The functions  $\psi_n(p_A, p_B)$  is more useful than the  $\pi_n$  because all the statistics of the alterable segments can be expressed in its terms. Each term in the polynomials corresponds to a different spin configuration, e.g.

$$\psi_2(p_A, p_B) = p_A^2 + 2p_A p_B$$

means the alterable segment of length 2 has one configuration with two spins up (the  $p_A^2$  term) and two configurations with one spin up and one spin down (the  $2p_A p_B$  term).

The knowledge of the  $\psi_n(p_A, p_B)$  allows me to calculate the thermodynamic properties. The probability that a site is in an alterable segment is

$$P_{alt} = \sum_{n=1}^{\infty} n \pi_n = (p_A^c)^2 (p_B^c)^4 \sum_{n=1}^{\infty} n \psi_n(p_A^c, p_B^c) \quad (3.19)$$

using Eq.(3.11). The form for the  $\psi_n(p_A, p_B)$  given in Eq.(3.18) means  $P_{alt}$  can be obtained by summing geometric series and simplifying using  $p_A^c + p_B^c = 1$ . The result,

$$P_{alt} = (p_A^c)^2 (1 + 3p_A^c - 4(p_A^c)^2 + (p_A^c)^3) \quad (3.20)$$

is shown as a function of  $p_c$  as one of the curves in Fig. 3.3.

One obtains next the internal energy (per site) and the specific heat. These quantities give physical insight into the properties of this model and its possible relevance to real materials. At temperatures equal to and above the transition temperature, the internal energy and heat capacity describe free spins. Below the transition temperature, only the alterable segments contribute to changes in the internal energy and the specific heat. Thus, one needs only consider the temperature dependence of the alterable segment contribution to the internal energy, which is

$$U(T)_{alt} = \sum_{n=1}^{\infty} \pi_n u_n(T). \quad (3.21)$$

The internal energy of an alterable segment of length  $n$  is

$$u_n(T) = h \frac{1}{\psi_n(p_A, p_B)} \left( p_A \frac{\partial}{\partial p_A} - p_B \frac{\partial}{\partial p_B} \right) \psi_n(p_A, p_B) \quad (3.22)$$

because the differentiations “count” the number of spin-up and spin-down sites.

For example, using Eq.(3.22) and  $p_A + p_B = 1$  gives  $u_1(T) = h(p_A - p_B)$  and

$$u_2(T) = \frac{h(2(p_A)^2)}{((p_A)^2 + 2p_A p_B)} \quad (3.23)$$

as one expects.

The sums needed to obtain  $U(T)_{alt}$  must be done numerically. They converge quickly, and Fig. 3.2 shows the temperature dependence of the internal energy for  $p_A^c = 0$  (free spins) and for  $p_A^c = 0.2, 0.3, 0.4$ . The corresponding specific heats  $C(T) = dU(T)/dT$  are shown in the inset. As one can see in Fig. 3.2, the suppression of spin flips dramatically reduces the specific heat below the transition.

Associated with the lower specific heat is an excess internal energy at  $T = 0$ , represented by the difference between the internal energy of the model and the internal energy of the free spins. Because the change in the free-spin internal energy from the transition temperature to zero temperature is  $-2hp_A^c$ ,

$$U_{excess} = 2hp_A^c - (U(T_c)_{alt} - U(0)_{alt}). \quad (3.24)$$

The excess internal energy can be evaluated exactly. Using Eq.(3.21),

$$U(T_c)_{alt} = -hp_A^c (1 - 5p_A^c + 4(p_A^c)^2 + (p_A^c)^3). \quad (3.25)$$

For  $T = 0$ , the configuration restrictions for alterable segments mean,  $u_n(0) = -h$  for odd  $n$  and  $u_n(0) = 0$  for even  $n$ . Thus,

$$U(0)_{alt} = -h \sum_{n=0}^{\infty} \pi_{2n+1}. \quad (3.26)$$



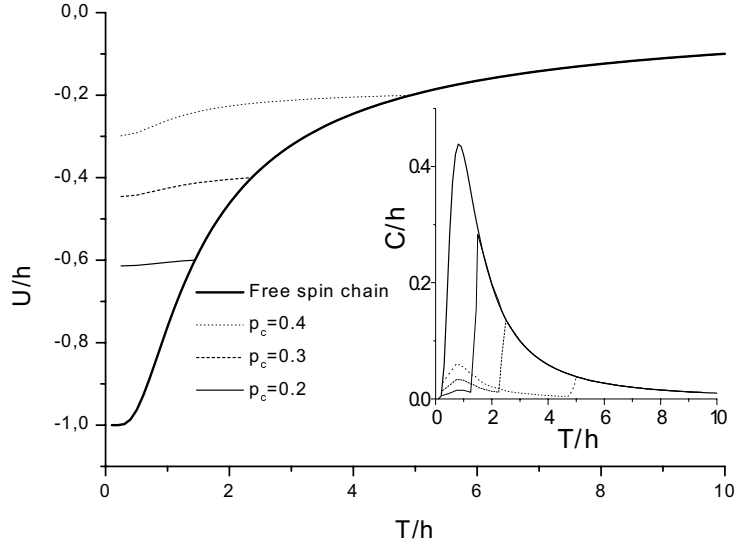


Figure 3.2: The internal energy  $U$  and the heat capacity  $C$  for a free spin chain and for  $p_A^c = 0.2, 0.3, 0.4$ .

Simplifying gives

$$U(0)_{alt} = -h \frac{(p_A^c p_B^c)^2}{1 + (p_A^c)^2} (1 - p_A^c (p_B^c)^2). \quad (3.27)$$

The  $p_A^c$  dependence of  $U_{excess}$  obtained using the above four equations is shown in Fig. 3.3.

There is also a residual zero-temperature entropy,  $S(0)$ , which is associated with the disorder fixed by cooling in the system. It can be evaluated starting from the equation

$$S(T) = S(T_c) - (S(T_c)_{alt} - S(T)_{alt}). \quad (3.28)$$

To find  $S(0)$ , two of the terms in Eq.(3.28) can be found exactly

$$S(T_c) = -(p_A^c \ln p_A^c + p_B^c \ln p_B^c) \quad (3.29)$$

and because segments with an even number of sites have a doubly degenerate ground state,

$$S(0)_{alt} = \ln(2) \sum_{n=1}^{\infty} \pi_{2n} = \ln(2) \frac{(p_A)^3 (p_B)^2 (2 - 2p_A + 2(p_A)^2 - (p_A)^3)}{(1 + (p_A)^2)}. \quad (3.30)$$

The alterable-segment contribution to the entropy at  $T_c$  can be obtained numerically in a variety of ways. Here I used

$$S(T)_{alt} = -\frac{dF}{dT} \quad (3.31)$$

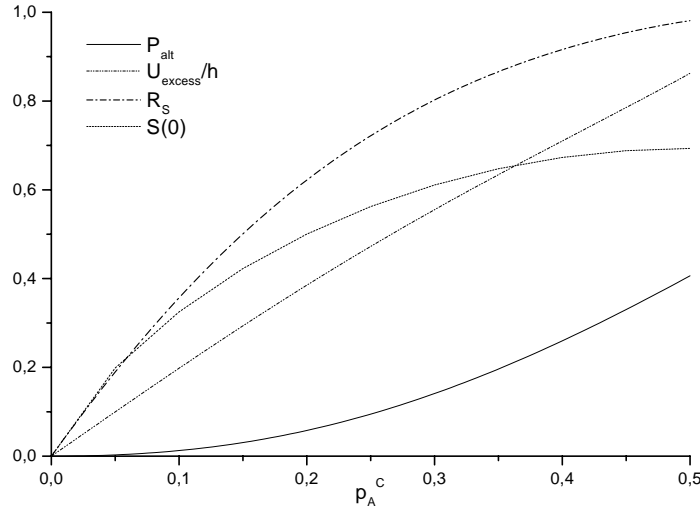


Figure 3.3: The probability for a spin to be within an alterable section  $P_{alt}$ , the excess internal energy  $U_{excess}/h$ , the scattering ratio  $R_S$  and the residual entropy  $S(0)$  as functions of  $p_A^c$ .

where the free energy function for the alterable segments is

$$F = -T \sum_{n=1}^{\infty} \pi_n \ln Z_n \quad (3.32)$$

and the partition function for each chain segment is

$$(e^{\beta h} + e^{-\beta h})^n \psi_n(p_A, p_B). \quad (3.33)$$

The residual entropy obtained from these expressions is shown as a function of  $p_A^c$  in Fig. 3.3. The entropy expression in Eq.(3.28) implies a continuous entropy function even at the transition temperature  $T_c$ . This means we have assumed there is no “collapse” of the system at the transition temperature. Such a collapse would occur if the positions of the static and alterable segments were specified. The entropy is continuous because all allowed partitions of the spin-chain into static and alterable segments is included in the counting of configurations. By assuming the system is the sum of all possible configurations, this model is translationally invariant even below  $T_c$ .

Despite the formal translational invariance, the modification of Fredrickson-Andersen model is disordered in the sense that it leads to diffuse elastic scattering. The diffuse scattering occurs because the model has a complicated thermal-averaged spin-spin correlation function  $\langle \sigma_i \sigma_j \rangle$ . The total scattering probability is the sum of

a forward (or Bragg) scattering part and a diffuse scattering part. The total scattering probability is proportional to  $\overline{\langle \sigma^2 \rangle}$ , where the "–" indicates an average over all lattice sites. Assuming the scattering amplitude from a site is proportional to  $\sigma$ , the forward scattering probability is proportional to  $\langle \bar{\sigma} \rangle^2$ . Letting  $R_S$  denotes the ratio of the diffuse scattering to the total scattering, and noting that  $\sigma^2 = 1$ ,

$$R_S = 1 - \frac{\langle \bar{\sigma} \rangle^2}{\langle \sigma^2 \rangle} = 1 - \left( \frac{U(T)}{h} \right)^2. \quad (3.34)$$

At high temperatures, the diffuse scattering fraction,  $R_S$ , is caused by thermal fluctuations. If all the spins could align at low temperatures,  $-U/h$  would be unity and the diffuse scattering fraction would vanish. Since the lowest value of the internal energy is  $-h + U_{excess}$  the diffuse scattering does not vanish even when  $T \rightarrow 0$ . This zero-temperature diffuse scattering is not associated with thermal fluctuations. Instead, it is caused by the disorder-like correlations which are introduced by cooling into the lattice. The diffuse scattering fraction is shown as a function  $p_A^c$  in Fig. 3.3.

### 3.1.5 Generalization from the Modified Model

Many of these results obtained in this modified one-dimensional case apply more generally. In particular, the modified Fredrickson-Anderson model yields a similar phase transition with  $T_c$  given by Eq.(3.8) on a square lattice (with  $n_R$  is 3 or 4) or a cubic lattice (with  $n_R = 4, 5, \text{ or } 6$ ). For  $T < T_c$  on the square or cubic lattices, there is a reduced specific heat leading to an excess internal energy at  $T = 0$  (compared to free spins). Associated with the reduced specific heat is a residual entropy at  $T = 0$  given by Eq.(3.28). There is also a diffuse scattering fraction given by Eq.(3.34).

The phase transitions and the simplifications described here are all associated with mean-field theory which limits the application to more complex systems. Partially, to overcome these restrictions and to study the behavior on time scales, I will go on with the dynamics of the Extended Fredrickson-Andersen model (EFAM).

### 3.1.6 Lattice Formulation of the Extended Model

The extension should also include the  $\beta_{JG}$ -process. Thus, it still remains the question of its meaning and its incorporation into the nSFM. There are sufficient strong indications that the  $\beta_{JG}$ -process can be observed in low molecular weight supercooled liquids [93] as well as in more complex structured systems. Experimental studies due to Kivelson [94, 95] suggest the existence of small regions with quasi-ordered short range structures with a diameter of some few nanometers above the melting temperature  $T_m$  and probably also below  $T_c$ . However, these objects are not appropriate to construct a macroscopic crystal in an Euclidean space. Since these frustration-limited domains form a macroscopic body they require structural singularities related to different local mobilities possible causing the  $\beta_{JG}$ -process. The

number of those local singularities is approximately constant due to the conservation of the geometrical frustrations. The molecules in the neighborhood of a singularity should have a higher mobility (agrees e.g. with an increasing mobility in the nearest environment of dislocations in crystalline solids). Furthermore, a diffusive motion of these singularities should be expected.

To incorporate these additional experimental features I want to analyze now the extended nSFM model (or extended Fredrickson-Andersen model) which was already suggested and numerically studied by Schulz [81, 82]. This model extends the ordinary nSFM in two ways. Firstly, we consider in the frame of a three-state model the influence of the above mentioned singularity components. These singularities correspond to empty states (vacancies) with  $\sigma_j = 0$ . Cells with mobile or immobile states ( $\sigma_j = \pm 1$ ) are denoted like yet introduced. The mobility is enhanced in the local environment of vacancies. Now we allow two elementary steps modeling the dynamics of the extended nSFM:

I The flip process of the usual Fredrickson-Andersen model (3.3) is realized with a transition probability  $\lambda_{BA}(T)$  for  $-1 \rightarrow +1$  and  $\lambda_{AB}(T)$  for  $+1 \rightarrow -1$  ( $2h$  is still the energy difference between the solid and liquid-like state). Whereas the first topological restriction for the flip,

1. at least  $n_R$  nearest neighbors at site  $i$  have  $\sigma_i = 1$ ,

$$\frac{1}{2} \sum_{j(i)} \sigma_j (1 + \sigma_j) \geq n_R \quad (3.35)$$

( $j(i)$  means all nearest neighbors) remains the same, the flip is additionally possible if

2. at least one nearest neighboring lattice site of  $i$  is a vacancy,

$$\prod_{j(i)} \sigma_j = 0 . \quad (3.36)$$

Concluding these two restrictions gives a transition rate for a flip  $\sigma_i \rightarrow -\sigma_i$

$$r_i(T) = Y_i [\lambda_{BA}(T) \delta_{\sigma_i, -1} + \lambda_{AB}(T) \delta_{\sigma_i, +1}] \quad (3.37)$$

( $Y_i$  is non-zero, if one or both of the two conditions (3.35) and (3.36) are fulfilled, zero otherwise).

II The diffusion process between the mobile state and the vacancy is given by

$$(\sigma_i = 1 \text{ and } \sigma_j = 0) \rightleftharpoons (\sigma_i = 0 \text{ and } \sigma_j = 1) \quad (3.38)$$

(if  $i, j$  nearest neighboring lattice sites). This exchange process of vacancies is determined by the transition rate  $\tilde{D}_0(T)$  and only high mobile, liquid-like (spin up) states interchange with the vacancy.

### 3.1.7 Second Quantized Master Equation

Taking these elementary steps one can start creating the one-step master equation. Because we consider a three-state model we apply the Para-Fermi statistics (see above in the section about it). Further, we additionally pay attention to dynamical restrictions due to the occupation of cells adjacent to the cell where the flip takes place. In case of  $s = 2$  the eigenvalues of the number operator  $z_n! = 2!$  for  $n = 1, 2$  (compare Eqs.(2.43) and (2.44)) are the same so I may rescale the operators

$$\hat{a}_{new} = \frac{\hat{a}}{\sqrt{2}} \text{ and } \hat{a}_{new}^\dagger = \frac{\hat{a}^\dagger}{\sqrt{2}}. \quad (3.39)$$

Hence, the eigenvalues  $z_{n,new} = 1$  for  $n = 1, 2$  in the picture of the new operators. For the further calculation within this section, I will only apply the new operators and neglect the subscript *new* again. To simplify the rules let us introduce the particle number operators for the mobile ( $\hat{A} = \hat{2}$ ), immobile ( $\hat{B} = \hat{0}$ ) and empty states ( $\hat{\Theta} = \hat{1}$ ),

$$\hat{A}_i = \hat{i}_i - \hat{a}_i \hat{a}_i^\dagger \quad \hat{B}_i = \hat{a}_i \hat{a}_i \hat{a}_i^\dagger \hat{a}_i^\dagger = \hat{i}_i - \hat{a}_i^\dagger \hat{a}_i \quad \hat{\Theta}_i = \hat{i}_i - \hat{A}_i - \hat{B}_i \quad (3.40)$$

with the typical projector properties if one uses the number-projectors

$$\hat{O}_i | n_i \rangle = \delta_{o,n_i} | n_i \rangle. \quad (3.41)$$

The letters denoting projectors should be preferred only for review purpose. Now I want to reformulate the restrictions (3.35) and (3.36) in terms of the letter operators. As discussed above a flip process  $A_i \leftrightarrow B_i$  at a lattice cell  $i$  is only allowed if

$$\sum_{j(i)} \langle n_j | \hat{A}_j | n_j \rangle \geq n_R \text{ or } \sum_{j(i)} \langle n_j | \hat{\Theta}_j | n_j \rangle > 0 \quad (3.42)$$

where  $j(i)$  means a summation over all adjacent cells of  $i$ ,  $n_R$  is again the restriction number of the  $n$ -facilitated kinetic Ising model. In our concrete example I will choose  $n_R$  as  $n_C/2$  later where  $n_C$  is the coordination number of underlying lattice. The first relation of Eq.(3.42) guarantees the cooperative dynamics of the modified nSFM studied in a large variety of numerical simulations [81–83]. The extension represents an allowance for a local flip process if at least one cell in the nearest neighborhood is empty. (This does not reflect the real atomic motion.) Further, one may include the diffusive motion between an empty and a liquid cell leading to more mobility in the system and therefore to shorter relaxation times. Finally, because I want to exploit the influence of the temperature on them I introduce temperature dependent operators  $\| \hat{O} \|$  abbreviating  $\exp[-\frac{\beta \hat{H}}{2}] \hat{O} \exp[\frac{\beta \hat{H}}{2}]$  with the Hamiltonian  $\hat{H}$  (which is not identical with the "quantum Hamiltonian"  $\hat{L}$ !). By means of results derived in the last chapter (Eqs.(2.107) and (2.118) for the flip (3.3)

as well as Eqs.(2.129) and (2.131) for the exchange (3.38)) the evolution operator takes the component form (compare also [20, 22])

$$\begin{aligned}
\hat{L} &= \hat{L}_U + \hat{L}_E \tag{3.43} \\
\hat{L}_U &= + \sum_i \tilde{\lambda}_{BA}(\hat{i} - \hat{a}_i \hat{a}_i) \|\hat{a}_i^\dagger \hat{a}_i^\dagger\| \left( \sum_{\langle m_1 \dots m_n \rangle} \hat{A}_{m_1} \dots \hat{A}_{m_n} + \sum_m \hat{\Theta}_m \right) \\
&\quad + \sum_i \tilde{\lambda}_{AB}(\hat{i} - \hat{a}_i^\dagger \hat{a}_i^\dagger) \|\hat{a}_i \hat{a}_i\| \left( \sum_{\langle m_1 \dots m_n \rangle} \hat{A}_{m_1} \dots \hat{A}_{m_n} + \sum_m \hat{\Theta}_m \right) \\
\hat{L}_E &= \sum_{\langle rs \rangle} \tilde{D}_0(\hat{a}_r^\dagger \hat{a}_s - \hat{i}) \hat{a}_r^\dagger \hat{a}_r \hat{a}_r \hat{a}_s^\dagger \hat{a}_s^\dagger \hat{a}_s \|\hat{a}_r^\dagger \hat{a}_s\| + \text{symmetric term}
\end{aligned}$$

where  $\tilde{\lambda}_{AB}$ ,  $\tilde{\lambda}_{BA}$  and  $\tilde{D}_0$  are the kinetic rates (which include some rescaling factors of the operators as well),  $r$  (the eigenvalue of the reference state) is set to 1 and  $\beta$  is the inverse temperature of a heat bath.

The first term of  $\hat{L}_U$  corresponds to a flip process  $B \rightarrow A$  and the second corresponds to a flip process  $A \rightarrow B$ .  $\hat{L}_E$  describes the exchange process  $A_i + \Theta_j \rightarrow \Theta_i + A_j$ . Further, each operator  $\|\hat{O}\|$  determines the correct thermodynamic weight for the realization of an elementary process in agreement with the principle of the detailed balance. Each  $\|\hat{O}\|$  generates a Boltzmann factor which represents the energy difference in the system before and after the elementary step. Thus, the dynamics will prefer a flip or exchange process minimizing the energy. In the present case  $\hat{H}$  corresponds to the Hamiltonian of the underlying modified nSFM (Spin-1 or Blume–Emery–Griffiths (BEG) model [96] neglecting any higher interactions)

$$\hat{H} = h \sum_i (\hat{A}_i - \hat{B}_i) + \Delta \sum_i (\hat{A}_i + \hat{B}_i). \tag{3.44}$$

The energy difference between the mobile (liquid-like) and the immobile (solid-like) state is denoted by  $2h$  and energy of a vacancy is given by  $-\Delta$ ; i.e. one obtains simply  $\hat{H} | A_i \rangle = (h + \Delta) | A_i \rangle$ ,  $\hat{H} | B_i \rangle = (-h + \Delta) | B_i \rangle$  and  $\hat{H} | \Theta_i \rangle = 0$ . Because the considered system has three different states, which correspond to the three possible settings of the spin in the Spin-1 model, this Hamiltonian leads to the correct equilibrium solution of the nSFM. By means of (3.44) one straightforwardly calculates the expressions  $\|\hat{O}\|$  yielding an exponential term. This is combined with the kinetic coefficients to give modified pre-factors denoted by  $\lambda_{AB}$ ,  $\lambda_{BA}$  and  $\tilde{D}_0$ . Applying the algebraic relations introduced before one obtains

$$\begin{aligned}
\|\hat{a}_r^\dagger \hat{a}_s\| &= \hat{a}_r^\dagger \hat{a}_s [(\hat{A}_s + \hat{B}_r) + (1 - \hat{A}_s + \hat{B}_r) \exp(-\beta\Delta)] \tag{3.45} \\
&= \hat{a}_r^\dagger \hat{a}_s \exp(-\beta\Delta(1 - \hat{A}_s + \hat{B}_r))
\end{aligned}$$

$$\begin{aligned}
\|\hat{a}_i^\dagger \hat{a}_i^\dagger\| &= \hat{a}_i^\dagger \hat{a}_i^\dagger [\hat{B}_i + (1 - \hat{B}_i) \exp(-\beta\Delta)] \exp[-\beta h] \tag{3.46} \\
&= \hat{a}_i^\dagger \hat{a}_i^\dagger \exp(-\beta\Delta(1 - \hat{B}_i) - \beta h) \text{ and}
\end{aligned}$$

$$\begin{aligned}
\|\hat{a}_i \hat{a}_i\| &= \hat{a}_i \hat{a}_i [\hat{A}_i + (1 - \hat{A}_i) \exp(-\beta\Delta)] \exp[\beta h] \tag{3.47} \\
&= \hat{a}_i \hat{a}_i \exp(-\beta\Delta(1 - \hat{A}_i) + \beta h).
\end{aligned}$$

Thus, we find the modified kinetic pre-factors to be

$$\bar{D}_0 = \tilde{D}_0, \lambda_{AB} = \tilde{\lambda}_{AB} \exp[\beta h] \text{ and } \lambda_{BA} = \tilde{\lambda}_{BA} \exp[-\beta h]. \quad (3.48)$$

The bracket term of Eq.(3.43)

$$\sum_{\langle m_1 \dots m_n \rangle_i} \hat{A}_{m_1} \dots \hat{A}_{m_n} + \sum_{m(i)} \hat{\Theta}_m \quad (3.49)$$

represents the kinetic restriction of the nearest neighborhood where

$$\langle m_1 \dots m_n \rangle_i$$

stands for all sets of  $n$  lattice cells adjacent to  $i$ . The operator  $\hat{A}_m$  yields a non-zero result only if  $m$  is a liquid cell as well as the action of  $\hat{\Theta}_m$  is non-zero only if the state at  $m$  is an empty one. Hence, (3.49) attains a non-zero value if it is applied to a cell  $i$  surrounded by at least  $n_R$  liquid cells or been adjacent to a vacancy.

Using Eq.(2.68) the time derivations of the two relevant observables  $\langle \hat{A}_k \rangle$  and  $\langle \hat{B}_k \rangle$  result in (notice, that  $\langle \hat{\Theta}_k \rangle = 1 - \langle \hat{A}_k \rangle - \langle \hat{B}_k \rangle$ )

$$\begin{aligned} \partial_t \langle \hat{B}_k \rangle &= -\lambda_{BA} \sum_{\langle m_1 \dots m_n \rangle} \langle \hat{B}_k \hat{A}_{m_1} \dots \hat{A}_{m_n} \rangle - \lambda_{BA} \sum_m \langle \hat{B}_k \hat{\Theta}_m \rangle \\ &\quad + \lambda_{AB} \sum_{\langle m_1 \dots m_n \rangle} \langle \hat{A}_k \hat{A}_{m_1} \dots \hat{A}_{m_n} \rangle + \lambda_{AB} \sum_m \langle \hat{A}_k \hat{\Theta}_m \rangle \\ \partial_t \langle \hat{A}_k \rangle &= -\partial_t \langle \hat{B}_k \rangle + 2D_0 [\langle \hat{\Theta}_k \Delta_k \hat{A}_k \rangle - \langle \hat{A}_k \Delta_k \hat{\Theta}_k \rangle] \end{aligned} \quad (3.50)$$

where

$$\begin{aligned} \Delta_k \hat{O}_k &= \frac{1}{l^2} \sum_{r(k)} (\hat{O}_r - \hat{O}_k) \\ D_0 &= \bar{D}_0 l^2. \end{aligned} \quad (3.51)$$

$l$  is the length of a lattice cell. For all further calculations I shall concentrate on a hypercubic lattice with  $n_R = d = n_C/2$  where  $d$  is the spatial dimension.

### 3.1.8 Mean-Field Approximation

Solving the coupled Eqs.(3.50) we apply the mean-field approach where all correlation functions between different cells are decoupled according to  $\langle \hat{O}_i \hat{O}_j \rangle \Rightarrow \langle \hat{O}_i \rangle \langle \hat{O}_j \rangle$ . Furthermore, we assume that the averages are independent of position, i.e.  $\langle \hat{O}_i \rangle \Rightarrow \langle \hat{O} \rangle$ . However, I will discuss the influence of spatial correlations later.

Performing this mean-field approximation I get the equilibrium solution (symbolized by the bar)

$$\partial_t \langle \hat{B} \rangle = \partial_t \langle \hat{A} \rangle = 0 \implies \lambda_{AB} \bar{A} = \lambda_{BA} \bar{B} \quad (3.52)$$

according with the kinetic Ising model and hence with (3.2), the restrictions only influence the dynamics and not the steady state ( $\bar{A}$  is nothing else but  $p_A$  if  $\bar{\Theta} = 0$  and  $\tilde{\lambda}_{AB}/\tilde{\lambda}_{BA} = 1$ ). Using  $\bar{B} = 1 - \bar{A} - \bar{\Theta}$  and taking into account (3.48) one obtains

$$\bar{A} = (1 - \bar{\Theta}) \frac{\lambda_{BA}}{\lambda_{AB} + \lambda_{BA}} = (1 - \bar{\Theta}) \frac{1}{\frac{\lambda_{AB}}{\lambda_{BA}} \exp(2\beta h) + 1}. \quad (3.53)$$

Testing the stability of the solution one may linearize the equations setting  $\langle \hat{A} \rangle = \bar{A} + \delta A(t)$  and  $\langle \hat{B} \rangle = \bar{B} + \delta B(t)$  leading to

$$\partial_t \begin{pmatrix} \delta A \\ \delta B \end{pmatrix} = \tilde{M}_{2 \times 2}(\bar{A}, \bar{B}, \bar{\Theta}) \begin{pmatrix} \delta A \\ \delta B \end{pmatrix}. \quad (3.54)$$

The eigenvalues of  $\tilde{M}_{2 \times 2}(\bar{A}, \bar{B}, \bar{\Theta})$  are identified (up to the sign) as inverse relaxation times

$$\tau_{1/2}^{-1} = R \pm \sqrt{R^2 - 2D_0 q^2 \lambda_{BA} (\zeta \bar{A}^d + n_C \bar{\Theta})} \quad (3.55)$$

with

$$R = \frac{1}{2} (\lambda_{BA} + \lambda_{AB}) (\zeta \bar{A}^d + n_C \bar{\Theta}) + 2D_0 (1 - \bar{B}) q^2,$$

$\zeta = 2d \cdot \dots \cdot (d+1)$  and  $q$  the wave number resulting from the Fourier transformation of the Laplacian and originated by the diffusive motion of the vacancies. Examining the relaxation times in case of vanishing diffusion ( $D_0 = 0$ ) one gets  $\tau_1^{-1} = 0$  and a remaining non-zero inverse relaxation time

$$\tau_2^{-1} = (\lambda_{BA} + \lambda_{AB}) (\zeta \bar{A}^d + n_C \bar{\Theta}). \quad (3.56)$$

This stationary solution is stable against small fluctuation. Analyzing the influence of the temperature  $\beta^{-1}$  under consideration of (3.53) the density of  $A$  states increases with decreasing  $\beta$  (or increasing temperature) and reaches a maximum for  $T \rightarrow \infty$ . Therefore, the system shows only a small cooperativity and the relaxation time  $\tau_2$  decreases exponentially  $\ln(\tau_2) \sim d\beta h$ . The evolution is independent of the dynamics of the empty states because small fluctuations relax quickly enough in due to mobile-states cells surrounding every lattice cell. This behavior completely differs from the low temperature regime as a result of less mobile neighbors in order to perform a flip. Neglecting empty states one gets a cross-over of  $\tau_2$  to a stronger slope in the Arrhenius plot. Because of the increasing cooperatively rearrangements with decreasing temperatures the corresponding relaxation time  $\tau_2$  should be identified with the usual  $\alpha$ -relaxation. Asymptotically one obtains  $\ln(\tau_2) \sim (2d - 1)\beta h$  (see Fig. 3.4,  $\tilde{\lambda}_{AB}/\tilde{\lambda}_{BA}$  is set to unity,  $\tau$  is measured in units of  $\tilde{\lambda}_{BA}^{-1}$  and the temperature is measured in units of  $hk^{-1}$  in all figures). The  $\alpha$ -process shows an increasing slope with decreasing temperature in agreement with numerical simulations [81, 84]. The asymptotic behavior indicates that the computation fails at sufficiently low temperature which is an inherent effect of each type of mean-field theory implying



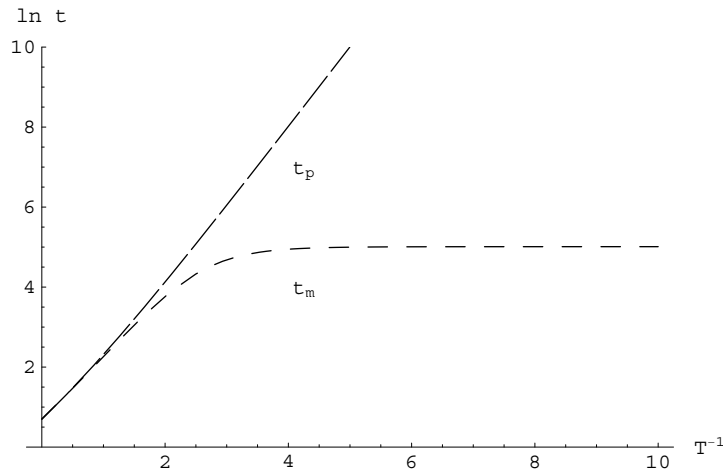


Figure 3.4: Relaxation times  $t_2$  without vacancies ( $t_p$ -long dash line) and with 2% vacancies ( $t_m$ -short dash line) in MFA ( $d=2$ , no diffusion,  $t$  reduced relaxation time with  $\ln(t) = \ln(\tau) - \beta h$ )

a particular pre-average of the configuration and hence leading to an effective one-particle theory.

If one takes into account the influence of the empty state  $\Theta$ , the cells have the facility to flip independently of the behavior of the solid-like phase. Thus, a small concentration (typically 0...5 %) of these empty cells determines the low temperature dynamics. There are only a few mobile cells at low temperature while the number of the empty cells is nearly constant over the whole temperature range. The influence of the  $\Theta$ -states is like the action of the restriction in the  $(n = 1)$ -facilitated nSFM. The crossover from the usual nSFM without any vacancies to the regime exclusively controlled by the vacancies occurs at

$$(\beta^* h^*) = \frac{1}{2} \ln \left[ (1 - \bar{\Theta}) \left( \frac{\zeta}{n_C \bar{\Theta}} \right)^{\frac{1}{d}} - 1 \right] \quad (3.57)$$

basing on the assumption that the influence of the two dynamics on the relaxation time  $\tau$  (3.56) are comparable when  $\zeta \bar{A}^d = n_C \bar{\Theta}$  and then applied Eq.(3.53) on it ( $\tilde{\lambda}_{AB}/\tilde{\lambda}_{BA}$  is set to unity).

Thus, the MFA relaxation time shows a low temperature dependence similar to the usual paramagnetic gas without any topological restrictions and a flip rate determined by the concentration of vacancies (see Fig. 3.4). The comparison between numerical simulations and the present MFA shows again a failure of mean-field theory at sufficiently low temperature. Only a small fraction of the cells takes part in a relatively fast motion in the neighborhood of the vacancies in numerical simulations. One obtains two well-separated relaxation times at low temperature. In

contrast, the simple mean field theory gives a weighted sum of the inverse of both times leading to an apparent smearing of the vacancies over all cells.

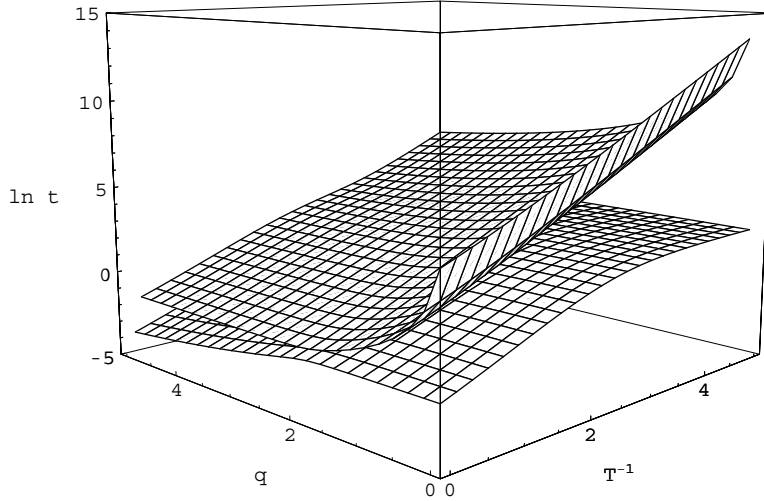


Figure 3.5: Relaxation times  $t_1$  (higher face) and  $t_2$  (lower face) in MFA with 2% vacancies ( $d=2$ ,  $t$  reduced relaxation time)

The diffusion also influences the relaxation time. Hence, one obtains wave vector dependent relaxation times  $\tau(q)$ . Inspecting Fig. 3.5 ( $q$  is measured in units of  $l^{-1}$  and  $D_0$  is set to  $\lambda_{BA}l^{-2}$ ), one observes the expected singularity of the relaxation time  $\tau_1$  in the hydrodynamic limit  $q \rightarrow 0$  in due to the vacancy diffusion. For increasing  $q$  the relaxation time decreases monotonically, because the disruption of the structure on a small length scale is faster. The decay of the fluctuations of the  $A$ - $B$  distributions is also controlled by the flip processes smoothing inhomogeneities on large length scales. Only the decay of the spatial vacancy fluctuations is exclusively determined by  $\tau_1$ .

To overcome the validity of the simple mean-field only at sufficiently high temperature I will stretch the method to lower temperatures. Let me consider in addition to the densities  $\hat{A}$  and  $\hat{B}$ , the nearest neighbor correlation functions

$$\hat{\Psi} = \hat{A}_k \hat{A}_l, \quad \hat{\Phi} = \hat{A}_k \hat{B}_l, \quad \hat{\chi} = \hat{B}_k \hat{B}_l \quad (3.58)$$

where cell  $k$  and  $l$  are adjacent. As a generalization of the above, we study the coupled system for these five quantities

$$\partial_t \langle \hat{A} \rangle = \langle f_A(\hat{A}, \hat{B}, \hat{\Psi}, \hat{\Phi}, \hat{\chi}) \rangle \dots \partial_t \langle \hat{\chi} \rangle = \langle f_\chi(\hat{A}, \hat{B}, \hat{\Psi}, \hat{\Phi}, \hat{\chi}) \rangle \quad (3.59)$$

using the algebraic properties of the operators and the mean-field decoupling of the resulting equations to derive this closed set of equations. Firstly, we discuss the

stationary solution to determine the equilibrium behavior

$$\partial_t \langle \hat{A} \rangle = \partial_t \langle \hat{B} \rangle = \partial_t \langle \hat{\Psi} \rangle = \partial_t \langle \hat{\Phi} \rangle = \partial_t \langle \hat{\chi} \rangle = 0. \quad (3.60)$$

The averages of the static nearest-neighbor correlation functions  $\bar{\Psi} = \bar{A}\bar{A}$ ,  $\bar{\Phi} = \bar{A}\bar{B}$ ,  $\bar{\chi} = \bar{B}\bar{B}$  decouple due to the lacking of static interaction between neighboring cells in the Hamiltonian. Thus, this approximation does not change the equilibrium values for  $\bar{A}$  and  $\bar{B}$ .

Now we investigate again the stability of the static solution by linearizing around the steady state:  $\langle \hat{A}(t) \rangle = \bar{A} + \delta A(t) \dots \langle \hat{\chi}(t) \rangle = \bar{\chi} + \delta \chi(t)$  yielding a system of equations

$$\partial_t \begin{pmatrix} \delta A \\ \delta B \\ \delta \Psi \\ \delta \Phi \\ \delta \chi \end{pmatrix} = \tilde{M}_{5 \times 5}(\bar{A}, \bar{B}, \bar{\Theta}) \begin{pmatrix} \delta A \\ \delta B \\ \delta \Psi \\ \delta \Phi \\ \delta \chi \end{pmatrix}. \quad (3.61)$$

Examining the eigenvalues of  $\tilde{M}_{5 \times 5}$  leads to a spectrum of relaxation times of which smallest  $\tau_1^{-1} = 0$  manifests the conservation of the empty states. In the limit that one of the dynamical processes vanishes ( $D_0 \rightarrow 0$  or  $\lambda_{BA} = \lambda_{AB} \rightarrow 0$ ) a second relaxation time increases drastically,  $\tau_2^{-1} \rightarrow 0$ . All non-zero eigenvalues of the matrix  $\tilde{M}_{5 \times 5}$  are negative indicating stable behavior against small perturbations. The relaxation time obtained in the simple mean-field approximation is split into three branches  $\tau_3$ ,  $\tau_4$  and  $\tau_5$  with different slopes in the low temperature region. In order to separate the different behavior we consider the case of absence of vacancies. Fig. 3.6 shows

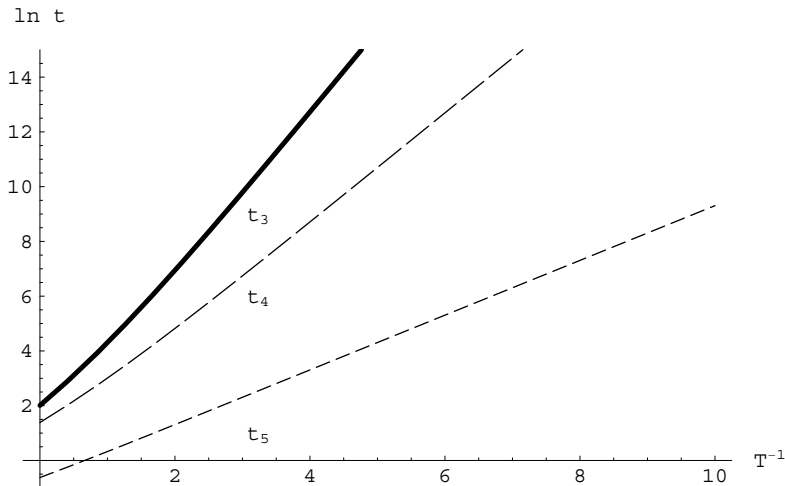


Figure 3.6: Relaxation times  $t_3$  (solid line),  $t_4$  (long dash line) and  $t_5$  (short dash line) in EMFA without vacancies ( $d=2$ , no diffusion,  $t$  reduced relaxation time)

a qualitative behavior similarly found in the simple mean-field approximation, but

the slopes of the branches are different now:  $\ln(\tau_3) \propto 2d\beta h$ ,  $\ln(\tau_4) \propto (2d-1)\beta h$  and  $\ln(\tau_5) \propto 2(d-1)\beta h$  for  $\beta \rightarrow \infty$ .

The low temperature asymptotic behavior indicates once more the restricted validity of mean-field-like approximation, but the valid temperature regime is extended to lower temperatures. The origin for the deviation from numerical simulations is again a smearing out of vacancies over the whole system. The improvement bases on the correct consideration of the nearest neighborhood in the calculation. Fig. 3.7

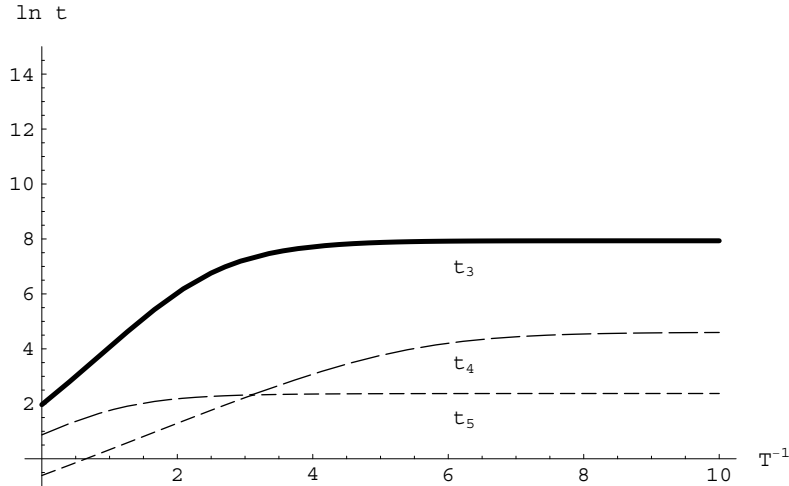


Figure 3.7: Relaxation times  $t_3$  (solid line),  $t_4$  (long dash line) and  $t_5$  (short dash line) in EMFA with 2% vacancies ( $d=2$ , no diffusion,  $t$  reduced relaxation time)

shows the relaxation times for a system with 2% vacancies which behaves at low temperature again like a usual paramagnetic gas without any topological restrictions (3.42). There is an apparently crossing between the two relaxation times  $\tau_4$  and  $\tau_5$  (see Fig. 3.8). From a knowledge of the relaxation times and the initial conditions, one can obtain the temporal decay of the correlation functions. Fig. 3.9 shows the time dependence of  $F(t) = \langle \hat{A}_k(t) \hat{A}_l(0) \rangle$ . These analytical results can be compared with numerical simulations [19] exhibiting a good qualitative agreement for  $d = 2$  (see Fig. 3.9).

### 3.1.9 Interpretation

From this computation one may conclude that the addition of strong localized processes to the slow cooperative dynamics leads to a new relaxation process. The model realization of this process causes a high mobility in the environment of vacancies which can be interpreted as regions with relatively large free volumes. Fig. 3.9 shows the characteristic decay of a correlation function. At high temperatures, only one effective common process occurs whereas below a characteristic temperature  $T_{char} (\approx \frac{1}{2}h)$  two processes exist, a fast  $\beta_{JG}$ -process and a slow  $\alpha$ -process.

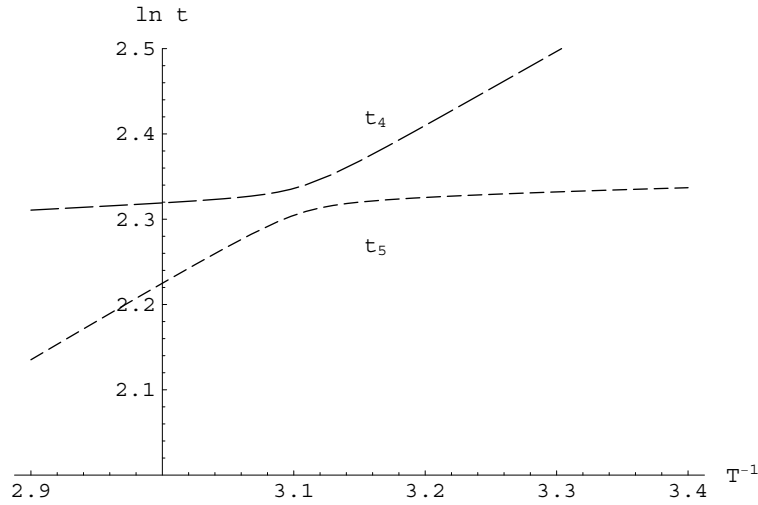


Figure 3.8: Relaxation times  $t_4$  (long dash line) and  $t_5$  (short dash line) in EMFA with 2% vacancies ( $d=2$ , no diffusion,  $t$  reduced relaxation time)

The origin of this behavior is the different thermodynamical weight of the two processes at various temperatures. At high temperatures the main contributions to a structural rearrangement comes from the flip dynamics of the bulk due to the negligible effect of the kinetic restrictions and of the influence of the empty states. Lowering the temperature, the cells solidify and the kinetic restrictions become increasingly important. Thus, the probability for an elementary flip process in the bulk decreases rapidly (almost all of the cells are neighbored by a sufficiently large number of solid cells) and only the cells surrounded by vacancies are not influenced by the kinetic restrictions. A structural rearrangement starts in the environment of the vacancies and proceeds slowly into the bulk. Furthermore, the diffusion of the vacancies contributes also to the decay of structural fluctuations, which can be qualitatively understood also in terms of the present model. This diffusion dominates the flip dynamics at sufficiently low temperatures and the  $\alpha$ -process shows again an Arrhenius-like behavior, but now with the activation energy of the diffusion process. An experimental indication of this behavior was recently realized [97]. The  $\beta_{JG}$ -process described here is not the remaining part of a dynamics which undergoes a ergodicity-non-ergodicity transition at a critical temperature  $T_c$  obtained from the mode coupling theory. The different elementary processes causing the  $\alpha$ - and the  $\beta_{JG}$ -process exist both above and below  $T_{char}$ . The relaxation time spectrum changes continuously in such a manner that a separation between both processes is only possible below  $T_{char}$ .

The strength of this approach is that algebraic properties of the operators allow to introduce restrictions of the dynamical processes explicitly. Despite the limitations of the mean-field approximation, one has obtained a qualitatively correct and

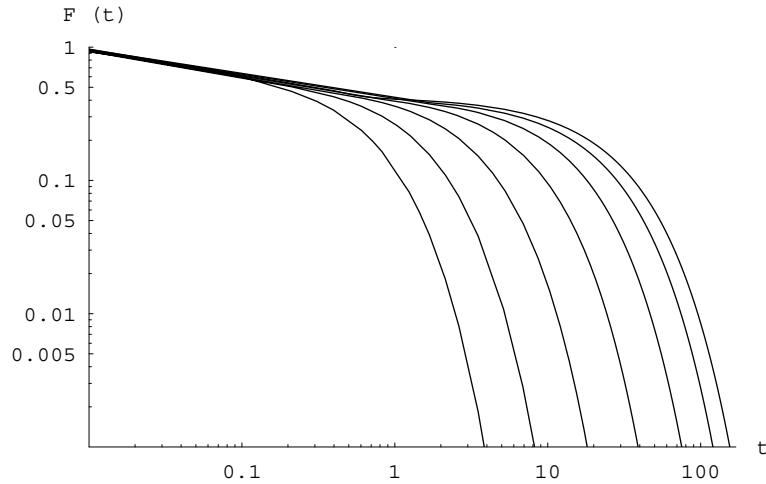


Figure 3.9: Correlation function  $F(t)$  in EMFA with 2% vacancies ( $\beta h = 0, 0.5, 0.75, 1, 1.25, 1.5$  ( $d=2$ ) from the left hand side to the right hand side)

convincing picture of the temperature dependence of the relaxation time spectrum for high and moderate temperatures. In particular, the evaluation of the derived equation of motion within this extended form of the mean-field approach is a sensible technique for this temperature range, but the mean-field approach fails at low temperatures. Local structures are smeared out. Hence, one obtains an effective one particle theory. The effects of the cooperativity are partly lost at low temperatures. However, the region of the apparent bifurcation between the  $\alpha$ -process and the  $\beta_{JG}$ -process around  $T_{char}$  seems to be qualitatively and quantitatively correct.

The mentioned apparent crossing between two relaxation times ( $\tau_4$  and  $\tau_5$ , see Fig. 3.8) indicates a typical behavior. A real crossing of the relaxation times in the Arrhenius-plot is not allowed if the dynamics of a system is based on two or more different coupled elementary processes. Relaxation times avoid each other because of the dynamical coupling between these processes, which is manifested as non-zero off-diagonal elements of the dynamical matrix (in the case of the above discussed linearized theory). The non-crossing of relaxation times seems to be an important general principle whose validity extends beyond mean-field theory. The near-crossing which occurs in a temperature region which is at the border of validity does not invalidate this conclusion. In particular, if the  $\alpha$ - and the  $\beta_{JG}$ -process are determined by different coupled elementary processes (e.g. the  $\alpha$ -process corresponds to a molecular motion whereas the  $\beta_{JG}$ -process is connected to changes of the local molecular configuration), a crossing of the associated relaxation times is avoided. Such an effect was observed qualitatively by various authors [98, 99].

## 3.2 Shocks in an Asymmetric Exclusion Model

In contrast to the previous section, this example demonstrates the application of the Fock-space formalism with ordinary Pauli operators and the connection to the  $q$ -deformed quantum group symmetry. These groups play an important rôle in the study of driven systems if  $q$  is a real number. The parameter  $q$  may be assigned to an energy gap driven system between two sites on a lattice in a ( $q \sim \exp(\beta\Delta E)$ ).  $\Delta E$  expresses the energy gap, and  $\beta$  is the inverse temperature. Imagine that in this energy landscape particles perform random walks of which hopping probabilities depend on  $q$ . Then these particles prefer to go in the direction of which transition probabilities are higher. Therefore,  $q$  represents the asymmetry in the hopping process of random walkers. If the particles possess a hard-core interaction with each other then they obey an exclusion principle. However, it is still more interesting to explore a collective behavior of random walk particles, e.g. shocks, sharp intrusions or decreases of the average density. In this section, I shall study the dynamics of a shock distribution as an initial state for an one-dimensional asymmetric simple exclusion process (ASEP) with a sublattice parallel update. As shown below, the time evolution of this shock distribution can be exactly calculated if the two initial densities of the shock satisfy a special relation. The resulting distribution is a linear combination of shock measures. Moreover, the motion of the shock position can be interpreted as if it would perform a discrete-time biased random walk, with hopping rules related to that of a single particle in the exclusion process. The expressions of the shock diffusion coefficient and of the shock velocity in terms of currents and densities reveal an underlying principle which may be generally valid for shocks.

The exploration of exclusion processes plays an important part in special fields of many-body systems, so the study of traffic (jams) [37, 100], self-diffusion (e.g. in zeolites) [38] or reading processes for RNA strands within cells [39].

As mentioned above the asymmetric simple exclusion process (ASEP) is a model of diffusing identical particles with hard-core interaction on a lattice. Every single particle performs a biased random walk, but at the same time they obey the exclusion principle which prohibits the occupation of a lattice site by more than one particle [7, 40]. Various exact results including stationary states, correlation functions and lengths were obtained not only by using probabilistic tools, but also by the Bethe ansatz and related quantum mechanical methods or the matrix product ansatz [101].

Here, I will concentrate on the temporal evolution of a shock in a special ASEP. One can compute the full time evolution of an initial shock measure which will be shown to evolve into a linear combination of similar shock distributions if a particular constraint between hopping probabilities of the exclusion particles and the shock densities is fulfilled. It will transpire that the shock – which represents the collective motion of many particles – may be described by only one parameter, the shock position. This position represents the increase or decrease of the densities in the ensemble average. Such a reduced description in terms of the stochastic

dynamics of a single coordinate can be motivated by every-day experience with traffic jams, but also by Monte-Carlo simulations of the exclusion process [102, 103] where the existence of a sharp shock is not a-priori clear. I want to stress that the particle dynamics in the exclusion process takes place on a mesoscopic scale whereas quantities like the shock position usually appears in a macroscopic framework of description. It is well-known that on a macroscopic level a shock can be viewed as a collective single particle excitation. However, usually the macroscopic results are only approximate but not exact due to the reduction of the degrees of freedom. Hence, it is surprising, that this exclusion model yields *exact* single particle dynamics for the shock even on the mesoscopic lattice scale. Thus, this is a rare example where the emergence of macroscopic degrees of freedom can be directly deduced from mesoscopic scales without invoking any approximation or taking any scaling limit.

There are also studies of the time evolution of shocks involving second-class (kind) particles [104, 105]. This technique yields exact (and rigorous) results in certain scaling limits without constraints on the hopping rates and boundary densities of the shock. In our approach second-class particles do not appear. Instead I shall apply the above introduced quantum algebra technique which allows me to relate the time evolution of a shock to the time evolution of a single particle [106]. Throughout my discussion I will restrict myself to a one-parameter family of shock distributions which satisfy the constraint mentioned above. From a mathematical point the quantum algebra symmetry requires to take the thermodynamic limit, a single-shock picture remains valid also in the continuous-time exclusion process on a finite lattice with open boundaries if a constraint on the boundary injection/absorption rates analogous to our constraint is satisfied [107].

In the next subsections I will reduce the shock dynamics to a single-particle dynamics and analyze the properties of the associated single-particle random walk which will be finally translated into the corresponding properties of the shock. The expressions of the exact drift velocity and diffusion coefficient in terms of the currents and densities enable me to draw some conclusions which may be valid in more general settings.

### 3.2.1 Shock Distribution in ASEP

#### The Asymmetric Exclusion Model

Following the idea proposed in [15, 108], here I want to study an exclusion process [109] which can be connected to a six vertex model [110]. In a chain of length  $4L$  (beginning from  $-2L + 1$ ) every lattice site can be occupied by a particle or not. The constraint of a finite chain will be lifted later for an infinite chain in the thermodynamic limit. Hard-core interaction between the particles is included, so if one place is occupied by a particle no other one can jump on it. For later



purpose I shall define  $|n_k\rangle = (0 \ 1)^T$  if the position  $k$  is occupied by a particle and  $|n_k\rangle = (1 \ 0)^T$  otherwise.

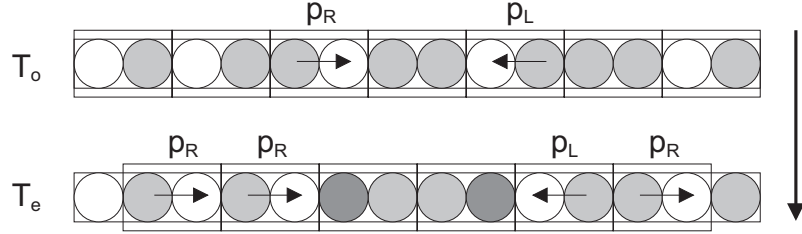


Figure 3.10: Parallel update sequence of an ASEP (in direction of the large arrow on the r.h.s.). Small arrows indicate possible jumps. Each cell represents a lattice site. Particles which have moved in the first half step (odd sublattice) are shown in dark grey in the second half step.

The stochastic time evolution of the system proceeds in two half-time steps. For this purpose one divides the chain into pairs of sites as shown in Fig. 3.10.

1. The pairs are chosen for the first half-time step,  $t \rightarrow t + \frac{1}{2}$ , in such a way that the first lattice index is odd. I.e.  $(-2L + 1, -2L + 2) \dots (2L - 1, 2L)$  form pairs, and the evolution only takes place between these two lattice points in a parallel update. Hence, if both sites are occupied or empty, they remain unchanged. However, if one of these sites is empty and the other not the particle jumps onto it with probability  $p_L$  ( $p_R$ ) if the jump is to the left (right).
2. In the second half time step,  $t + \frac{1}{2} \rightarrow t + 1$ , the pairing is shifted by one lattice unit and the even pairs  $(-2L + 2, -2L + 3) \dots (2L - 2, 2L - 1)$  will be updated in the same manner as above. Notice that the first and the last site are excluded in this update step whereas the boundary sites are involved during the first time step.

With this choice of reflecting boundary conditions the model satisfies detailed balance. The steady state is identical to that of the usual exclusion process in continuous-time and is described in detail in [16]. The continuous-time exclusion process is obtained from this discrete-time model by taking the limit  $p_R, p_L \rightarrow 0$  with the fixed ratio

$$q^2 = \frac{p_R}{p_L} \quad (3.62)$$

expressing the asymmetry in the hopping process. The continuous time parameter  $\tau$  (setting the hopping time scale) is obtained by taking the limit  $t \rightarrow \infty$ , keeping  $\tau = t(p_R + p_L)$  fixed.

In the next step I want to specify the dynamics of this parallel update ASEP model in terms of the Fock space formalism. If we denote the first temporal step

$\hat{T}_o$ , the second one  $\hat{T}_e$  and the total temporal evolution  $\hat{T}$  one may express the total time evolution as follows

$$\hat{T} = \hat{T}_e \hat{T}_o. \quad (3.63)$$

The discrete operator  $\hat{T}_o$  can be encoded in the form

$$\hat{T}_o = \prod_{k=-L+1}^L \hat{T}_{o,(2k-1)} = \prod_{k=-L+1}^L \begin{pmatrix} 1 & 0 & 0 & 0 \\ 0 & 1-p_L & p_R & 0 \\ 0 & p_L & 1-p_R & 0 \\ 0 & 0 & 0 & 1 \end{pmatrix}_{2k-1,2k} \quad (3.64)$$

where (using rules of the exchange dynamics for fermions, see (2.125))

$$\hat{T}_{o,(2k-1)} = 1 - p_R [\hat{N}_{2k-1}(1 - \hat{N}_{2k}) - a_{2k-1} a_{2k}^\dagger] - p_L [(1 - \hat{N}_{2k-1})\hat{N}_{2k} - a_{2k-1}^\dagger a_{2k}], \quad (3.65)$$

and  $\hat{N}_k$  are the number operators giving the occupation number at site  $k$ . The symbols

$$a_k = \begin{pmatrix} 0 & 1 \\ 0 & 0 \end{pmatrix}_k, \quad a_k^\dagger = \begin{pmatrix} 0 & 0 \\ 1 & 0 \end{pmatrix}_k \quad (3.66)$$

abbreviate the lowering and raising operators acting non-trivially on site  $k$  but as unit elements on all other sites, i.e. for any single-site operator  $G$

$$G_k = \mathbf{1} \otimes \dots \otimes \mathbf{1} \otimes G \otimes \mathbf{1} \dots \otimes \mathbf{1}. \quad (3.67)$$

Analogously one can define  $\hat{T}_e$ , but the update sequence changes to  $2k, 2k+1$  with  $k \in [-L+1, L-1]$ . Within the bulk, stationarity of this chain is only possible if two different densities for the odd and even, respectively, sublattices exist, i.e.

$$\rho^A = \frac{1}{2L} \sum_{k=-L+1}^L \langle \hat{N}_{2k-1} \rangle \quad \text{and} \quad \rho^B = \frac{1}{2L} \sum_{k=-L+1}^L \langle \hat{N}_{2k} \rangle \quad (3.68)$$

reflecting the sublattice structure of the transfer matrix. This form is a special case of the expectation value of the number operator at site  $i$ , given by

$$\rho_i = \langle \vec{r} | \hat{N}_i | \Pi(t) \rangle. \quad (3.69)$$

Assuming one considers bulk sites on the odd and even sublattices with the density  $\rho^A$  and  $\rho^B$  and applies the transfer matrix  $\hat{T}$  so that for the evolution the product measure remains invariant, i.e.

$$\begin{aligned} & \hat{T} \left\{ \dots \otimes \begin{pmatrix} 1 - \rho^A \\ \rho^A \end{pmatrix}_{2k-1} \otimes \begin{pmatrix} 1 - \rho^B \\ \rho^B \end{pmatrix}_{2k} \otimes \dots \right\} \\ &= \hat{T}_e \hat{T}_o \left\{ \dots \otimes \begin{pmatrix} 1 - \rho^A \\ \rho^A \end{pmatrix}_{2k-1} \otimes \begin{pmatrix} 1 - \rho^B \\ \rho^B \end{pmatrix}_{2k} \otimes \dots \right\} \\ &= \hat{T}_e \left\{ \dots \otimes \begin{pmatrix} 1 - \rho^B \\ \rho^B \end{pmatrix}_{2k-1} \otimes \begin{pmatrix} 1 - \rho^A \\ \rho^A \end{pmatrix}_{2k} \otimes \dots \right\} \\ &= \left\{ \dots \otimes \begin{pmatrix} 1 - \rho^A \\ \rho^A \end{pmatrix}_{2k-1} \otimes \begin{pmatrix} 1 - \rho^B \\ \rho^B \end{pmatrix}_{2k} \otimes \dots \right\}. \end{aligned} \quad (3.70)$$

Or equivalently one obtains

$$\begin{aligned} \hat{T} | \Pi^* \rangle &= \hat{T} \left[ (1 - \rho^A) \begin{pmatrix} 1 \\ \frac{\rho^A}{1 - \rho^A} \end{pmatrix} \otimes (1 - \rho^B) \begin{pmatrix} 1 \\ \frac{\rho^B}{1 - \rho^B} \end{pmatrix} \right]^{\otimes 2L} \\ &= \left[ (1 - \rho^A) \begin{pmatrix} 1 \\ \frac{\rho^A}{1 - \rho^A} \end{pmatrix} \otimes (1 - \rho^B) \begin{pmatrix} 1 \\ \frac{\rho^B}{1 - \rho^B} \end{pmatrix} \right]^{\otimes 2L} \end{aligned} \quad (3.71)$$

neglecting boundary effects. One may write

$$\begin{aligned} &\left[ (1 - \rho^A) \begin{pmatrix} 1 \\ \frac{\rho^A}{1 - \rho^A} \end{pmatrix} \otimes (1 - \rho^B) \begin{pmatrix} 1 \\ \frac{\rho^B}{1 - \rho^B} \end{pmatrix} \right] \\ &= \frac{1}{1 + \xi^A} \hat{\Xi}^A \otimes \frac{1}{1 + \xi^B} \hat{\Xi}^B | \vec{r} \rangle \equiv | \rho^A \rangle \otimes | \rho^B \rangle \end{aligned} \quad (3.72)$$

if one sets

$$\hat{\Xi}^{A/B} = \begin{pmatrix} 1 & 0 \\ 0 & \xi^{A/B} \end{pmatrix} \text{ and } \xi^{A/B} = \frac{\rho^{A/B}}{1 - \rho^{A/B}}. \quad (3.73)$$

Hence, this product measure is the stationary state of the finite *periodic* system [108] and also of the infinite system with equal asymptotic sublattice densities. Eq.(3.71) implies a relation between the two sublattice densities

$$(1 - p_R) \xi^A = (1 - p_L) \xi^B. \quad (3.74)$$

The average bulk density is defined by the sum  $\rho = \frac{1}{2} (\rho^A + \rho^B)$ .

### Definition of a Shock

In this subsection I will calculate the temporal distribution for a family of shock initial states. Although I intend to carry out the computation in the thermodynamic limit I will begin with a finite chain of  $4L$  sites. The evolution of the system will be described by the transfer matrix  $\hat{T}$  mentioned above.

Our shock at position  $2k + 1$  is defined in the following manner: Up to a position  $2k$  the product measure on  $\{0, 1\}$  has the density

$$\rho_1 = \frac{1}{2} (\rho_1^A + \rho_1^B) \quad (3.75)$$

whereas all other sites  $\geq 2k + 1$  have the density

$$\rho_2 = \frac{1}{2} (\rho_2^A + \rho_2^B) \quad (3.76)$$

with  $\rho_{1/2} \in [0, 1]$  (Fig. 3.2). This jump in the densities forms a domain wall connecting stationary regions. In order to have a stable shock which does not smear

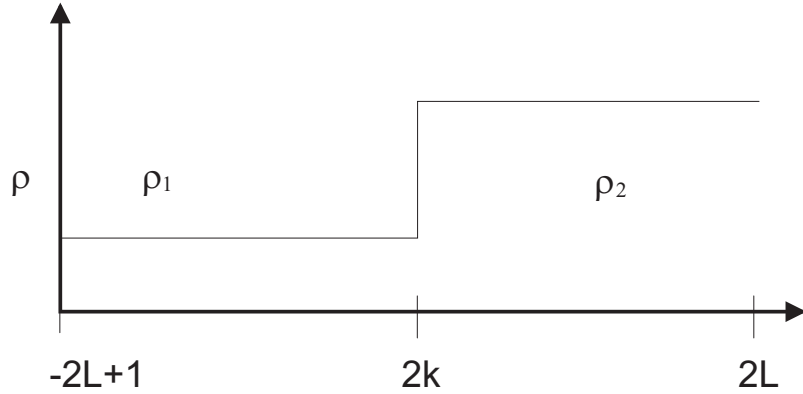


Figure 3.11: Schematic representation of the density profile in an upward shock at site  $2k$ .

out in time I assume  $\rho_1 < \rho_2$ . We will demand that the densities fulfil a relation involving the ratio of the hopping probabilities  $q^2$ . This choice enables me to calculate the exact temporal evolution of the shock family. I call this measure a *shock measure* at  $2k + 1$  and denote it with  $\mu_{2k+1}$ . Shocks at an even position  $2k$  are defined as follows: up to site  $2k - 2$  the density is  $\rho_1$ . At site  $2k - 1$  ( $2k$ ) the density is  $\rho_1^A(\rho_2^B)$ . At all other sites the density is  $\rho_2$ . The shock  $\mu_k$  can be represented as a vector  $|\mu_k\rangle$  in the Fock space, see below.

### Dynamics of the Shock

Firstly, we introduce a diagonal operator

$$\hat{Q}_k := \prod_{l=k}^{2L} \begin{pmatrix} 1 & 0 \\ 0 & q^2 \end{pmatrix}_l \equiv \prod_{l=k}^{2L} \Omega_l \quad (3.77)$$

( $k$  may be even or odd) which is related to the shock as will be shown below. Let me start with one-time step evolution of  $\hat{Q}_k$

$$\langle \hat{Q}_k(t+1) \rangle = \langle \vec{r} | \hat{Q}_k \tilde{T} \hat{V}^T | \Pi(t) \rangle = \langle \vec{r} | \hat{Q}_k \tilde{T}_o \tilde{T}_e \hat{V}^T | \Pi(0) \rangle \quad (3.78)$$

with the initial distribution  $\hat{V}^T | \Pi(t) \rangle$ ,  $\hat{V}$  is a diagonal operator and the appropriate reference vector  $\langle \vec{r} | = \langle r |^{\otimes 4L}$  where  $\langle r | = (1 \ 1)^T$ , i.e. all components are equal to 1 ( $r = 1$ ). Here I used a slightly different stochastic transfer matrix  $\tilde{T} = \tilde{T}_o \tilde{T}_e$ . Compared to above I changed the update sequence and exchanged the hopping probabilities  $p_R \Leftrightarrow p_L$ . It is known from the quantum group symmetry of the  $SU_q(2)$  (the  $q$ -deformed group of  $SU(2)$ , compare e.g. [111] with  $q^2$  as the asymmetry ratio (3.62)) that the time evolution of  $\hat{Q}_k$  yields a closed set of equations in the site index  $k$  which can be interpreted as an one-particle dynamics [16, 112].

Now I want to exploit this result by applying it to our original dynamics. Transposing the expectation value (3.78) yields

$$\langle \Pi(0) | \hat{V} \tilde{T}_e^T \tilde{T}_o^T \hat{Q}_k | \vec{r} \rangle. \quad (3.79)$$

$\hat{V} \hat{Q}_k$  should be chosen such that  $\hat{V} \hat{Q}_k | \vec{r} \rangle$  is a shock at position  $k$  which contains stationary regions in front of and behind the shock like defined above. Because  $\hat{V}$  and  $\hat{Q}_k$  (both diagonal) commute,  $\hat{V} | \vec{r} \rangle$  should become a stationary state of the whole system whereas  $\hat{Q}_k$  fixes the position where the density changes. Given the alternating density of the stationary state one may write  $\hat{V} = \otimes_{k=-L+1}^L (\hat{V}^A \otimes \hat{V}^B)$  where  $\hat{V}^{A,B}$  are diagonal  $2 \times 2$  matrices and  $\otimes$  denotes the tensor product. This determines the elements of  $\hat{V}$  up to an irrelevant constant factor

$$\hat{V}^A \otimes \hat{V}^B = \hat{\Xi}^A \otimes \hat{\Xi}^B = \begin{pmatrix} 1 & 0 & 0 & 0 \\ 0 & \xi^B & 0 & 0 \\ 0 & 0 & \xi^A & 0 \\ 0 & 0 & 0 & \xi^A \xi^B \end{pmatrix} \quad (3.80)$$

with the ratio

$$\xi^{A/B} = \frac{\rho^{A/B}}{1 - \rho^{A/B}}. \quad (3.81)$$

Up to now the total chain has the density  $\rho$  which I may set without loss of generality to  $\rho_1$ . Starting from position  $k$  I want to "create" the density  $\rho_2$  instead of  $\rho_1$ . To achieve this goal one uses the operator

$$\Omega_l = \begin{pmatrix} 1 & 0 \\ 0 & q^2 \end{pmatrix}_l \quad (3.82)$$

and obtains the action of the operator  $\Omega_l$  on a state  $| (\rho_1)_l \rangle$  at one lattice site  $l$

$$\frac{1 + \xi_1^{A/B}}{1 + \xi_2^{A/B}} \Omega_l | (\rho_1^{A/B})_l \rangle = \frac{1}{1 + \xi_2^{A/B}} \hat{\Xi}_2^{A/B} | r_l \rangle = | (\rho_2^{A/B})_l \rangle. \quad (3.83)$$

One recognizes that one generates a state with a different density on site  $l$  defined by the constraint

$$q^2 = \frac{\xi_2^A}{\xi_1^A} = \frac{\xi_2^B}{\xi_1^B}. \quad (3.84)$$

By applying  $\Omega_l$  to all sites of the chain larger than  $k$ , i.e. acting with  $\hat{Q}_k$  on the product state  $| \rho_1 \rangle$  yields a state corresponding to a shock measure with shock densities  $\rho_{1,2}^{A/B}$  related by (3.84). The operator  $\hat{Q}_{2k+1}$  of the whole chain,  $\rho_2$  beginning from  $2k+1$ , therefore may be written

$$\hat{Q}_{2k+1} = \mathbf{1}^{\otimes 2(L+k)} \otimes \left[ \begin{pmatrix} 1 & 0 \\ 0 & \frac{\xi_2^A}{\xi_1^A} \end{pmatrix} \otimes \begin{pmatrix} 1 & 0 \\ 0 & \frac{\xi_2^B}{\xi_1^B} \end{pmatrix} \right]^{\otimes (L-k)} \quad (3.85)$$

from which the shock representation follows immediately (up to the normalization)

$$\hat{V}\hat{Q}_{2k+1} = (\hat{\Xi}_1^A \otimes \hat{\Xi}_1^B)^{\otimes(L+k)} \otimes (\hat{\Xi}_2^A \otimes \hat{\Xi}_2^B)^{\otimes(L-k)}. \quad (3.86)$$

Returning to the time evolution of  $\hat{Q}_k$  one continues computing and obtains

$$\langle \Pi(0) | (\hat{V}\hat{T}_e^T \hat{T}_o^T \hat{V}^{-1}) \hat{V}\hat{Q}_k | \vec{r} \rangle = \langle \Pi(0) | (\hat{V}\hat{T}_e^T \hat{X}^{-1}) (\hat{X}\hat{T}_o^T \hat{V}^{-1}) \hat{V}\hat{Q}_k | \vec{r} \rangle \quad (3.87)$$

where  $\hat{X}$  is a further diagonal matrix to be determined. Notice that the transpose matrices  $\hat{T}_e^T$  and  $\hat{T}_o^T$  are not longer stochastic. To retain stochastic matrices one has to require that

$$(\hat{V}\hat{T}_e^T \hat{X}^{-1}) = \hat{T}_e \text{ and } (\hat{X}\hat{T}_o^T \hat{V}^{-1}) = \hat{T}_o. \quad (3.88)$$

Thus, one obtains the original transfer matrix (3.63) again. To determine  $\hat{X}$  one applies the linear shift operator  $\hat{\Delta}_S$  to shift all operators from one sublattice to the other and gets by means of (3.88)

$$\hat{\Delta}_S \hat{V} \hat{\Delta}_S^{-1} = \hat{X} \quad (3.89)$$

Summarizing the matrices satisfy the relations

$$\hat{V}\hat{T}_e^T \hat{\Delta}_S \hat{V}^{-1} \hat{\Delta}_S^{-1} = \hat{T}_e \text{ and } \hat{\Delta}_S \hat{V} \hat{\Delta}_S^{-1} \hat{T}_o^T \hat{V}^{-1} = \hat{T}_o. \quad (3.90)$$

Together with the condition of the stationarity one recovers from this relation the constraint (3.74) inside a domain (of course separately valid for each domain 1 and 2, that is the reason why we will call it the *intra-domain relation*).

In the next step I proceed with the shock as a wall separating two domains of stationary states with densities  $\rho_1$  and  $\rho_2$ , respectively. Starting from the representation of the stationary state for  $\hat{V}$  (3.80),  $\hat{Q}_{2k+1}$  (3.85) and the requirement that  $\hat{V}\hat{Q}_{2k+1} | \vec{r} \rangle$  should be a normalized shock the initial distribution for an odd-type shock at position  $2k+1$  results in

$$\begin{aligned} |\mu_{2k+1}\rangle &= \hat{V}\hat{Q}_{2k+1} | \vec{r} \rangle \quad (3.91) \\ &= C^{-1} \left( \frac{(1 + \xi_2^B)(1 + \xi_2^A)}{(1 + \xi_1^B)(1 + \xi_1^A)} \right)^{L+k} \left( \hat{\Xi}_1^A \right)^{\hat{N}_o^{2k-1}} \left( \hat{\Xi}_1^B \right)^{\hat{N}_e^{2k}} \times \\ &\quad \times \left( \hat{\Xi}_2^A \right)^{\hat{N}_o - \hat{N}_o^{2k-1}} \left( \hat{\Xi}_2^B \right)^{\hat{N}_e - \hat{N}_e^{2k}} | \vec{r} \rangle \end{aligned}$$

where

$$C = ((1 + \xi_2^B)(1 + \xi_2^A))^{2L} \quad (3.92)$$

is the normalization and

$$\hat{N}_o^{2k-1} = \sum_{i=1-L}^k \hat{N}_{2i-1}, \quad \hat{N}_e^{2k} = \sum_{i=1-L}^k \hat{N}_{2i}, \quad \hat{N}_o = \sum_{i=1-L}^L \hat{N}_{2i-1}, \quad \hat{N}_e = \sum_{i=1-L}^L \hat{N}_{2i} \quad (3.93)$$

are sums of number operators. For an even-type shock at position  $2k$  the distribution reads

$$|\mu_{2k}\rangle = \left( \hat{\Xi}_2^B \right)^{\hat{N}_{2k}} \left( \hat{\Xi}_1^B \right)^{-\hat{N}_{2k}} \frac{(1 + \xi_1^B)}{(1 + \xi_2^B)} | \mu_{2k+1}\rangle. \quad (3.94)$$

### Shock Dynamics as an One-Particle Equation

Taking the odd-position shock representation (3.91), it is easy to see that in the first half-time step (odd sublattice) there is only an update inside the domains because it does not exist any pair  $(\rho_1, \rho_2)$  inside the chain. Thus, the shock does not move. However, in the second half-time step (even sublattice) there is a sequence  $(\rho_1, \rho_2)$  at pair positions  $2k, 2k + 1$ . To achieve shock distributions again and to conserve the stationarity state of the domains (besides of the boundary which I consider later) it exist three possible sequences inside this pair after the temporal update. Taking these constraints into account the equation of motion  $|\mu_{2k+1}(t+1)\rangle = \hat{T}_e \hat{T}_o |\mu_{2k+1}(t)\rangle$  leads to four partial equations

$$\hat{T}_e \hat{T}_o |\mu_{2k+1}(t)\rangle = \pi_R |\mu_{2k+2}(t)\rangle + \pi_L |\mu_{2k}(t)\rangle + \pi_S |\mu_{2k+1}(t)\rangle \quad (3.95)$$

for three coefficients  $\pi_L, \pi_S$  and  $\pi_R$ . These equations are correct up to the treatment of the boundary discussed below. Thus, one can understand the many-particle motion of a shock as a discrete random walk of only one particle by identifying the position of the shock with the position of the random walker. Therefore one could reduce degrees of freedom without loss of relevant information. From (3.95) one reads off the probabilities

$$\pi_R = p_R \frac{1 + \xi_1^B}{1 + \xi_2^B} \quad (3.96)$$

$$\pi_S = (1 - p_L - p_R) \frac{1 + \xi_2^A}{1 + \xi_1^A} \frac{1 + \xi_1^B}{1 + \xi_2^B} \quad (3.97)$$

$$\pi_L = p_L \frac{1 + \xi_2^A}{1 + \xi_1^A} \quad (3.98)$$

by using the constraint (3.84) between the shock densities (which one may denote *inter-domain relation* in contrast to the intra-domain relation (3.74)).

Notice that the shock position  $k$  is determined by the position where the second density starts, independently of the sublattice structure. One obtains for the even shock in the same manner

$$\begin{aligned} \hat{T} |\mu_{2k}\rangle &= \pi_S \pi_L |\mu_{2k-1}\rangle + \pi_S \pi_R |\mu_{2k+1}\rangle + \\ &+ (2\pi_L \pi_R + \pi_S) |\mu_{2k}\rangle + \pi_L^2 |\mu_{2k-2}\rangle + \pi_R^2 |\mu_{2k+2}\rangle \end{aligned} \quad (3.99)$$

As seen, the shock distribution turns into a linear combination of the same distributions with weights identical with the jump probabilities for the evolution of the discrete time random walk. By iterating the evolution equations (3.95) and (3.99) one may summarize

$$|\mu_k(t)\rangle = \sum_l p_l^k(t) |\mu_l\rangle \quad (3.100)$$

where  $p_l^k(t)$  is the transition probability of the shock from site  $k$  to site  $l$  after  $t$  time steps, with the transition probabilities (3.96) - (3.98) and the rules described above.

From these rules it is clear that the motion of a shock can be reformulated and understood as a random walk of a single particle with sublattice update according to the following updating scheme: In the first half-time step one considers only the even sublattice. If the particle is at position  $2k$  then it moves with the probability  $\pi_L$  and  $\pi_R$  to the left and to the right, respectively. In the second half-time step one shifts to the odd sublattice and lets the particle evolves in the same manner like in the first half-time step. This procedure leads immediately to the hopping rules (3.99). In the same manner one recovers (3.95) if there was a particle at site  $2k + 1$  at the beginning of the first half-step. The solution of this random walk problem yields the transition probabilities  $p_l^k(t)$ .

### Boundary Effects

The result of the previous subsection is the equation of motion holding for the bulk, but with the incorrect consideration of the boundary (I regarded the finite chain with  $4L$  sites.). The next step is to remedy the influence of the boundary by taking the limit for  $L$  to infinity. Up to this point the ends are "incorrectly" treated, i.e. after one time step there are the density  $\rho_B^1$  instead of  $\rho_A^1$  at the end point  $-2L + 1$  and the density  $\rho_A^2$  instead of  $\rho_B^2$  at the other end points  $2L$ , but the shock distribution is still properly normalized. With the proper treatment of the boundary the equation (3.95) reads

$$\hat{T} | \mu_{2k+1} \rangle = \pi_S | \mu_{2k+1} \rangle_{-2L+1,2L} + \pi_L | \mu_{2k} \rangle_{-2L+1,2L} + \pi_R | \mu_{2k+2} \rangle_{-2L+1,2L} \quad (3.101)$$

where the indices mark the deviation at the boundary for the odd-type shock. For the even-type shock one obtains

$$\begin{aligned} \hat{T} | \mu_{2k} \rangle = & \pi_S \pi_L | \mu_{2k-1} \rangle_{-2L+1,2L} + \pi_S \pi_R | \mu_{2k+1} \rangle_{-2L+1,2L} + \\ & + (2\pi_L \pi_R + \pi_S) | \mu_{2k} \rangle_{-2L+1,2L} + \pi_L^2 | \mu_{2k-2} \rangle_{-2L+1,2L} + \pi_R^2 | \mu_{2k+2} \rangle_{-2L+1,2L} \end{aligned} \quad (3.102)$$

The disturbances of the boundary would evolve and destroy finally the shock distribution. However, this spreading of the disturbance takes place with a finite speed of two lattice units per time step. Thus, for  $L \rightarrow \infty$  and finite time, there is always an infinite unaffected region around the shock position, i.e. one may conclude

$$\lim_{L \rightarrow \infty} | \mu_k(t) \rangle_{-2L+1,2L} = \lim_{L \rightarrow \infty} | \mu_k(t) \rangle \quad (3.103)$$

for all fixed number of time steps  $t$ .

Of course, the conservation of probability is still guaranteed because the boundary effects do not affect the normalization. Hence, in the thermodynamic limit Eqs.(3.95) and (3.99) are exact. The shock evolves into a linear combination of shock distributions if all constraints, i.e. the inter-domain relation (3.84) between the shock densities (resulting from the  $SU_q(2)$  symmetry) and the intra-domain relation (3.74) (for stationarity within the domains) are fulfilled.



### 3.2.2 Drift Velocity and Diffusion Coefficient for the One Particle Random Walk

The shock  $|\mu_k\rangle$  is labeled with the index expressing its position ( $k$ ) which may be assigned to a particle performing a random walk. I denote its position as a Fock space vector  $|k\rangle$  for the following computation. From its random walk dynamics it may be calculated its drift velocity and its diffusion coefficient which one can relate to the shock velocity and the shock diffusion coefficient later.

Using the coupled equation system (3.101) and (3.102) one can explicitly calculate the higher moments  $\langle k^n(t) \rangle$

$$\langle k^n(t) \rangle = \sum_{k=-\infty}^{\infty} k^n P(k, t) = \langle k_e^n(t) \rangle + \langle k_o^n(t) \rangle \quad (3.104)$$

by means of the definition

$$\langle k_e^n(t) \rangle := \sum_{k=-\infty}^{\infty} (2k)^n P(2k, t) \quad \text{and} \quad \langle k_o^n(t) \rangle := \sum_{k=-\infty}^{\infty} (2k+1)^n P(2k+1, t). \quad (3.105)$$

These quantities are moments of the spatial probability distribution of the random walker. They lead to the drift velocity

$$v = \lim_{t \rightarrow \infty} (\langle k(t+1) \rangle - \langle k(t) \rangle) \quad (3.106)$$

and the diffusion coefficient

$$D = \lim_{t \rightarrow \infty} \langle (k(t+1) - \langle k(t+1) \rangle)^2 \rangle - \langle (k(t) - \langle k(t) \rangle)^2 \rangle. \quad (3.107)$$

To calculate these moments one derives the master equation for the probabilities  $P(k, t)$ . This can be formally done by starting from the master equation (2.51) under consideration of the probability representation (2.58), with  $r = 1$ ,

$$\begin{aligned} \hat{T} |\Pi(t)\rangle &= \hat{T} \sum_l |l\rangle = \hat{T} \sum_l P((2l, t) | 2l) + P(2l+1, t) | 2l+1\rangle \\ &= + \sum_l \{ [\pi_L^2 P(2l, t)] | 2l-2\rangle + [\pi_L \pi_S P(2l, t)] | 2l-1\rangle \} \\ &\quad + \sum_l [\pi_L P(2l+1, t) + \pi_S P(2l, t) + 2\pi_R \pi_L P(2l, t)] | 2l\rangle \\ &\quad + \sum_l [\pi_S P(2l+1, t) + \pi_R \pi_S P(2l, t)] | 2l+1\rangle \\ &\quad + \sum_l [\pi_R P(2l+1, t) + \pi_R^2 P(2l, t)] | 2l+2\rangle \end{aligned} \quad (3.108)$$

One obtains the odd-type master equation (which, of course, may be directly found from the definition of the process)

$$\begin{aligned} P(2k+1, t+1) &= \langle 2k+1 | \hat{T} | \Pi(t) \rangle \\ &= \pi_S P(2k+1, t) + \pi_L \pi_S P(2k+2, t) + \pi_R \pi_S P(2k, t) \end{aligned} \quad (3.109)$$

if one exploits the orthogonality of the states. Inserting the master equation into the odd part of the zeroth moments (3.105) yields

$$\begin{aligned} \langle k_o^0(t+1) \rangle &= \sum_k P(2k+1, t+1) \\ &= \pi_S \langle k_o^0(t) \rangle + (1 - \pi_S) \pi_S \langle k_e^0(t) \rangle \end{aligned} \quad (3.110)$$

bearing the probability conservation  $\pi_S + \pi_L + \pi_R = 1$  in mind.

In the case of the even-type dynamics one equivalently gets

$$\begin{aligned} P(2k, t+1) &= \langle 2k | \hat{T} | \Pi(t) \rangle \\ &= (2\pi_L \pi_R + \pi_S) P(2k, t) + \pi_L P(2k+1, t) + \pi_R P(2k-1, t) \\ &\quad + \pi_L^2 P(2k+2, t) + \pi_R^2 P(2k-2, t). \end{aligned} \quad (3.111)$$

Taking the even part of (3.105) the master equation results in

$$\begin{aligned} \langle k_e^0(t+1) \rangle &= \sum_k P(2k, t+1) \\ &= (1 - \pi_S) \langle k_o^0(t) \rangle + [(1 - \pi_S)^2 + \pi_S] \langle k_e^0(t) \rangle. \end{aligned} \quad (3.112)$$

Not surprisingly, due to the conservation  $\langle k_e^0(t) + k_o^0(t) \rangle = 1$  the Eqs.(3.110) and (3.112) are not independent. Their stationary solution is given by

$$\langle k_e^0 \rangle = \frac{1}{1 + \pi_S} \quad \text{and} \quad \langle k_o^0 \rangle = \frac{\pi_S}{1 + \pi_S} \quad (3.113)$$

This gives the stationary probability of finding the random walker (i.e. the shock position) on the even and odd sublattice, respectively.

To simplify the subsequent calculations I assume as the initial condition that the particle can be found at an arbitrary position  $x$  on the odd lattice, i.e.

$$P(k, 0) = \delta_{k,x}. \quad (3.114)$$

However, this initial assumption does not influence the asymptotic behavior. One successively determines the higher moments from the known lower moments. Thus, one gets two coupled equations for the first moments

$$\langle k_o^1(t+1) \rangle = \pi_S \langle k_o^1(t) \rangle + (1 - \pi_S) \pi_S \langle k_e^1(t) \rangle + (\pi_R - \pi_L) \pi_S \langle k_e^0(t) \rangle \quad (3.115)$$

and

$$\begin{aligned} \langle k_e^1(t+1) \rangle &= (1 - \pi_S) \langle k_o^1(t) \rangle + [(1 - \pi_S)^2 + \pi_S] \langle k_e^1(t) \rangle \\ &\quad + 2(1 - \pi_S)(\pi_R - \pi_L) \langle k_o^0(t) \rangle + (\pi_R - \pi_L) \langle k_e^0(t) \rangle. \end{aligned} \quad (3.116)$$

Solving this difference system under consideration of (3.113) and looking for the asymptotic limit of the particle drift velocity  $v$  (3.106) one finds

$$v = 2 \frac{\pi_R - \pi_L}{1 + \pi_S}. \quad (3.117)$$

If one interprets

$$\Pi_{R/L} = \frac{\pi_{R/L}}{1 + \pi_S} \quad (3.118)$$

as an effective jump probability  $v$  can be written as

$$v = 2(\Pi_R - \Pi_L). \quad (3.119)$$

To determine the diffusion coefficient one still needs the second moments

$$\begin{aligned} \langle k_o^2(t+1) \rangle &= \pi_S \langle k_o^2(t) \rangle + (1 - \pi_S) \pi_S \langle k_e^2(t) \rangle \\ &\quad + 2(\pi_R - \pi_L) \pi_S \langle k_e^1(t) \rangle + (1 - \pi_S) \pi_S \langle k_e^0(t) \rangle \end{aligned} \quad (3.120)$$

and

$$\begin{aligned} \langle k_e^2(t+1) \rangle &= (1 - \pi_S) \langle k_o^2(t) \rangle + [(1 - \pi_S)^2 + \pi_S] \langle k_e^2(t) \rangle \\ &\quad + 4(1 - \pi_S)(\pi_R - \pi_L) \langle k_o^1(t) \rangle + 2(\pi_R - \pi_L) \langle k_e^1(t) \rangle \\ &\quad + (1 - \pi_S) \langle k_o^0(t) \rangle + 2[(1 - \pi_S)^2 + (\pi_R - \pi_L)^2] \langle k_e^0(t) \rangle. \end{aligned} \quad (3.121)$$

Computing this second difference equation system using (3.113) and the results of the first difference equation system (3.115, 3.116) one gets the asymptotic limit of the particle diffusion coefficient  $D$  (3.107)

$$D = 2 \frac{1 - \pi_S}{1 + \pi_S} \left[ 1 - \left( \frac{v}{2} \right)^2 \right] \quad (3.122)$$

using the velocity (3.117). In terms of the effective jump probabilities one has

$$D = 2(\Pi_R + \Pi_L) [1 - (\Pi_R - \Pi_L)^2]. \quad (3.123)$$

Notice that these expressions for the drift velocity and the diffusion coefficient are the same as those for a single exclusion particle with the sublattice dynamics of the exclusion process described above. Even though the microscopic dynamics of a single exclusion particle is different from the random walk discussed here the long-time properties are identical.

### 3.2.3 Conclusions

Using the quantum algebra symmetry of the ASEP with sublattice parallel update one could obtain the time evolution of an initial shock distribution by going through steps analogous to those taken in Ref. [106]. Perhaps the most important observation is the possibility of the description for the collective many-body dynamics by a stochastic single-particle motion without having to resort to a some approximation or a scaling argument. The price which one has to pay for achieving the exact time-dependent shock measure is a constraint (3.84) on the shock densities which results from the underlying  $SU_q(2)$ .

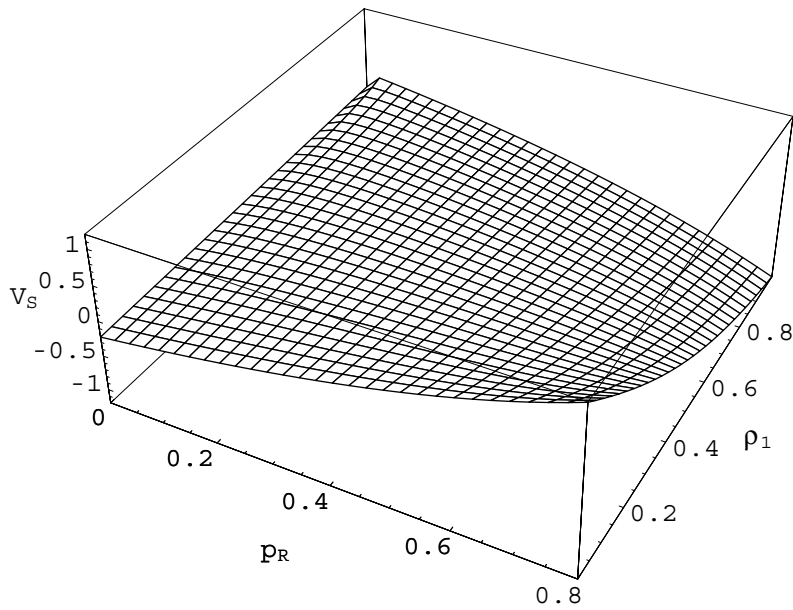


Figure 3.12: Shock velocity  $v_S$  as the function of  $p_R$  and  $\rho_1$  ( $p_L = 0.2$ , therefore  $q = 0 \dots 2$ )

The analysis of the properties of the associated random walk problem enables me to calculate the exact drift velocity and diffusion coefficient of the shock. The shock velocity  $v_S$  corresponds to the drift velocity of the random walk if one inserts the transition probabilities  $\pi_S, \pi_R$  and  $\pi_L$  of (3.96-3.98) into (3.117). One gets

$$\begin{aligned} v_S &= \frac{2(p_R - p_L)(1 - \rho_2^B - \rho_1^A)}{(1 - p_R) + (1 - p_L) + (p_R - p_L)(\rho_2^B - \rho_1^A)} \\ &= \frac{(p_R - p_L)(1 - \rho_2^B - \rho_1^A)}{\rho_2 - \rho_1} (\rho_2^A - \rho_1^B). \end{aligned} \quad (3.124)$$

If one takes the current of both stationary domains [108],

$$j = p_R \rho^A (1 - \rho^B) - p_L \rho^B (1 - \rho^A) \quad (3.125)$$

and the total densities on both sides, Eqs.(3.75) and (3.76), one can rewrite the shock velocity,

$$v_S = \frac{j_2 - j_1}{\rho_2 - \rho_1}. \quad (3.126)$$

It is clear that while (3.126) was directly derived only under the assumption that the constraint (3.84) holds, it must be generally valid. This is a simple consequence of mass conservation and reflects the more general principles of shock dynamics independent of the microscopic details and the update scheme. The parameter dependence of the shock velocity is shown in Fig. 3.12.

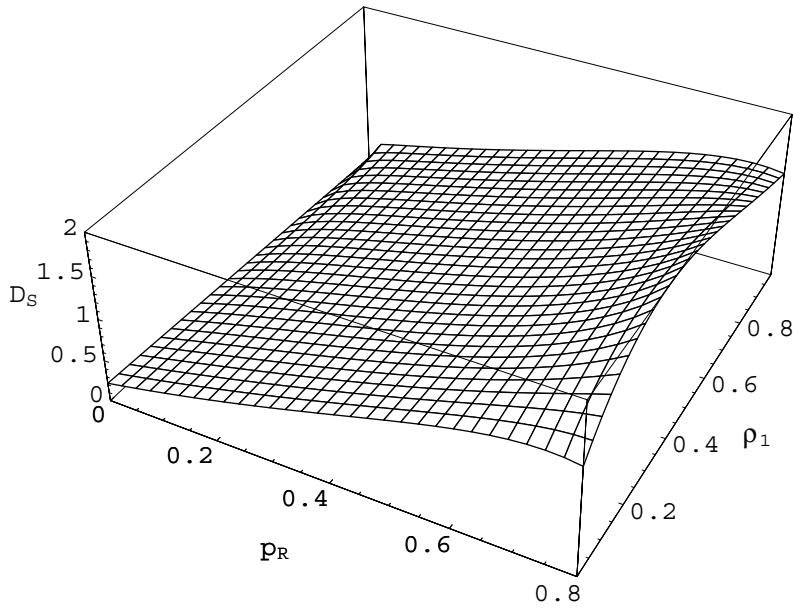


Figure 3.13: Shock diffusion constant  $D_S$  as the function of  $p_R$  and  $\rho_1$  ( $p_L = 0.2$ , therefore  $q = 0 \dots 2$ )

If one inserts the transition probabilities (3.96-3.98) into the particle diffusion coefficient (3.122) one may compute the shock diffusion coefficient,

$$D_S = \frac{2(p_R + p_L) + 2(p_R - p_L)(\rho_2^B - \rho_1^A)}{(1 - p_R) + (1 - p_L) + (p_R - p_L)(\rho_2^B - \rho_1^A)} \left[ 1 - \left( \frac{v_S}{2} \right)^2 \right] \quad (3.127)$$

which represents the width of the shock distribution and thus gives a measure for its fluctuation. The hopping probability dependence of the diffusion coefficient is shown in Fig. 3.13. It is remarkable that also the diffusion coefficient can be expressed in terms of currents and densities of the shock domains. Using (3.125) one obtains

$$D_S = \frac{j_2 + j_1}{\rho_2 - \rho_1} \left[ 1 - \left( \frac{v_S}{2} \right)^2 \right]. \quad (3.128)$$

It seems that not only the expression (3.126) for the drift velocity is generally valid, but also the expression (3.128). I.e. also if the constraint (3.84) is not satisfied and hence a single particle picture is not strictly valid on the lattice scale, (3.128) should remain valid, even though an underlying general principle is still unknown. This expression for the diffusion coefficient is different from that of the time-continuous exclusion process [103, 104]. Thus, it depends on the details of the stochastic dynamics. There is, however, an analogy to the time-continuous exclusion process in so far as in both models the shock dynamics have the same characteristic long-time properties as single particles in the respective processes. I.e. drift velocity and diffusion coefficient are the same for shock and particle respectively if one replaces the particle hopping rates (probabilities) by effective hopping rates (probabilities) for the shock. Since the expression of the shock diffusion coefficient in terms of the currents and densities in the time-continuous exclusion process is generally valid it seems plausible that this would remain true also for the present discrete-time realization of the exclusion process.

### 3.3 *Q*-deformed Models

In contrast to the last section where  $q$  is a real number (representing the asymmetry of the hopping probabilities) we want to study applications if  $q$  is a complex root of unity. Such  $q$ -deformed models could be relevant for the motion on fractals, deposition-desorption processes and queuing & servicing problems. The here explored models of the surface growth and of a parking lot problem should be examples demonstrating a possibly wide range of applications to other physical and non-physical systems of interest.

#### 3.3.1 The Surface Growth

Let me start with a 2-dimensional crystal growth model (a review can be found e.g. in [41]). One possible method to produce crystal layers is the molecular beam epitaxy where a beam of atoms falls down on a surface. Usually, the particles diffuse to energy-preferred sites but I want to restrict the consideration to cases with a small diffusion rate (against the desorption rate). The particles should stick at the sites where they were deposited, so that one may reduce the dimension later, i.e. the diffusion coefficient are sufficiently small enough against all other quantities. On the other hand, desorption effects should be included which are caused by a surface potential. Further, assuming that the stiffness of the surface approaches zero thus one may neglect the interface bending force as well. The substrate should grow by adsorbing particles over a plane surface starting from a complete layer. The actual height at local position  $r$  is expressed by the thickness of the layer  $z(r)$ . Hence, the energy functional of the model is given by

$$E[z(r)] = \int dz(r) [V[z(r)] - hz(r)] \quad (3.129)$$

where  $h$  is the supercooling force or deposition rate.  $V[z(r)]$  is the pinning potential, which can lead either to the attraction or to the desorption of particles, and therefore describes the layering. It can be expanded in first order to its fundamental (higher harmonics are irrelevant [41])

$$V[z(r)] = -V_0 \cos\left(\frac{2\pi}{a}z(r)\right) \quad (3.130)$$

with  $a$  as the difference between two complete surface layers. In a phenomenological, thermodynamic view a non-equilibrium equation can be derived from the variation of the energy. In this sense, the local rate of the displacement of the height,  $\partial_t z(r)$ , is proportional to the thermodynamic force  $\frac{\delta E[z(r)]}{\delta z(r)}$ . Hence, the temporal evolution of the deposition height can be described, following the model A of the Halperin-Hohenberg [113, 114] classification, as a Langevin equation

$$\partial_t z(r) = -\Gamma \frac{\delta E[z(r)]}{\delta z(r)} + \eta(r, t) \quad (3.131)$$

where  $\Gamma$  is the proportional factor. The added white noise  $\eta$  with  $\langle \eta(r, t) \rangle = 0$  is caused e.g. by the fluctuations in the epitatic beam (shot noise). Using this ansatz and inserting the energy functional (3.129) one obtains the stochastic equation

$$\partial_t z(r) = \Gamma \left( -V_0 \frac{2\pi}{a} \sin \left( \frac{2\pi}{a} z(r) \right) + h \right) + \eta(r, t). \quad (3.132)$$

Notice, if one replaced the deposition rate  $h$  by a diffusive term  $\gamma \Delta h$  one would recover the Chui-Weeks equation [115]

$$\partial_t z(r) = -V_0 \frac{2\pi}{a} \sin \left( \frac{2\pi}{a} z(r) \right) + \gamma \Delta h + \eta(r, t). \quad (3.133)$$

Setting the time derivative to zero,

$$\partial_t z(r) = 0 \quad (3.134)$$

the stationary state of the deterministic system emerges after averaging

$$\bar{z}(r) = \frac{a}{2\pi} \arcsin \left( \frac{ah}{2\pi V_0} \right). \quad (3.135)$$

Moreover, I want to restrict the dynamics to only one lattice point  $r_0$ , the kink position, due to the reason mentioned above. Therefore, the dimension of the system which has to be considered may be reduced from 2 to 1. Let me abbreviate the elevation  $z$  at  $r_0$  with  $z_0$ . Then, I want to express the height  $z_0$  in units of  $a$  counting the number  $N \in [0, s]$  of adsorbed particles in the ratio to its maximal value  $(s + 1)$  per complete layer, i.e.

$$z_0 = \frac{Na}{2(s + 1)}. \quad (3.136)$$

Carrying out the following replacements of the kinetic parameter, of the potential and of the supercooling force

$$\Gamma = 1, V_0 = \frac{\kappa a^2}{4\pi(s + 1) \sin \left( \frac{\pi}{s+1} \right)} \simeq \frac{\kappa a^2}{4\pi^2} \text{ and } h = \frac{\lambda a}{2(s + 1)} \quad (3.137)$$

in (3.132) and inserting the height of the co-ordinate  $z_0$  (3.136) yields the equation of motion for the number of adsorbed atoms

$$\partial_t N = -\kappa \frac{\sin \left( \frac{N\pi}{s+1} \right)}{\sin \left( \frac{\pi}{s+1} \right)} + \lambda + \eta(r_0, t). \quad (3.138)$$

On the assumption that the highest state  $s$  is rarely occupied the relation is equivalent to

$$\partial_t N = -\kappa |[N]| + \lambda(1 - s) + \eta(r_0, t) \quad (3.139)$$



remembering the definition of the symmetric-deformed number for  $q = j_{s+1}^{\frac{1}{2}}$

$$|[N]| = \frac{j_{s+1}^{\frac{N}{2}} - j_{s+1}^{-\frac{N}{2}}}{j_{s+1}^{\frac{1}{2}} - j_{s+1}^{-\frac{1}{2}}} = \frac{\sin\left(\frac{N\pi}{s+1}\right)}{\sin\left(\frac{\pi}{s+1}\right)}. \quad (3.140)$$

Considering the ensemble of deposition-desorption processes one still has to average over all terms leading to equation of motion for the occupation number

$$\partial_t \langle N \rangle = -\kappa \langle |[N]| \rangle + \lambda \langle (1-s) \rangle. \quad (3.141)$$

If one neglects the last state  $s$  again its stationary solution is given by the expression

$$\langle |[N]| \rangle = \frac{\lambda}{\kappa} \quad (3.142)$$

or in terms of the number of steps  $\frac{a}{(s+1)}$

$$\langle \bar{N} \rangle = \frac{s+1}{\pi} \arcsin\left(\frac{\lambda}{\kappa} \sin\left(\frac{\pi}{s+1}\right)\right) \quad (3.143)$$

which goes for small arguments as  $\frac{\lambda}{\kappa}$ . This result corresponds with (3.135) taking (3.136) into account. Below I will deduce this very last equation exploiting the properties of  $q$ -deformed operators in a  $q$ -deformed model.

### 3.3.2 The Parking Lot Problem

Another possible application is the filling of a parking lot with cars. This problem belongs to a class of waiting and queuing line problems [42]. On the other hand, one can regard it as a general birth and death process as well. Supposing a parking lot with  $s$  places is given. The cars should be enter with the rate  $\lambda$  independently of the number of already parking cars, but only as empty space is available. Hence, the probability for a non-arriving of a car within a time period is exponentially distributed (Poisson type). Every car can leave the lot with the probability  $\kappa$ . Imagine one has a narrow lot so that cars can block each other. For a sufficiently small number  $n$  of cars (in comparison to the maximum number of sites) they can be considered as fairly-independently from each other, so the rate is  $\kappa n$  that one car can leave. For a more occupied lot the cars obstruct themselves, thus the rate is not longer proportional to  $n$ . For a almost full lot only  $s+1-n$  cars can independently leave the parking lot. Hence, the releasing rate is given in a rough interpolation by

$$\kappa \frac{\sin\left(\frac{n\pi}{s+1}\right)}{\sin\left(\frac{\pi}{s+1}\right)} = \kappa |[n]|. \quad (3.144)$$

If  $P(n, t)$  denotes the probability that  $n$  cars park at the lot at time  $t$  then the basic differential equation takes the form

$$\begin{aligned} \partial_t P(n, t) = & \kappa [|n+1| P(n+1, t) - |n| P(n, t)] \\ & + \lambda [P(n-1, t) - P(n, t)(1 - \delta_{n,s})] \end{aligned} \quad (3.145)$$

which we will recover below. Due to the restriction and the symmetric-deformed number  $|n|$  one gets a truncate general Poisson process.

### 3.3.3 A $q$ -deformed Evolution Process

Now, I will try to recover the equation of interest of the preceding sections by introducing  $q$ -deformed operators, deriving the assigned master equation and showing its equivalence to the master equations (3.141) and (3.145). The present  $q$ -deformed model is an extension of the usual spin-flip model using Glauber dynamics introduced in the corresponding subsection above. The idea to study such a model stems from a  $q$ -deformed pore model [24]. Whereas  $q$  is a real number in this paper,  $q$  is set to be a root of unity here. The dynamics is restricted to only one site enables us to neglect the lattice index. But I want to allow that this site can possess  $s+1$  different states which may be assigned to e.g. the number of adsorbed particles or parking cars. Further, it is assumed that only one particle or car can be added with the probability  $\lambda\Delta t$  within a time period  $\Delta t$ . However, cars or particles can be ejected from the system with a state-dependent probability  $|n|\kappa\Delta t$ , i.e. the decay of the state  $n$  is sinusoidally driven.

Equivalently, one may consider the process as a random walk of one particle (indicating the maximal occupied state) in a chain of  $(s+1)$  different sites where the particle can hop with different rates to both sides. The system is closed in this sense that the particle can never leave. Additionally, the hopping rates should depend on the state for the decreasing process whereas the increasing rate is state-independent.

In analogy to the usual spin-flip model I start with the one-step ( $n=1$ ) generating process  $\hat{L}_{o,G}^1$  in (2.102) where  $\hat{O}$  is chosen in such a way that the last state  $s$  is excluded. The decreasing part is the annihilation operator  $\hat{L}_{o,A}^1$  in (2.114) neglecting the inverse of the number operator  $|\hat{Z}_{n+1}|$  (indicated by the prime) and excluding the state 0. Summing up both dynamics by paying attention to the rates yields

$$\begin{aligned} \hat{L}_{GA}^1 &= \lambda \hat{L}_G^1(\hat{i} - \hat{S}) + \kappa (\hat{L}'_A)^1(\hat{i} - \hat{O}) \\ &= (\hat{C}_+ - \hat{i})[\lambda(\hat{i} - \hat{S}) - (\bar{r}\kappa) \hat{c}_-(\hat{i} - \hat{O})]. \end{aligned} \quad (3.146)$$

Converting the time evolution operator in terms of the  $q$ -statistics (where  $q$  is a

simple root of unity) reads

$$\hat{L}_{GA}^1 = - \left( \frac{\hat{b}_-^\dagger}{\bar{r}} + \frac{(\bar{r}\hat{b}_-)^s}{|[s]|!} - \hat{i} \right) \left( (\bar{r}\kappa)\hat{b}_- - \lambda \left( \hat{i} - \frac{\hat{b}_-^\dagger \hat{b}_-^s}{|[s]|!} \right) \right). \quad (3.147)$$

Before I will continue to explore the time evolution operator for arbitrary  $s$  it seems interesting to regard two limit cases. To get the case  $s \rightarrow 1$ , i.e. the fermion limit, one may conclude from Eqs.(2.104) and (2.116). Denoting the variables for the simplification as

$$\begin{aligned} \hat{b}_- &= \hat{a} \text{ and} \\ \hat{b}_-^\dagger &= \hat{a}^\dagger, \end{aligned} \quad (3.148)$$

one can easily reproduce the evolution operator of the fermion Glauber dynamics (compare e.g. [14])

$$\lambda (\bar{r}^{-1} - \hat{a}) \hat{a}^\dagger + \kappa (\bar{r} - \hat{a}^\dagger) \hat{a}. \quad (3.149)$$

The other case is  $s \rightarrow \infty$ , i.e. the boson limit of the  $q$ -statistics. Simplifying again like in (3.148) and applying the Eqs.(2.96) and (2.110) the evolution operator results in the known form of the boson Glauber dynamics (compare e.g. [6])

$$\lambda (\bar{r}^{-1} \hat{a}^\dagger - \hat{i}) + \kappa (\bar{r} - \hat{a}^\dagger) \hat{a}. \quad (3.150)$$

Returning to the general case the evolution can be expressed by the transfer matrix ( $M_m^n$ ) as defined in (2.71)

$$\begin{aligned} (M_m^n) &= \hat{L}_{GA}^1 \frac{\langle r|n\rangle}{\langle r|m\rangle} \\ &= \begin{pmatrix} -\lambda & \kappa |[1]| & \cdots & 0 & 0 \\ \lambda & -(\lambda + \kappa |[1]|) & \ddots & 0 & 0 \\ \vdots & \ddots & \ddots & \ddots & \vdots \\ 0 & 0 & \ddots & -(\lambda + \kappa |[s-1]|) & \kappa |[s]| \\ 0 & 0 & \cdots & \lambda & -\kappa |[s]| \end{pmatrix}. \end{aligned} \quad (3.151)$$

Using the probability evolution equation (2.71) the one-step master equation of the probability follows immediately

$$\begin{aligned} \partial_t P(n, t) &= \kappa |[n+1]| P(n+1, t) - |[n]| P(n, t) \\ &\quad + \lambda [P(n-1, t) - P(n, t) (1 - \delta_{n,s})]. \end{aligned} \quad (3.152)$$

This equation is equivalent to Eq.(14) in [24] if one replaces  $|[n]|$  by  $[n]$ , sets  $q$  real and neglects the boundary. Moreover, it is identical with the master equation of

the parking lot problem (3.145). Naturally, the master equation includes only real parameters if the kinetic coefficient as well as the eigenvalues of the symmetric-deformed number operator are real. The transition rates towards smaller states depend on  $n$  whereas the rates to larger states remain constant. The probability current between two neighbored  $n$  is then given by

$$J_n^{n+1} = -\kappa |[n+1]| P(n+1, t) + \lambda P(n, t), \quad (3.153)$$

hence one can rewrite the time derivative of the probability in form of an equation of continuity

$$\partial_t P(n, t) = J_{n-1}^n - J_n^{n+1}. \quad (3.154)$$

Since absorbing and injecting states do not exist all currents are zero if the system is stationary, i.e.  $\partial_t \bar{P}(n, t) = 0$ . Therefore, from  $J_n^{n+1} = 0$  follows immediately the detailed balance condition

$$\frac{\bar{P}(n+1)}{\bar{P}(n)} = \frac{M_n^{n+1}}{M_{n+1}^n} = \frac{\lambda}{\kappa |[n+1]|} \quad (3.155)$$

where  $\bar{P}(n)$  denote the equilibrium probabilities. The detailed balance condition leads to the stationary solution of the master equation (3.152). Thus, the equilibrium solution and the probability distribution satisfying the detailed balance are equivalent. The equilibrium probabilities may be expressed by

$$\bar{P}(n) = P_0^{-1} \left( \frac{\lambda}{\kappa} \right)^n \frac{1}{|[n]|!} \quad (3.156)$$

with the normalization

$$P_0^{-1} = \left[ \sum_{n=0}^s \left( \frac{\lambda}{\kappa} \right)^n \frac{1}{|[n]|!} \right]^{-1} := \overline{\exp}_j^{-1} \left( \frac{\lambda}{\kappa} \right) \quad (3.157)$$

guaranteeing that the sum  $\sum_{n=0}^s \bar{P}(n) = 1$ . The function  $\overline{\exp}_j(x)$  is the symmetric  $q$ -deformed exponential function in contrast to (2.34). For the boson limit  $s \rightarrow \infty$   $|[n]|!$  approaches the ordinary factorial and  $\bar{P}(n)$  becomes the Poisson distribution. Hence, one can consider  $\bar{P}(n)$ , sketched in Fig. 3.14 for  $s = 7$ , as a generalized (or truncated) Poisson distribution. As shown for small enough  $\tilde{N} := \frac{\lambda}{\kappa}$  (small injections rates) the equilibrium distributions behaves similar to a Poisson distribution. The number of particles (or cars) remains small against the number of possible places. The particles or cars do not "feel" the restriction of the finite system and behave quite independently from each other. The maximum remains near 0. However, if the injection rate increases the distribution shows significant deviations. The equilibrium distribution  $\bar{P}(n)$  can establish two local maxima in a medium range of the parameter  $\tilde{N}$ , one for small  $n$  and the other at the boundary like present here

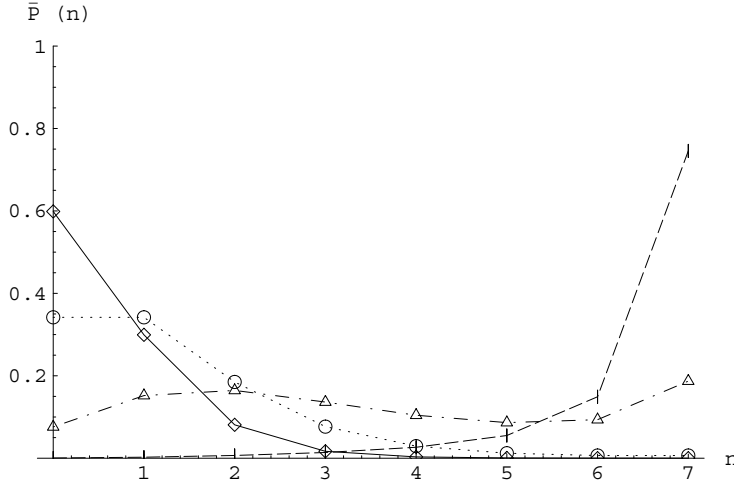


Figure 3.14: Equilibrium distribution  $\bar{P}(n)$  for  $s = 7$ . The lines are only inserted to guide the eyes. The ratio  $\tilde{N}$  is 0.5 (straight line/diamonds), 1 (dot line/circles), 2 (dot-dash line/triangles) and 5 (dash line/dashes).

for  $\tilde{N} = 2$ . The non-boundary maximum vanishes if  $\tilde{N}$  is further increased. The system is most probably in the highest states, the parking lot would be completely full the most time.

Another interesting quantity is the expectation value of the occupation number of adsorbed particles (or parked cars),  $\bar{N}$ , in the equilibrium which is given by

$$\bar{N} = P_0^{-1} \sum_{n=0}^s \left( \frac{\lambda}{\kappa} \right)^n \frac{n}{|[n]|!}. \quad (3.158)$$

$\bar{N}$  is shown for different maximal numbers  $s$  in Fig. 3.15. For small  $\tilde{N}$  all curves reflect the more or less bosonic property of the system (the curve corresponding to the boson limit is the asymptote for small  $\tilde{N}$ ). For increasing  $\tilde{N}$  all graphs apart from the curve for  $s = 2$  establish an inflection point  $N_I$  representing the transition from the boson-like behavior to the fermion-like behavior which is an indication for the finiteness of the system. The line of all inflection points is presented in Fig. 3.16. For small  $s$  the transition line to the fermion-like behavior has a slope of roughly  $\frac{1}{3}$ . For large systems the transition line approaches  $N_I = 1 + \frac{1}{5}s$ . Below this line the system can be fairly considered as a boson system where the cars or particles do not obstruct each other. But at relative low limit the mutual independence is lifted and the system must be considered as a fermion-like system. Naturally,  $\bar{N}$  approaches  $s$  if  $\tilde{N}$  goes to infinity.

For large  $s$  and  $n \neq s$  one may approximate the equation of the evolution (3.152)

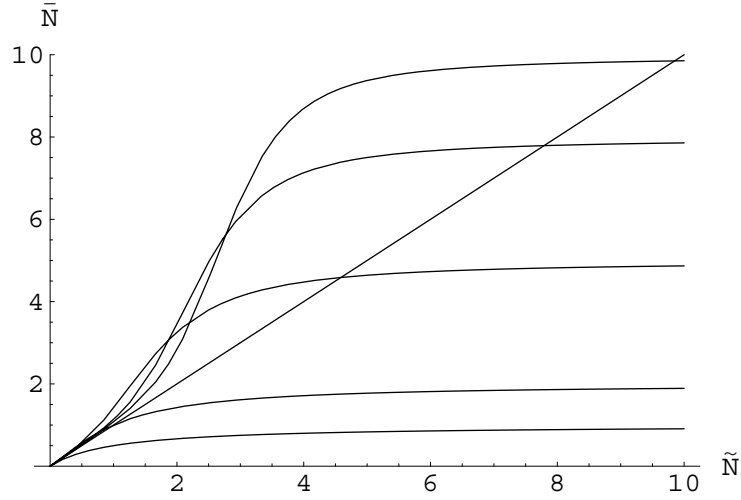


Figure 3.15: Static expectation value  $\bar{N}$  as function of  $\tilde{N}$  for different  $s$  (from bottom to the top: 1, 2, 5, 8, 10). The straight line is the boson limit corresponding to  $s \rightarrow \infty$ .

in a continuum Kramers-Moyal form. Then one gets for  $n$  far from the boundaries

$$\partial_t P(n, t) = -\partial_n [v(n) P(n, t)] + \frac{1}{2} \partial_n^2 [D(n) P(n, t)] \quad (3.159)$$

where the generalized velocity and the diffusion coefficient are given by

$$v(n) = \lambda - \kappa |[n]| \quad \text{and} \quad D(n) = \lambda + \kappa |[n]|. \quad (3.160)$$

### 3.3.4 The Equation of Evolution of the Number Operator

As already mentioned above, the expectation value of the number operator reveals the information about the adsorbed particles or parked cars. Therefore, it is preferable to possess its equation of motion. To create it I exploit the time evolution operator of the  $q$ -deformed model (3.147) and apply the relations for the expectation values (2.93). Therefore, the time evolution of the expectation value for a quantity  $\hat{G}$  is given by

$$\partial_t \langle \hat{G}\{\hat{N}\} \rangle = \langle \hat{G}\{\hat{N}\} \hat{L}_{GA}^1 \rangle. \quad (3.161)$$

The straight forward calculation yields the exact expression for its time evolution of the  $q$ -deformed model

$$\begin{aligned} \partial_t \langle \hat{G}\{\hat{N}\} \rangle &= \lambda \langle (1 - \hat{S})(\hat{G}\{\hat{N} + 1\} - \hat{G}\{\hat{N}\}) \rangle \\ &\quad - \kappa \langle (\hat{G}\{\hat{N}\} - \hat{G}\{\hat{N} - 1\}) |[[\hat{N}]] \rangle. \end{aligned} \quad (3.162)$$

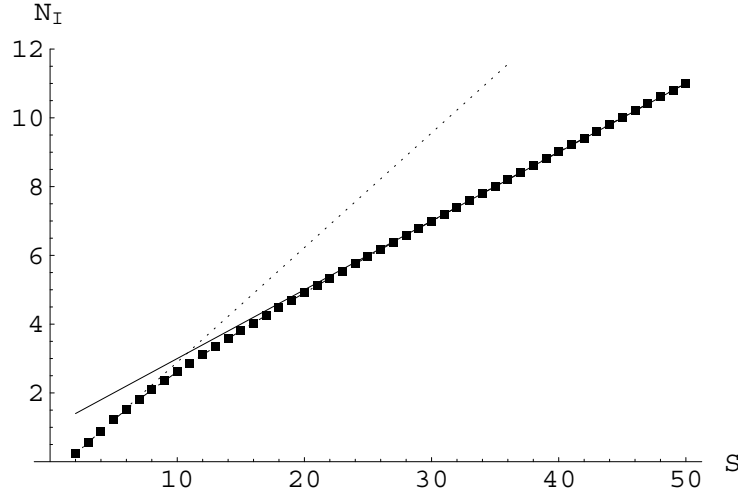


Figure 3.16: Limit line (given by the inflection points  $N_I$ ) between the boson-like behavior (below the line) and the fermion-like behavior (above the line) of the system as a function of  $s$ . The squares indicate integer values of  $s$ . The lines between them should only guide the eyes and do not represent the real physical value for the fractional  $s$  at this point (this is a more complicate curve). The asymptote for small  $s$  has the slope  $\frac{1}{3}$ . For large enough  $s$  the curve approaches  $N_I = 1 + \frac{s}{5}$ .

In general, this equation leads to the start point of an infinite hierarchy of equations. As one can recognize the time derivative of the expectation value  $\langle \hat{N}^m \rangle$  produces higher order terms  $\langle \hat{N}^{m'} \rangle$  with  $m' \geq m$  on the right hand side. Therefore, one has to determine the temporal development of the expectation values of these quantities as well. It usually leads to an infinite number of equations. One way out to achieve at least an approximative solution is to break up higher correlations and to get a closed system of equations. The price paying for this is to partially neglect the influence of fluctuations in the system. E.g. one obtains for two arbitrary quantities  $G_1$  and  $G_2$  the relation

$$\langle G_1 G_2 \rangle - \langle \delta G_1 \delta G_2 \rangle = \langle G_1 G_2 \rangle - \langle (G_1 - \langle G_1 \rangle) (G_2 - \langle G_2 \rangle) \rangle = \langle G_1 \rangle \langle G_2 \rangle \quad (3.163)$$

leading in lowest order to

$$\langle G_1 G_2 \rangle \simeq \langle G_1 \rangle \langle G_2 \rangle. \quad (3.164)$$

If it is important to take correlations into account simple mean-field theory is not sufficient. Then it is more sophisticate to include higher order correlation functions.

If one identifies the operator  $\hat{G}$  with the number operator itself, i.e.  $\hat{G}\{\hat{N}\} = \hat{N}$ , the equation of evolution takes the form

$$\partial_t \langle \hat{N} \rangle = \lambda \langle (1 - \hat{S}) \rangle - \kappa \langle |[\hat{N}]| \rangle. \quad (3.165)$$

As one can recover this time evolution is completely equivalently to the equation of the deposition-desorption model (3.141). Hence, the  $q$ -deformed operators allow a proper description of this phenomenon.

Firstly, it seems interesting to check the limits for the spectrum of  $q$ . In case of  $s = 1$  (fermion limit) one obtains the time evolution

$$\partial_t \langle \hat{N} \rangle = \lambda - (\kappa + \lambda) \langle \hat{N} \rangle = \tau_{q=-1}^{-1} [\bar{N}_{q=-1} - \langle \hat{N} \rangle] \quad (3.166)$$

bearing in mind the equivalence  $\hat{S} \equiv \hat{N}$ . This differential equation is easy to solve resulting in

$$\langle \hat{N}(t) \rangle = (N(0) - \bar{N}_{q=-1}) \exp\left(-\frac{t}{\tau_{q=-1}}\right) + \bar{N}_{q=-1} \quad (3.167)$$

with the initial value at time zero  $N(0)$ . The typical time scale where the system equilibrates is given by the relaxation time

$$\tau_{q=-1} = (\kappa + \lambda)^{-1}. \quad (3.168)$$

The system approaches the equilibrium value

$$\bar{N}_{q=-1} = \frac{\lambda}{\kappa + \lambda} \quad (3.169)$$

if the time goes to infinity in case  $N(0) \neq \bar{N}_{q=-1}$ . The fermion case poses not much sense for the deposition-desorption model or for the parking lot problem, but gives us the dynamics of a spin system flipping between two states only. The rates  $\lambda$  and  $\kappa$  are usually temperature-dependent so that the two states are occupied according to the temperature.

Considering instead the master equation for  $s = \infty$  (boson limit) leads to a slightly different equation of evolution

$$\partial_t \langle \hat{N} \rangle = \lambda - \kappa \langle \hat{N} \rangle = \tau_{q=1}^{-1} [\bar{N}_{q=1} - \langle \hat{N} \rangle]. \quad (3.170)$$

Here, the fact of the non-existence of a highest state was used. Notice, that the system possesses still a lower boundary 0. The solution has the same form like in the fermion case (3.167) but with a different relaxation time

$$\tau_{q=1}^{-1} = \kappa \quad (3.171)$$

and a different equilibrium expectation value

$$\bar{N}_{q=1} = \frac{\lambda}{\kappa}. \quad (3.172)$$

As expected for the Poisson process the equilibrium number of particles is the ratio of the rates. The process equilibrates faster than the two level system does due to



the missing upper limit of the states. Herein these both cases, it was not a serious problem to gain a dynamical solution. However, the general solution of Eq.(3.165) reveals as more complicated.

Obviously, that the equilibrium expectation values computed by means of  $\bar{P}(n)$  in (3.156) actually fulfil the stationary condition of the equation of evolution (3.165). The equilibrium solution  $\bar{N}$  is given if

$$\partial_t \langle \bar{N} \rangle = \tilde{\tau}^{-1} \left( \tilde{N} \langle 1 - \bar{S} \rangle - \langle |[\bar{N}]| \rangle \right) = 0 \quad (3.173)$$

where  $\tilde{\tau}^{-1} = \kappa$  and  $\tilde{N} = \frac{\lambda}{\kappa}$  like introduced above. As one can recognize both parameters seem identical to those in the boson case, but they indicate neither the equilibrium solution nor the relaxation time.

Only if one neglects the upper boundary  $\bar{S} = 0$ , it follows the stationary solution of (3.165)

$$|[\bar{N}]| = \tilde{N} \quad (3.174)$$

of which special case ( $q = 1$ ) one could see above. This result is solely valid if the occupancy of the last state can be ignored. I.e. the parameter ( $\kappa$  and  $\lambda$ ) and the initial condition must be chosen in such a way that the higher states will be rarely involved in the dynamics.

Returning to the equilibrium solution (3.173)  $|[\bar{N}]|$  is the expectation value of the symmetric-deformed number operator in the thermal equilibrium (3.156),

$$|[\bar{N}]| = \sum_{m=0}^s |m| \bar{P}(m) = P_0^{-1} \sum_{m=1}^s \frac{\tilde{N}^m}{|[m-1]|!}. \quad (3.175)$$

On the other hand, the equilibrium expectation value of the projector  $\hat{S}$  is found,

$$\bar{S} = P_0^{-1} \sum_{m=0}^s \delta_{m,s} \bar{P}(m) = P_0^{-1} \frac{\tilde{N}^s}{|[s]|!}. \quad (3.176)$$

Therefore, the central term in (3.173) vanishes in case of the equilibrium solution, i.e.

$$\tilde{N} (1 - \bar{S}) - |[\bar{N}]| = P_0^{-1} \left( \tilde{N} P_0 - \tilde{N} \frac{\tilde{N}^s}{|[s]|!} - \sum_{m=1}^s \frac{\tilde{N}^m}{|[m-1]|!} \right) = 0. \quad (3.177)$$

As expected the system being in the thermal equilibrium fulfils the stationary master equation (3.173) .

### 3.3.5 The Decomposition of Projectors and Number Operators

One possible way evaluating the evolution equation (3.165) is to find a unique expansion of  $\hat{S}$  and  $[[\hat{N}]]$  in terms of the ordinary number operator  $\hat{N}$ , i.e.

$$\hat{S} = \sum_{m=0}^s \sigma_m \hat{N}^m \quad \text{and} \quad [[\hat{N}]] = \sum_{m=0}^s \nu_m \hat{N}^m. \quad (3.178)$$

Obviously, the symmetry of the symmetric-deformed number operator,

$$[[\hat{N}]] = [[\hat{S} + 1 - \hat{N}]], \quad (3.179)$$

should be reflected in the  $\nu_m$ . The coefficient  $\nu_0$  is always zero in due to the properties of the number operator

$$[[\hat{N}]]|0\rangle = \hat{N}^m|0\rangle \equiv 0. \quad (3.180)$$

The same argument also holds for  $\sigma_0$ . There is always a unique solution of (3.178) if the determinant

$$Det_0 \equiv \det \begin{pmatrix} 1 & 1^2 & \dots & 1^s \\ 2 & 2^2 & \dots & 2^s \\ \vdots & \vdots & \ddots & \vdots \\ s & s^2 & \dots & s^s \end{pmatrix} \quad (3.181)$$

and all determinants  $Det_m$ , wherein the  $m$ th column of  $Det_0$  is substituted by numbers from 1 to  $[[s]]$ , remain non-zero. Then the coefficients of the expansion  $\nu_m$  can be read off

$$\nu_m = \frac{Det_m}{Det_0}. \quad (3.182)$$

The denominator determinant  $Det_0$  can be calculated to  $\prod_{m=1}^s m!$ . The numerator determinant  $Det_m$  is revealed as more complicated and has to be calculated for every special case. For instance, taking the case  $s = 2$  yields the decomposition of the symmetric-deformed number operator

$$[[\hat{N}]]_{s=2} = -\frac{1}{2}\hat{N}(\hat{N} - 3). \quad (3.183)$$

In same manner one may exercise to compute  $\sigma_m$  replacing the  $m$ th column of  $Det_0$  by zeros apart from the last element equal to 1. In this sense one can rewrite the master equation (3.165) including only terms of powers of the ordinary number operator  $\langle \hat{N}^k \rangle$ .

### 3.3.6 The $q$ -deformed Evolution Process for $s = 2$

To illustrate the approach by using the decomposition in terms of the ordinary number operator, the computation should be demonstrated for the simplest non-trivial  $s = 2$ . Specifying the representations for the last-state projector and the symmetric-deformed number operator,

$$\hat{S}_{s=2} = \frac{1}{2}\hat{N}(\hat{N} - 1) \text{ and } |[\hat{N}]|_{s=2} = -\frac{1}{2}\hat{N}(\hat{N} - 3), \quad (3.184)$$

and applying these series, the master equation (3.165) transforms into

$$\partial_t \langle \hat{N} \rangle = -\frac{1}{2\tilde{\tau}} [(\tilde{N} - 1)\langle \hat{N}^2 \rangle - (\tilde{N} - 3)\langle \hat{N} \rangle - 2\tilde{N}]. \quad (3.185)$$

Further, setting the equation of evolution to zero yields a relation for the equilibrium expectation values  $\overline{N^k}$

$$(\tilde{N} - 1)\overline{N^2} - (\tilde{N} - 3)\bar{N} - 2\tilde{N} = 0. \quad (3.186)$$

Because this equation is still exact the equilibrium values of the higher moments of the number operator

$$\overline{N^k} = P_0^{-1} \sum_{m=0}^s \tilde{N}^m \frac{m^k}{|[m]|!} \quad (3.187)$$

satisfy the stationary solution with the replacements  $\bar{N}$  by  $\frac{2\tilde{N}^2 + \tilde{N}}{\tilde{N}^2 + \tilde{N} + 1}$  and  $\overline{N^2}$  by  $\frac{4\tilde{N}^2 + \tilde{N}}{\tilde{N}^2 + \tilde{N} + 1}$ .

#### Stationary Solution ( $s = 2$ )

In order to check the quality of an approximative solution (here mean-field) I want to commence with the exploration of the stationary case. Its solution should be nearly coincident with the solution getting from the equilibrium expectation values (3.187).

The mean-field approach (3.164) breaks up all correlations and neglects therefore the influence of the fluctuations. Now, one will see as this approximation alters the exact result. The stationary form in (3.186) has a singularity at point  $\tilde{N} = 1$  leading to the unique solution  $\bar{N} = 1$  where the mean-field solution coincides with the exact solution. In all other points,  $\tilde{N} \neq 1$ ,  $\overline{N^2}$  is broken up into  $\bar{N}_{MFA}^2 \equiv \bar{N}^2$  leading to two roots

$$N_{MFA}^{\pm} = \frac{1}{2(\tilde{N} - 1)} [(\tilde{N} - 3) \pm \sqrt{(\tilde{N} - 3)^2 + 8\tilde{N}(\tilde{N} - 1)}]. \quad (3.188)$$

The negative branch shows a real singularity at  $\tilde{N} = 1$  whereas the positive branch has a liftable singularity at this point which is shown in Fig. 3.17. One can recognize

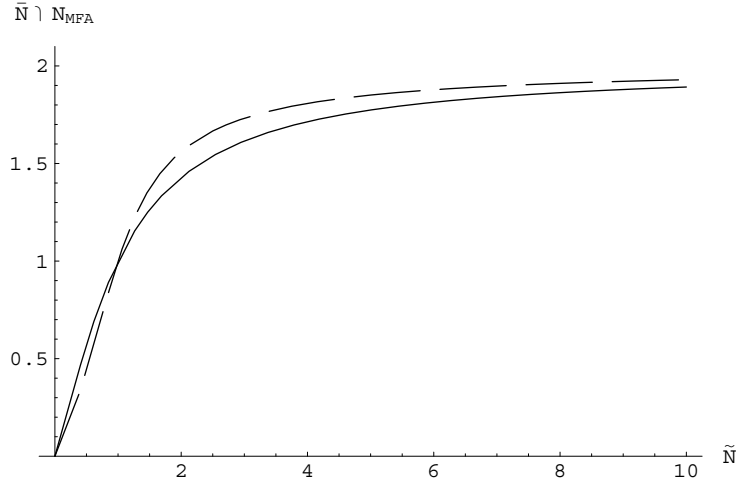


Figure 3.17: The comparison between the stationary solution  $\bar{N}$  (straight line) and its mean-field approximation  $N_{MFA}^+$  (dash line) as a function of  $\tilde{N}$  for  $s = 2$ . The intersection point is the singularity at  $\tilde{N} = 1$ .

that the approximation shows only a small deviation from the right value  $\bar{N}$ . Therefore, the stationary mean-field solution reflects the stationary behavior of the system in an adequate manner. Additionally, only the positive branch proves as a physically sensible solution (only in this case the  $\bar{N}$  remains in the range  $0 \leq \bar{N}_{MFA} \leq 2$ ). This statement can be supported by the linear stability analysis. Making the ansatz with a small deviation  $\delta N(t)$  around the expectation value

$$\langle \hat{N}(t) \rangle = \bar{N}_{MFA}^{\pm} + \delta N(t) \quad (3.189)$$

setting in (3.186) leads to a simple differential equation. Its solution is given by

$$\delta N(t) = \delta N(0) \exp\left(\mp \frac{1}{2} \sqrt{R} \frac{t}{\tau}\right) \quad (3.190)$$

with  $R = (\tilde{N} - 3)^2 + 8\tilde{N}(\tilde{N} - 1)$  as the root in (3.188). The upper sign is related to the positive branch whereas the lower sign is related to the negative branch. Hence, small perturbations will be averaged in the former case leading to the stable solution.

### Dynamic Solution ( $s = 2$ )

The more interesting task remains to gain information about the temporal evolution of the system, to solve Eq.(3.165). Unfortunately, only one of the eigenvalues of the matrix (3.151) is known for all  $s$  and equals zero due to conservation of the total probability. It seems impossible to determine analytically the other eigenvalues as

well as to find another exact solutions in general case for  $s > 4$ . Instead using the mean-field approach again results in the solution

$$N_{MFA}(t) = \bar{N}_{MFA}^{\pm} + \frac{\sqrt{R}}{2(\tilde{N} - 1)} \times \left( \frac{\tanh\left[\frac{\sqrt{R}t}{4\tilde{\tau}}\right] \mp 1 + \frac{2(\tilde{N}-1)}{\sqrt{R}}(N(0) - \bar{N}_{MFA}^{\pm})}{1 - \tanh\left[\frac{\sqrt{R}t}{4\tilde{\tau}}\right] \left[\mp 1 + \frac{2(\tilde{N}-1)}{\sqrt{R}}(N(0) - \bar{N}_{MFA}^{\pm})\right]} \pm 1 \right) \quad (3.191)$$

where  $N_{MFA}^{\pm}(t) = \langle \hat{N}(t) \rangle$  in mean-field approximation and  $N(0)$  is the initial condition. In Fig. 3.18 (with the initial condition  $N(0) = 0$ ) one may recognize the smooth approach of the mean-field solution to its stationary value  $\bar{N}_{MFA}^+$ .

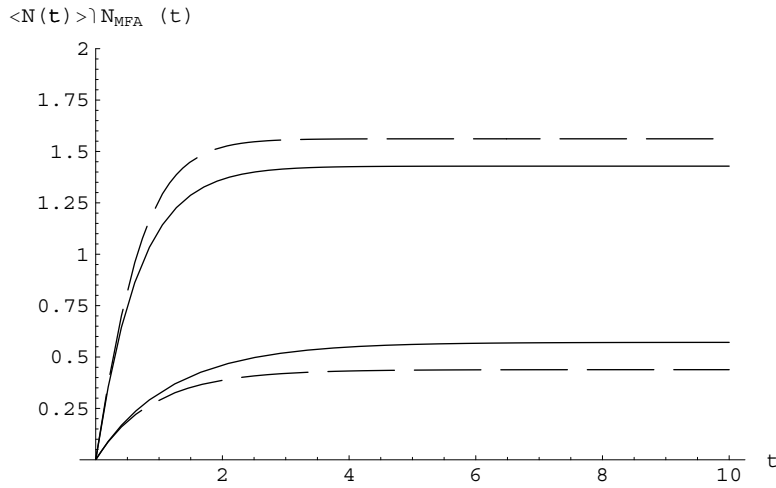


Figure 3.18: The comparison between the dynamic expectation value  $\langle N \rangle$  (straight lines) and its mean-field approximation  $N_{MFA}^+(t)$  (dash lines) as a temporal function (scaled time  $\frac{t}{\tilde{\tau}}$  with  $\tilde{\tau}$  set to unity) for  $s = 2$ . The both upper curves represent  $\tilde{N} = 2$  whereas the both lower curves sketch the evolution for  $\tilde{N} = 0.5$ .

Naturally, that  $N_{MFA}(t) \equiv \bar{N}_{MFA}^{\pm}$  remains for all times if one sets the initial value to the stationary solution. If one analytically computes the solution in the infinite time limit the mean-field equilibrium solution  $\bar{N}_{MFA}^+$  follows. In the singular point  $\tilde{N} = 1$ ,  $N_{MFA}^{\pm}(t)$  can be simplified to

$$N_{MFA}(t) = \bar{N}_{MFA}^{\pm} + (N(0) - \bar{N}_{MFA}^{\pm}) \exp\left(\mp \frac{t}{\tilde{\tau}}\right). \quad (3.192)$$

Physically relevant is only the upper sign. The next step is to determine the exact result to check the quality of the mean-field approach. Because of unique representations of pure states 2 and 0 these initial conditions are ideal to compare the exact

solution with its approximation. Therefore, the variance for pure states 2 and 0 at the start point are zero according to the idea of the mean-field analysis to neglect all fluctuations. The exact solution, e.g. for the initial state 0, is given by

$$\begin{aligned} \langle N(t) \rangle &= \bar{N} - \bar{N} \exp\left(-\left(1 + \tilde{N}\right) \frac{t}{\tilde{\tau}}\right) \cosh\left(\sqrt{\tilde{N}} \frac{t}{\tilde{\tau}}\right) \\ &\quad - \frac{\sqrt{\tilde{N}}(2\tilde{N} + \tilde{N}^2)}{1 + \tilde{N} + \tilde{N}^2} \exp\left(-\left(1 + \tilde{N}\right) \frac{t}{\tilde{\tau}}\right) \sinh\left(\sqrt{\tilde{N}} \frac{t}{\tilde{\tau}}\right). \end{aligned} \quad (3.193)$$

This result can be directly derived from the expansion of the probability vector using the eigenvalues of the matrix (3.151)

$$\begin{aligned} \vec{P}(t) = \begin{pmatrix} P(0,t) \\ P(1,t) \\ P(2,t) \end{pmatrix} &= c_1 \begin{pmatrix} \tilde{N}^{-1} \\ 1 \\ \tilde{N} \end{pmatrix} \\ &+ c_2 \begin{pmatrix} -\sqrt{\tilde{N}^{-1}} \\ -1 + \sqrt{\tilde{N}^{-1}} \\ 1 \end{pmatrix} \exp\left(-\left(1 + \tilde{N} - \sqrt{\tilde{N}}\right) \frac{t}{\tilde{\tau}}\right) \\ &+ c_3 \begin{pmatrix} \sqrt{\tilde{N}^{-1}} \\ -1 - \sqrt{\tilde{N}^{-1}} \\ 1 \end{pmatrix} \exp\left(-\left(1 + \tilde{N} + \sqrt{\tilde{N}}\right) \frac{t}{\tilde{\tau}}\right). \end{aligned} \quad (3.194)$$

The parameter  $c_1$  can be obtained from the normalization condition

$$\sum_{n=0}^2 P(n,t) = 1. \quad (3.195)$$

and the other both coefficients directly stem from the initial condition. Regarding the Fig. 3.18 and comparing mean-field solution and the exact solution shows an almost equivalent behavior in the time regime for the initial value  $N(0) = 0$ , there is only a small deviation from the exact solution. Hence, the mean-field approximation well describes not only the statics but also the temporal evolution of the system.

### 3.3.7 Conclusions

Using  $q$ -deformed operators in a generalized flip model or birth-death model one recovers a master equation which is applicable to problems of the surface growth or the queuing. Its stationary state can be exactly calculated. One obtains a generalized Poisson distribution which is similar to the ordinary Poisson distribution for small parameters  $\tilde{N}$  but shows strong deviations for medium  $\tilde{N}$  (two local maxima) and for large  $\tilde{N}$  (maximum at the upper boundary). Unfortunately, a direct, dynamical solution of the master equation by exploring e.g. a generating function or

the eigenvalues of the matrix seems impossible for high enough  $s$ . As one potential way out it remains approximative computations like mean-field theory. It could be demonstrated in case of  $s = 2$  that this approximation can provide sufficiently exact results. Moreover, it can be supposed supported by further calculations that the mean-field approach qualitatively yields valid results also for higher maximum states  $s$ . The difficulty remains to figure out the right root of the solution.

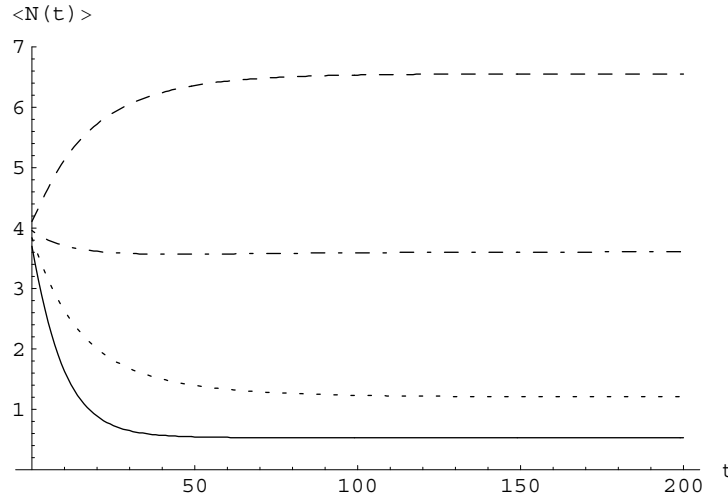


Figure 3.19: Computer simulation ( $s = 7$ ) for the temporal evolution of  $\langle N \rangle$  for different values of  $\tilde{N} = 0.5$  (straight line), 1 (dot line), 2 (dot-dash line) and 5 (dash line).  $t$  represents the number of discrete time steps.  $N(0) = 4$  for all curves.

Numerical simulations are an additional mean to reveal dynamical and stationary properties of the system as presented in Fig. 3.19. In this figure the dynamical solution of the evolution equation (3.165) for the case  $s = 7$  is depicted of which equilibrium solution was shown in Fig. 3.14. The corresponding curves are indicated by the same type of lines. As the most interesting case it reveals  $\tilde{N} = 2$ , bearing in mind that the corresponding equilibrium solution possesses two local maxima. Starting from the pure state  $N(0) = 4$  the system mainly develops in direction to the local maximum at 2, so that the expectation value firstly decreases under the stationary state  $\tilde{N}$ . After a short while the system "realizes" that there is another preferable state at the boundary which is further away from the start point than the first maximum. Therefore,  $\langle N \rangle$  increases again to approach the stationary state. In the numerical simulation only small rates are applied because then they can be approximated by probabilities in an equivalent discrete model. To make the simulations effectively depend only on one parameter  $\tilde{N}$  the product of the both kinetic parameter  $\lambda$  and  $\tilde{z}$  is kept constant ( $\lambda \tilde{z} = 0.1$ ). All other curves show similar slopes like studied already in the  $s = 2$  case.

In general,  $q$ -deformed models possess the exciting property to interpolate be-

tween a fermion-like and a boson-like behavior of the system. Therefore it exist the hope that this kind of models can find a wide range of applications in physics, chemistry and biology.



### 3.4 Functional Integral of a $q$ -deformed Object

A striking method for computation in statistical physics is the application of functional integral (path integral). Firstly thought for applications in quantum theory the functional integral developed into a universal tool with a wide range of usage. Surveys about this topic are given e.g. by Feynman [43], Kleinert [44], Zinn-Justin [116] and Negele [117]. Functional integrals can help to calculate the transition probabilities and correlation functions. So e.g. the propagator of an ordinary motion of a free particle can be computed by functional integrals (see e.g. [44]). Naturally, it seems attractive to ask for the propagator of a motion of a particle which is  $q$ -deformed. Moreover, the knowledge that particles obeying the Newtonian equation of motion can be transformed to the harmonic oscillator ([45–47]) arises the question after a more general relation between a deformed motion and general oscillators. As one will see the motion of a particle undergoing the free  $q$ -deformed equation of motion can be actually related to a pulsed oscillator. Both different objects can be combined to one  $q$ -deformed object of which propagator can be computed. The special cases of the general propagator like the free particle can be recovered again.

A periodically pulsed oscillator (with period  $T_P$ ) should be explored [118] in this section sharing certain common properties with the  $q$ -deformed motion of a free particle. Astonishing, the two systems are characterized by the same common deformation parameter  $q$ , and reduce to a usual free particle as  $q$  tends to unity in the boson limit. For the deformed free particle,  $q$  is a real number, whereas for the pulsed oscillator it belongs to  $\mathbf{S}^1$ . Later the propagator for the so-called Chebyshev process will be derived from which the propagator for the  $T_P$ -evolution of the deformed free particle will be obtained.

#### 3.4.1 Introduction

The damped harmonic oscillator can be seen as a harmonic oscillator via a scale transformation (see, e.g., [119]). In the same fashion, the harmonic oscillator may be conceived as a free particle via the de Alfaro-Fubini-Furlen-Jackiw transformation [45–47],

$$\mathbf{r}(t) = \mathbf{R}(s) \sec(\omega s) \quad t = \tan(\omega s) \quad (3.196)$$

where  $s$  is a new time-like parameter.

Here, the argumentation is carried out in a slightly different manner, i.e. a  $q$ -deformed free particle may be viewed as the pulsed harmonic oscillator in a more generalized sense.

As  $q$ -deformed free particle one understands a particle obeying the  $q$ -counterpart of Newton's force-free equation of motion

$$\partial_{s,q}^2 y(s) = 0, \quad (3.197)$$

exploiting the symmetric form of the  $q$ -derivative applied to a function  $f(s)$

$$\partial_{s;q}f(s) = \frac{f(q^{\frac{1}{2}}s) - f(q^{-\frac{1}{2}}s)}{(q^{\frac{1}{2}} - q^{-\frac{1}{2}})s}. \quad (3.198)$$

The equation of motion can be written equivalently as a  $q$ -difference equation

$$q^{-\frac{1}{2}}y(qs) - (q^{\frac{1}{2}} + q^{-\frac{1}{2}})y(s) + q^{\frac{1}{2}}y(q^{-1}s) = 0, \quad (3.199)$$

where  $s$  is the time parameter. The  $q$ -free particle becomes the usual Newtonian free particle only when  $q \rightarrow 1$ .

The *pulsed harmonic oscillator* (pulsed oscillator) is not identical to the kicked harmonic oscillator (a harmonic oscillator subjected to periodic kicks), but is a free particle subject to the periodic pulses of the Hooke's force. Right after the  $m$ th pulse, when  $t = mT_P$ , it obeys the difference equation

$$x(t + T_P) - (2 - \omega^2 T_P^2)x(t) + x(t - T_P) = 0 \quad (3.200)$$

where  $\omega$  is a constant and  $T_P$  is the period of pulses.

The above two difference equations can be reduced to the recursion relation for the Chebyshev polynomials and that both the  $q$ -deformed free particle and the pulsed oscillator can be characterized by a common deformation parameter  $q$ . Later, a generic  $q$ -object (a generalized pulsed oscillator) will be introduced unifies the two systems under the condition  $q^{\frac{1}{2}} + q^{-\frac{1}{2}} \in \mathbf{R}$ . For this  $q$ -object one can compute a path integration of the  $q$ -dependent propagator and then specify for different sectors of  $q$  ( $q \in \mathbf{R}$  for  $q$ -deformed free particle and  $q \in \mathbf{S}^1$  for the pulsed oscillator). Then the caustics and the harmonic oscillator can be represented by particular values of the deformation parameter  $q$ .

### 3.4.2 The $q$ -Deformed Free Particle

In order to derive the  $q$ -deformed equation of motion one needs a derivative which fits to the  $q$ -calculus. This creates a relation to the above derived different kind of  $q$ -deformed commutators connected to  $q$ -deformed oscillators (*Biedenharn-Macfarlane oscillator* [55,56]). As mentioned above the symmetric  $q$ -derivative (or the symmetric Jackson derivative)  $\partial_{s;q}$  of a function  $f(s)$ , corresponding to the deformation (2.28), is defined by

$$\partial_{s;q}^2 f(s) = \frac{f(q^{\frac{1}{2}}s) - f(q^{-\frac{1}{2}}s)}{(q^{\frac{1}{2}} - q^{-\frac{1}{2}})s}. \quad (3.201)$$

The  $q$ -counterpart of Newton's equation in one dimension is

$$\partial_{s;q}^2 y(s) = F(y) \quad (3.202)$$

where  $F(y)$  is a force exerted to the system.

What one may be referring to as a  $q$ -deformed free particle is the system obeying the force-free equation ( $F(y) = 0$ ); the difference equation (3.199). One solution of (3.199) is indeed the usual free particle solution

$$y(s) = as + c \quad (a, c : \text{constant} \in \mathbf{R}). \quad (3.203)$$

Insofar as the time parameter  $s$  changes translationally and uniformly, the  $q$ -deformed free particle is nothing more than the ordinary free particle. Yet, the  $q$ -deformed free particle equation (3.199) differs from the difference equation corresponding to the usual force-free Newtonian equation,

$$x(t + T_P) - 2x(t) + x(t - T_P) = 0. \quad (3.204)$$

This is also a special case of the difference equation for the pulsed oscillator (3.200) with  $\omega = 0$  (where  $T_P$  is no longer the pulsing period but any finite time interval). The solution of (3.204),  $x(t) = at + b$ , is the same as (3.203) in form, but not in content unless  $q$  tends to unity because the  $q$ -free particle equation (3.199) reduces to the Newtonian form (3.204) only in the limit  $q \rightarrow 1$ .

The difference equation (3.204) dictates the time-evolution of the particle under the discrete time-translation  $t - T_P \rightarrow t \rightarrow t + T_P$ , whereas the deformed difference equation (3.199) stipulates the progression of the particle under the time-scaling  $q^{-1}s \rightarrow s \rightarrow qs$ . In fact, the time transformation [120]

$$s = q^{t/T_P} \quad (3.205)$$

with  $q \neq 0$  relates the time-translation to the time-scaling as

$$q^{\frac{1}{2}}s = q^{(t+T_P/2)/T_P}, \quad (3.206)$$

and the symmetric  $q$ -derivative to the ordinary discrete derivative as

$$\frac{y(q^{\frac{1}{2}}s) - y(q^{-\frac{1}{2}}s)}{(q^{\frac{1}{2}} - q^{-\frac{1}{2}})s} = \frac{T_P}{q^{\frac{1}{2}} - q^{-\frac{1}{2}}} \frac{y(t + T_P/2) - y(t - T_P/2)}{T_P}, \quad (3.207)$$

or more formally

$$\partial_{s;q}y(s) = \frac{T_P}{q^{\frac{1}{2}} - q^{-\frac{1}{2}}} \Delta_{t;T_P}y(t). \quad (3.208)$$

Therefore, the trajectory of a  $q$ -deformed free particle evolving with the Newtonian time  $t$  is given by

$$y(t) = aq^{t/T_P} + c. \quad (3.209)$$

In the transformation (3.205),  $q$  may be a complex number and the resulting value of  $s$  can be complex as well. However, for a real trajectory of a  $q$ -deformed free particle, as described by (3.209),  $q$  must be a real number.

Focusing the attention on the  $q$ -progression I consider  $m$  times of the  $q$ -progression from a fixed value  $s_0$  (e.g.,  $s_0 = 1$  corresponding to  $t = 0$ ) of  $s$ . This leads to

$$q^{-\frac{1}{2}}y(q^{m+1}s_0) - (q^{\frac{1}{2}} + q^{-\frac{1}{2}})y(q^m s_0) + q^{\frac{1}{2}}y(q^{m-1}s_0) = 0. \quad (3.210)$$

by substituting  $s = q^m s_0$  into (3.199). Then setting

$$u_m(q^{\frac{1}{2}}) = y(q^m s_0)/q^{\frac{m}{2}} \quad (3.211)$$

to rewrite (3.210) in the form,

$$u_{m+1}(q^{\frac{1}{2}}) - (q^{\frac{1}{2}} + q^{-\frac{1}{2}})u_m(q^{\frac{1}{2}}) + u_{m-1}(q^{\frac{1}{2}}) = 0, \quad (3.212)$$

yields the  $q$ -progress equation of the  $q$ -deformed free particle. A general solution of this equation is

$$u_m(q^{\frac{1}{2}}) = bq^{\frac{m}{2}} + cq^{-\frac{m}{2}} \quad (b, c : \text{constant}). \quad (3.213)$$

Correspondingly,

$$y(q^m s_0) = aq^m s_0 + c, \quad (3.214)$$

where  $b$  is chosen to be  $as_0$ . This solution for the  $m$ th progression is directly obtainable from (3.209) by letting  $t = t_0 + mT_P$  with  $s_0 = e^{t_0/T_P}$ . More generally, replacing  $s_0$  by  $s$ , one can write (3.214) as

$$y(q^m s) = aq^m s + c. \quad (3.215)$$

The corresponding  $m$ th step momentum,

$$p_y(q^m s) = \mu \partial_{s;q} y(q^m s) = \mu a q^m, \quad (3.216)$$

where  $\mu$  is the mass of the particle, satisfies, if divided by  $q^{\frac{m}{2}}$ , the same  $q$ -progress equation (3.212).

Noticeably, the  $q$ -progress equation (3.212) is the recursion relation for the Chebyshev polynomials of type I and type II (see, e.g., [121]) given, respectively, by

$$T_m[\cos \varphi] = \cos m\varphi \quad \text{and} \quad U_m[\cos \varphi] = \frac{\sin(m+1)\varphi}{\sin \varphi} \quad (3.217)$$

when  $q^{\frac{1}{2}} = e^{-i\varphi}$  ( $\varphi \in \mathbf{R}$ ). The solution of (3.212), satisfying the boundary conditions  $u_m(1) = 0$  and  $u_1(q^{\frac{1}{2}}) = 1$ , is indeed the symmetric deformed number  $||[m]||$  (2.31) (which is the Chebyshev polynomial of type II if  $q^{\frac{1}{2}} = e^{-i\varphi}$ ). I will refer to an evolution obeying the recursion relation (3.212) as a Chebyshev process.

### 3.4.3 The Pulsed Oscillator

The pulsed oscillator is a free particle which undergoes periodic pulses of Hooke's force  $F(t) = -\mu\omega^2 x \delta(t/T_P - m)$  where  $\mu\omega^2$  is Hooke's constant,  $T_P$  is the period of pulses and  $m \in \mathbf{Z}$ . Its Lagrangian is given by

$$L = \frac{1}{2}\mu\dot{x}^2 - \sum_m \frac{1}{2}\mu\omega^2 T_P x^2 \delta(t - t_m) \quad (3.218)$$

where  $t_m = mT_P$ . Hooke's force is exerted not continuously but periodically and instantaneously at  $t = t_m$ . During the period between two consecutive pulses, the system is a free particle.

The action integral for a time interval  $\tau = t'' - t'$  is

$$S(t'', t') = \int_{t'}^{t''} \left[ \frac{1}{2}\mu\dot{x}^2 - \frac{1}{2}\mu\omega^2 T_P x^2 \sum_m \delta(t - t_m) \right] dt. \quad (3.219)$$

The action integral for a short time interval  $\tau_j = t_j - t_{j-1} \ll T_P = t_m - t_{m-1}$  may be chosen as

$$\begin{aligned} S_j &= \int_{t_{j-1}}^{t_j} \left[ \frac{1}{2}\mu\dot{x}^2 - \frac{1}{4}\mu\omega^2 T_P x^2 \{ \delta(t - t_m) + \delta(t - t_{m-1}) \} \right] dt, \\ &= \frac{\mu}{2\tau_j} (x_j - x_{j-1})^2 - \frac{1}{4}\mu\omega^2 T_P \{ x_m^2 \delta(m, j) + x_{m-1}^2 \delta(m-1, j) \}, \end{aligned} \quad (3.220)$$

where  $x_k = x(t_k)$  and

$$\delta(k, j) = \begin{cases} 1 & \text{if } t_{j-1} < kT_P < t_j \\ 0 & \text{otherwise.} \end{cases}$$

Naturally, the action evaluated along the classical path from  $t = t_{m-1} + \epsilon$  to  $t = t_m - \epsilon$  ( $0 < \epsilon \ll T_P$ ) without involving pulses yields the action of a free particle:

$$S_0(t_m, t_{m-1}) = \lim_{\epsilon \rightarrow 0} S(t_m + \epsilon, t_{m-1} - \epsilon) = \frac{\mu}{2T_P} (x_m - x_{m-1})^2. \quad (3.221)$$

But involving pulses, the action becomes

$$S(t_m, t_{m-1}) = \lim_{\epsilon \rightarrow 0} S(t_m + \epsilon, t_{m-1} - \epsilon) = \frac{\mu}{2T_P} (x_m - x_{m-1})^2 - \frac{1}{4}\mu\omega^2 T_P (x_m^2 + x_{m-1}^2). \quad (3.222)$$

Here, I prefer the symmetric form with respect to  $x_m$  and  $x_{m-1}$  for convenience noting that the non-symmetric form is possible as well.

Calculating the canonical momenta from the symmetrized action (3.222) by

$$p_m = \partial S / \partial x_m = \frac{\mu}{T_P} (x_m - x_{m-1}) - \left( \frac{1}{2}\mu\omega^2 T_P \right) x_m, \quad (3.223)$$

$$p_{m-1} = -\partial S / \partial x_{m-1} = \frac{\mu}{T_P} (x_m - x_{m-1}) + \left( \frac{1}{2}\mu\omega^2 T_P \right) x_{m-1}, \quad (3.224)$$

we find the area preserved linear map in phase space:

$$\begin{aligned} x_m &= x_{m-1} + \frac{T_P}{2\mu \left(1 - \frac{1}{4}\omega^2 T_P^2\right)} (p_m + p_{m-1}), \\ p_m &= p_{m-1} - \frac{1}{2}\mu\omega^2 T_P (x_m + x_{m-1}). \end{aligned} \quad (3.225)$$

The evolution of the classical trajectory in phase space obeying the linear map (3.225) is not chaotic. It is interesting that both  $x_m$  and  $p_m$  in (3.225) obey the well-known recursion relation for the Chebyshev polynomials,

$$u_{m+1}(z) - 2z u_m(z) + u_{m-1}(z) = 0, \quad (3.226)$$

when the following identification

$$z = 1 - \frac{1}{2}\omega^2 T_P^2 \quad (3.227)$$

is made. With  $z = \cos \varphi$ , the solutions of the recursion relation (3.226) are given in terms of the Chebyshev polynomials of (3.217). If  $0 < \omega^2 T_P^2 < 4$ , then  $\varphi \in \mathbf{R}$ . Hence, the classical discrete solutions for  $x(t)$  and  $p(t)$  oscillate sinusoidally, which are indeed physical solutions for the proper pulsed oscillator. If  $\omega^2 T_P^2 < 0$  or  $4 < \omega^2 T_P^2$ , then  $\varphi$  has to be complex; so the solutions of (3.226) are not oscillatory and do not physically represent the pulsed oscillator. Nevertheless, one may handle the physically proper solutions and the physically improper solutions together as solutions of the pulsed oscillator in a generalized sense.

It should be noted that although the area-preserving linear maps, obtainable from the non-symmetric one-period actions, differ in form from (3.225), each of  $x_m$  and  $p_m$  resulting from the non-symmetric actions also satisfies the same recursion relation (3.226).

### 3.4.4 $Q$ -Objects

It is remarkable that the recursion relation for the pulsed oscillator (3.226) coincides with the  $q$ -progress equation (3.212) for the  $q$ -deformed free particle if  $q^{\frac{1}{2}} = e^{-i\varphi}$ . Apparently, the time-evolution of both systems is basically the Chebyshev process. While the  $q$ -difference equation for the  $q$ -deformed free particle takes the Newtonian form in the limit  $q^{\frac{1}{2}} \rightarrow 1$ , the pulsed oscillator approaches the free particle in the limit  $e^{-i\varphi} \rightarrow 1$  ( $\omega \rightarrow 0$ ). Therefore, by relating  $q$  to  $\varphi$  by  $q^{\frac{1}{2}} = e^{-i\varphi}$ , one should be able to treat both the  $q$ -deformed free particle and the pulsed oscillator in a unified manner. In other words, one may consider the two systems as special cases of a generic  $q$ -object with  $q^{\frac{1}{2}} = e^{-i\varphi}$ .

The generic  $q$ -object may be defined with a non-zero complex valued  $q$ . However, I restrict myself to the case where  $z = \cos \varphi = \frac{1}{2}(q^{\frac{1}{2}} + q^{-\frac{1}{2}})$  is real. Under this

condition,  $q \in \mathbf{R}$  or  $q \in \mathbf{S}^1$ . In fact, such a  $q$ -object is equivalent to the generalized pulsed oscillator possessing the proper and improper solutions. Therefore, it is convenient to utilize the oscillator's frequency  $\omega$  as a parameter even for the  $q$ -object. We may classify the solutions of the  $q$ -object into three classes as follows:

$$\begin{aligned} \text{(i)} \quad & 0 < \omega^2 T_P^2 < 4; \quad \varphi = \cos^{-1}(1 - \omega^2 T_P^2/2) \in \mathbf{R}; \quad q^{\frac{1}{2}} \in \mathbf{S}^1 \\ \text{(ii)} \quad & \omega^2 T_P^2 < 0; \quad i\varphi = \cosh^{-1}(1 + |\omega|^2 T_P^2/2) \in \mathbf{R}; \quad q^{\frac{1}{2}} \in \mathbf{R}^+ \\ \text{(iii)} \quad & 4 < \omega^2 T_P^2; \quad i\varphi = i\pi + \cosh^{-1}(\omega^2 T_P^2/2 - 1) \in \mathbf{R}; \quad q^{\frac{1}{2}} \in \mathbf{R}^- \end{aligned}$$

Evidently, case (i) corresponds to the proper pulsed oscillator. As it has been mentioned earlier, for the real trajectory (3.209) of the  $q$ -deformed free particle,  $q^{\frac{1}{2}}$  must be real. However, for a continuous evolution with the Newtonian time  $t$ ,  $y(t)$  can be real only when  $q^{\frac{1}{2}}$  is positive. Hence, case (ii) should correspond to the (proper) evolution of the  $q$ -deformed free particle. As each discrete translation of time by  $T_P$  causes the scaling of  $s$  by  $q$ ,  $y_m$  remains to be real even if  $q^{\frac{1}{2}}$  is a negative real number provided  $s_0$  is real. For a continuous evolution with a negative  $q^{\frac{1}{2}}$ ,  $y(t)$  takes complex values in general. Thus, the discrete evolution of the hopping  $q$ -deformed free particle belongs to case (iii). In this manner, the  $q$ -deformed free particle may be viewed as a form of the improper pulsed oscillator.

### 3.4.5 The Propagator for the Chebyshev Process

The next step is calculating the propagator for the pulsed oscillator and exploring the dependency on the deformation parameter  $q$ . Then it will be more generally interpreted as the propagator (in the  $T_P$ -evolution) for the generic  $q$ -object obeying the Chebyshev process.

Using the Lagrangian (3.218) the propagator can be calculated from Feynman's path integral [43],

$$K(x'', x'; \tau) = \lim_{N \rightarrow \infty} \int_{x'=x(t_0)}^{x''=x(t_N)} \prod_{j=1}^{N-1} dx_j \prod_{j=1}^N \exp \left[ \frac{i}{\hbar} S_j \right] \prod_{j=1}^N \left[ \frac{\mu}{2\pi i \hbar \tau_j} \right]^{1/2}, \quad (3.228)$$

where  $\tau = t_N - t_0$  is the fixed total time interval. The propagator must fulfil the following properties:

$$K(x'', t''; x', t') = \int dx(t) K(x'', t''; x, t) K(x, t; x', t'), \quad (3.229)$$

$$\lim_{t'' \rightarrow t'} K(x'', t''; x', t') = \delta(x'' - x'). \quad (3.230)$$

To calculate the one-period propagator, one firstly combines it by applying the convolution property (3.229) to the form

$$\begin{aligned} K(x_m, x_{m-1}; T_P) &= \lim_{\epsilon \rightarrow 0} \int dx_2 dx_1 K(x'', t_m + \epsilon; x_2, t_m - \epsilon) \times \\ &\times K(x_2, t_m - \epsilon; x_1, t_{m-1} + \epsilon) K(x_1, t_{m-1} + \epsilon; x', t_{m-1} - \epsilon), \end{aligned} \quad (3.231)$$

where  $x'' = x(t_m + \epsilon)$ ,  $x_2 = x(t_m - \epsilon)$ ,  $x_1 = x(t_{m-1} + \epsilon)$  and  $x' = x(t_{m-1} - \epsilon)$ . Then I use the symmetric action (3.222) to find the three propagators in the integrand and to complete the integral on the right hand side of (3.231). Namely, one finds

$$\begin{aligned}
\lim_{\epsilon \rightarrow 0} K(x_2, t_m - \epsilon; x_1, t_{m-1} + \epsilon) &= \lim_{\epsilon \rightarrow 0} \sqrt{\frac{\mu}{2\pi i \hbar T_P}} \exp \left[ \frac{i}{\hbar} S_0(t_m - \epsilon, t_{m-1} + \epsilon) \right], \\
\lim_{\epsilon \rightarrow 0} K(x'', t_m + \epsilon; x_2, t_m - \epsilon) &= \lim_{\epsilon \rightarrow 0} \sqrt{\frac{\mu}{2\pi i \hbar T_P}} \exp \left[ \frac{i}{\hbar} S_0(t_m + \epsilon, t_m - \epsilon) \right] \times \\
&\quad \times \exp \left[ -\frac{i}{4\hbar} \mu \omega^2 T_P x_m^2 \right] \\
&= \delta(x_m - x_2) \exp \left[ -\frac{i}{4\hbar} \mu \omega^2 T_P x_m^2 \right], \\
\lim_{\epsilon \rightarrow 0} K(x_1, t_{m-1} + \epsilon; x', t_{m-1} - \epsilon) &= \lim_{\epsilon \rightarrow 0} \sqrt{\frac{\mu}{2\pi i \hbar T_P}} \exp \left[ \frac{i}{\hbar} S_0(t_{m-1} + \epsilon, t_{m-1} - \epsilon) \right] \times \\
&\quad \times \exp \left[ -\frac{i}{4\hbar} \mu \omega^2 T_P x_{m-1}^2 \right] \\
&= \delta(x_1 - x_{m-1}) \exp \left[ -\frac{i}{4\hbar} \mu \omega^2 T_P x_{m-1}^2 \right] \quad (3.232)
\end{aligned}$$

using the relation

$$\lim_{\epsilon \rightarrow 0} [a/\epsilon]^{1/2} e^{-(a/\epsilon)(x-x')^2} = \delta(x - x'). \quad (3.233)$$

Substituting these results into (3.231) one gets

$$\begin{aligned}
K(x_m, x_{m-1}; T_P) &= \sqrt{\frac{\mu}{2\pi i \hbar T_P}} \exp \left[ \frac{i}{\hbar} S_0(t_m, t_{m-1}) \right] \times \\
&\quad \times \exp \left[ -\frac{1}{4\hbar} \mu \omega^2 T_P (x_m^2 + x_{m-1}^2) \right], \quad (3.234)
\end{aligned}$$

or

$$K(x_m, x_{m-1}; T_P) = \sqrt{\frac{\mu}{2\pi i \hbar T_P}} \exp \left[ \frac{i}{\hbar} S(t_m, t_{m-1}) \right], \quad (3.235)$$

where  $S_0(t_m, t_{m-1})$  in (3.234) is the free particle action (3.221) and  $S(t_m, t_{m-1})$  in (3.235) is the symmetric one-period action (3.222), respectively. The propagator (3.232) evaluated from  $t_{m-1} + \epsilon$  to  $t_m - \epsilon$  is the free particle propagator:

$$\begin{aligned}
K^{free}(x_m, x_{m-1}; T_P) &= \sqrt{\frac{\mu}{2\pi i \hbar T_P}} \exp \left[ \frac{i}{\hbar} S_0(t_m, t_{m-1}) \right] \\
&= \sqrt{\frac{\mu}{2\pi i \hbar T_P}} \exp \left[ \frac{i\mu}{2\hbar T_P} (x_m - x_{m-1})^2 \right]. \quad (3.236)
\end{aligned}$$



The state function  $\psi(x_m)$  at the  $m$ th pulse is to be determined from the state  $\psi(x_{m-1})$  at the  $(m-1)$ th pulse by

$$\psi(x_m) = \int_{-\infty}^{\infty} dx_{m-1} K(x_m, x_{m-1}; T_P) \psi(x_{m-1}), \quad (3.237)$$

and the propagator for a double period  $2T_P$  can be found by convolution,

$$K(x_{m+1}, x_{m-1}; 2T_P) = \int dx_m K(x_{m+1}, x_m; T_P) K(x_m, x_{m-1}; T_P). \quad (3.238)$$

In finding the two-period propagator via (3.238), one expands the one-period propagator in a series of the orthogonal polynomials and carries out the convolution by means of the orthogonality of the polynomials. For this purpose, it is convenient to rewrite the symmetric one-period action (3.222) as

$$S(x_m, x_{m-1}) = \frac{\mu}{2T_P} \left( 1 - \frac{1}{2} \omega^2 T_P^2 \right) (x_m^2 + x_{m-1}^2) - \frac{\mu}{T_P} (x_m x_{m-1}). \quad (3.239)$$

If one lets

$$\cos \varphi = 1 - \frac{\omega^2 T_P^2}{2}, \quad \text{or} \quad \sin \frac{\varphi}{2} = \frac{\omega T_P}{2} \quad (3.240)$$

and

$$\xi = \alpha x \quad \text{with} \quad \alpha = \sqrt{\frac{\mu}{\hbar T_P}} \sin \varphi, \quad (3.241)$$

the one-period action (3.239) may be expressed as

$$S(\xi_m, \xi_{m-1}) = \frac{1}{2} \hbar \cot(\varphi) (\xi_m^2 + \xi_{m-1}^2) - \hbar \csc(\varphi) \xi_m \xi_{m-1}. \quad (3.242)$$

At this point it is reasonable to relate  $\varphi$  to the deformation parameter  $q$  by

$$\varphi = \frac{1}{2} i \ln q \quad (3.243)$$

as has been mentioned at the end of the previous section. Then one may express the one-period propagator for this action as

$$\begin{aligned} K(\xi_m, \xi_{m-1}; T_P) &= \sqrt{\frac{\mu}{2\pi i \hbar T_P}} \exp \left[ -\frac{1}{2} (\xi_m^2 + \xi_{m-1}^2) \right] \times \\ &\times \exp \left[ \frac{2\xi_m \xi_{m-1} q^{\frac{1}{2}} - (\xi_m^2 + \xi_{m-1}^2) q}{1 - q} \right]. \end{aligned} \quad (3.244)$$

Applying Mehler's formula for the Hermit polynomials  $H_n(x)$  (see, e.g., [122]),

$$(1 - q)^{-1/2} \exp \left[ \frac{2xyq^{\frac{1}{2}} - (x^2 + y^2)q}{1 - q} \right] = \sum_{k=0}^{\infty} \frac{q^{\frac{1}{2}k} H_k(x) H_k(y)}{2^k k!}, \quad (3.245)$$

leads to the propagator (3.244) in its series form,

$$K(\xi_m, \xi_{m-1}; T_P) = \frac{\alpha}{\sqrt{\pi}} \exp \left[ -\frac{(\xi_m^2 + \xi_{m-1}^2)}{2} \right] \sum_{k=0}^{\infty} \frac{q^{\frac{1}{2}(k+\frac{1}{2})}}{2^k k!} H_k(\xi_m) H_k(\xi_{m-1}). \quad (3.246)$$

Substituting this into the integrand of (3.238) and performing the integration with the help of the orthogonality relation for the Hermit polynomials,

$$\int_{-\infty}^{\infty} e^{-\xi^2} H_k(\xi) H_{k'}(\xi) d\xi = 2^k k! \sqrt{\pi} \delta_{k,k'}, \quad (3.247)$$

one arrives at the double period propagator,

$$K(\xi_{m+1}, \xi_{m-1}; 2T_P) = \frac{\alpha}{\sqrt{\pi}} \exp \left[ -\frac{(\xi_{m+1}^2 + \xi_{m-1}^2)}{2} \right] \sum_{k=0}^{\infty} \frac{q^{(k+\frac{1}{2})}}{2^k k!} H_k(\xi_{m+1}) H_k(\xi_{m-1}). \quad (3.248)$$

Similarly, the  $n$ -period propagator with  $m = 1$  is given by

$$K(\xi_n, \xi_0; nT_P) = \frac{\alpha}{\sqrt{\pi}} \exp \left[ -\frac{(\xi_n^2 + \xi_0^2)}{2} \right] \sum_{k=0}^{\infty} \frac{q^{\frac{n}{2}(k+\frac{1}{2})}}{2^k k!} H_k(\xi_n) H_k(\xi_0). \quad (3.249)$$

This can be easily proven by induction applying the convolution formula (3.238) and the orthogonality (3.247). It is important that the  $n$ -period propagator is characterized by the  $n$ th power of the deformation parameter  $q^{\frac{1}{2}}$ .

Again, using the expansion formula (3.245) and noticing that

$$\alpha = \sqrt{\frac{\mu}{\hbar T_P} \sin(\varphi)} = \sqrt{\frac{\mu}{2i\hbar T_P} \left( q^{\frac{1}{2}} - q^{-\frac{1}{2}} \right)} \quad (3.250)$$

one may transform the series solution (3.249) back to a closed form expression:

$$K(x_n, x_0; nT_P) = \sqrt{\frac{\mu}{2\pi i \hbar T_P |[n]|}} \exp \left[ \frac{i\mu \{ (x_n^2 + x_0^2) (q^{\frac{n}{2}} + q^{-\frac{n}{2}}) - 4x_n x_0 \}}{4\hbar T_P |[n]|} \right] \quad (3.251)$$

remembering the definition  $|[n]|$  in (2.31). However, if one starts counting pulses  $n$  times after the  $m$ th pulse, one must replace  $x_0$  by  $x_m$  and  $x_n$  by  $x_{m+n}$  in (3.249). The corresponding  $n$ -period propagator is

$$K(x_{m+n}, x_m; nT_P) = \sqrt{\frac{\mu}{2\pi i \hbar T_P |[n]|}} \times \exp \left[ \frac{i\mu \{ (x_{m+n}^2 + x_m^2) (q^{\frac{n}{2}} + q^{-\frac{n}{2}}) - 4x_{m+n} x_m \}}{4\hbar T_P |[n]|} \right] \quad (3.252)$$

The  $q^{\frac{n}{2}}$  dependence of the  $n$ -period propagator remains invariant under the shift of the initial position.

The  $n$ -period propagator (3.251) or (3.252) is the  $q$ -representation of the propagator for the pulsed oscillator (or more generally for the  $q$ -object). With  $q^{\frac{1}{2}} = e^{-i\varphi}$ , one can express the propagator (3.251) in the  $\varphi$ -dependent form:

$$K(x_n, x_0; nT_P) = \sqrt{\frac{\mu}{2\pi i \hbar T_P U_{n-1}[\cos \varphi]}} \times \quad (3.253)$$

$$\times \exp \left[ \frac{i\mu \{ (x_n^2 + x_0^2) T_n[\cos \varphi] - 2x_n x_0 \}}{2\hbar T_P U_{n-1}[\cos \varphi]} \right],$$

where  $T_n[\cos \varphi]$  and  $U_n[\cos \varphi]$  are the Chebyshev polynomials given in (3.217).

For the proper pulsed oscillator  $\varphi$  has to be real as is in case (i). However, extending the propagator (3.252) or (3.253) by analytic continuation under the condition  $q^{\frac{1}{2}} + q^{-\frac{1}{2}} \in \mathbf{R}$  to include cases (ii) and (iii), one should interpret it as the propagator for the  $q$ -object.

### 3.4.6 Special Cases

Now I will discuss the propagator for the special  $q$ -objects:

#### 1. Pulsed Harmonic Oscillator

The  $n$ -period propagator for the proper pulsed oscillator follows immediately from the  $\varphi$ -dependent propagator (3.253) which also can be expressed in terms of the sinusoidal functions,

$$K(x_n, x_0; nT_P) = \sqrt{\frac{\mu \sin(\varphi(T_P))}{2\pi i \hbar T_P \sin(n\varphi(T_P))}} \times \quad (3.254)$$

$$\times \exp \left[ \frac{i\mu \sin(\varphi(T_P)) \{ (x_n^2 + x_0^2) \cos(n\varphi(T_P)) - 2x_n x_0 \}}{2\hbar T_P \sin(n\varphi(T_P))} \right].$$

In this case, the angle  $\varphi$  must be inevitably related to the period  $T_P$  by

$$\varphi(T_P) = \cos^{-1} \left( 1 - \omega^2 T_P^2 / 2 \right)$$

under the condition  $0 < \omega^2 T_P^2 < 4$ . The corresponding deformation parameter is

$$q^{\frac{1}{2}} = e^{-i\varphi} = \exp \left[ -i \left( 1 - \frac{\omega^2 T_P^2}{2} \right) \right] \in \mathbf{S}^1.$$

## 2. Caustics of the Pulsed Oscillator

It is evident that the zeros of  $U_{n-1}[\cos \varphi]$  in the pre-factor lead the propagator (3.253) to divergence. The zeros occur only when

$$n\varphi = k\pi \quad (k = 0, \pm 1, \pm 2, \dots);$$

i.e. only for the real pulsed oscillator with frequency  $\omega$  meeting the restriction  $0 < \omega^2 T_P^2 < 4$ . In other words,  $q^{\frac{n}{2}} = e^{-ik\pi}$  with  $k \in \mathbf{Z}$  corresponds to the caustics of the propagator for the proper pulsed oscillator (3.253).

## 3. The Harmonic Limit of the Pulsed Oscillator

In the limit of the zero period ( $T_P \rightarrow 0$ ), the pulsed action of Hooke's force on the system becomes a continuous influence of the harmonic oscillator potential on the particle. Thus, the propagator of the standard harmonic oscillator should result from the  $n$ -period propagator (3.252) by the limiting process:  $T_P \rightarrow 0$  and  $n \rightarrow \infty$  such that the total time interval  $nT_P = \bar{\tau}$  remains constant. In this limit,

$$\varphi = \sin^{-1} \left[ \omega T_P \left( 1 - \frac{\omega^2 T_P^2}{4} \right)^{1/2} \right] \rightarrow \omega T_P. \quad (3.255)$$

Hence,  $q^{\frac{1}{2}} \rightarrow e^{-i\omega T_P} \rightarrow 1$ , but  $q^{\frac{n}{2}} \rightarrow e^{-i\omega \bar{\tau}} \neq 1$ . Consequently, the  $n$ -period propagator for the pulsed oscillator (3.253) approaches the standard result for the harmonic oscillator propagator:

$$K(x'', x'; \bar{\tau}) = \sqrt{\frac{\mu\omega}{2\pi i\hbar \sin(\omega\bar{\tau})}} \exp \left[ \frac{i\mu\omega \{ (x''^2 + x'^2) \cos(\omega\bar{\tau}) - 2x'x'' \}}{2\hbar \sin(\omega\bar{\tau})} \right]. \quad (3.256)$$

where  $x'' = x_\infty$ ,  $x' = x_0$  and  $\bar{\tau} = nT_P$ . Apparently, the caustics of the pulsed oscillator remain to be those of the harmonic oscillator.

## 4. $q$ -free Particle

To extract the  $n$ -period propagator for the  $T_P$ -evolution of the  $q$ -free particle from (3.252), one first remembers that the coordinate variable  $y_m$  of the  $q$ -free particle is related to the variable  $x_m$  satisfying the Chebyshev recursion relation (3.212) by  $x_m = q^{-m}y_m$ . Thus, converting back  $x_m$  into  $y_m$ , one obtains

$$K(y_{m+n}, y_m; nT_P) = \sqrt{\frac{\mu}{2\pi i\hbar T_P |[n]|}} \times \exp \left[ \frac{i\mu \{ (q^{-n}y_{m+n}^2 + y_m^2)(q^{\frac{n}{2}} + q^{-\frac{n}{2}}) - 4q^{-\frac{n}{2}}y_{m+n}y_m \}}{4\hbar T_P |[n]|} \right] \quad (3.257)$$

with  $q^{\frac{1}{2}} \in \mathbf{R}$ . Here  $y_m = y(q^m s_0)$  with the initial time parameter  $s_0 = q^{t_0/T_P}$ . There are two types of  $q$ -free particles, those for  $q^{\frac{1}{2}} \in \mathbf{R}^+$  and for  $q^{\frac{1}{2}} \in \mathbf{R}^-$ . The former has real trajectories, while the latter has complex trajectories but retains real values at  $t = nT_P$ . If one takes the time-evolution  $t = nT_P$  (which corresponds to  $q$ -progression by  $q^n$ ), the propagator (3.257) is valid for both types.

For the  $q$ -free particle of the first type ( $\omega^2 T_P^2 < 0$ ), letting

$$q^{\frac{1}{2}} = e^{-\chi} \in \mathbf{R}^+$$

with  $\chi = \cosh^{-1}(1 + |\omega|^2 T_P^2/2) \in \mathbf{R}$ , the propagator (3.257) takes the form,

$$\begin{aligned} K(y_{m+n}, y_m; nT_P) &= \sqrt{\frac{\mu}{2\pi i \hbar T_P U_{n-1}[\cosh \chi]}} \times \\ &\times \exp \left[ \frac{i\mu \{ (e^{2\chi} y_{m+n}^2 + y_m^2) T_n[\cosh \chi] - 2e^\chi y_{m+n} y_m \}}{2\hbar T_P U_{n-1}[\cosh \chi]} \right]. \end{aligned} \quad (3.258)$$

For the  $q$ -free particle of the second type ( $4 < \omega^2 T_P^2$ ), we let

$$q^{\frac{1}{2}} = -e^{-\chi} \in \mathbf{R}^-$$

with  $\chi = \cosh^{-1}(\omega^2 T_P^2 - 1) \in \mathbf{R}$ . Then one gets

$$\begin{aligned} K(y_{m+n}, y_m; nT_P) &= \sqrt{\frac{i(-1)^n \mu}{2\pi \hbar T_P U_{n-1}[\cosh \chi]}} \times \\ &\times \exp \left[ -\frac{i\mu \{ (e^{2\chi} y_{m+n}^2 + y_m^2) T_n[\cosh \chi] - 2e^\chi y_{m+n} y_m \}}{2\hbar T_P U_{n-1}[\cosh \chi]} \right]. \end{aligned} \quad (3.259)$$

#### 5. Newtonian Free Particle

As the deformation parameter  $q^{\frac{1}{2}}$  tends to unity (or  $\omega \rightarrow 0$ ), the deformed number

$$|[n]| = \frac{q^{\frac{n}{2}} - q^{-\frac{n}{2}}}{q^{\frac{1}{2}} - q^{-\frac{1}{2}}} \quad (3.260)$$

approaches  $n$ . Hence, the propagators (3.252) and (3.256) both reduce to the standard free propagator:

$$K(x_n, x_0; nT_P) = \sqrt{\frac{\mu}{2\pi i \hbar n T_P}} \exp \left[ \frac{i\mu (x_n - x_0)^2}{2\hbar n T_P} \right]. \quad (3.261)$$

This agrees with the expected result.

### 3.4.7 Conclusions

The computation reveals the similarity between the deformed free particle and the pulsed harmonic oscillator via their recursion relation. By using this interesting nature, the two systems can be treated as special cases of a single  $q$ -deformed system ( $q$ -object). Hence, one was able to evaluate them together as the propagator for the Chebyshev process. From this unified treatment, an  $n$ -period propagator for the  $T_P$ -evolution of the  $q$ -free particle as well as of the pulsed oscillator can be derived. Whereas the boson limit  $q = 1$  gives the ordinary free particle propagator, the sector  $q \in \mathbf{R}$  gives the propagator for the  $q$ -free particle and  $q \in \mathbf{S}^1$  for the pulsed oscillator.

# Chapter 4

## Summary

*Die Menschen können lange Zeit das ihnen Nützliche verkennen, aber stets kommt die Zeit, da sie Klarheit gewinnen und von ihr Gebrauch machen.* [123]

Nowadays the exploration of systems far away from the equilibrium becomes more and more a key topic of the scientific research in physics, chemistry and biology. Among other techniques of statistical physics the master equation proves itself as a strong mathematical tool handling such complex systems. In the frame of this work relevant extensions of methods applied to the master equation are given. Moreover, these extensions represent a unifications of different, already known approaches. Illustrating examples were added to this methodical part in order to demonstrate its wide range of applications to many-particles systems. In this connection, the master equation in a Fock-space representation (including second quantized operators) and the functional integral formed the methods of interest. In order to compute the temporal evolution of classical systems with an extended exclusion principle, para-fermion and  $q$ -deformed operators were firstly introduced into the Fock-space formalism of the master equation. These operators include limit cases of fermion-like and boson-like representation of the dynamics, which shows their interpolating property. The commutation relationships ((2.23), (2.32) and (2.45)) were adapted and became an important mathematical tool for the computation of e.g. correlation functions. The reference state (2.86), which is necessary for the calculation of expectation values and corresponds to the bra-vector of the bilinear expectation values of the quantum mechanics, was extended according with the new operators. Apart from the rules for the computation of expectation values a general representation for two fundamental, dynamical processes, Glauber or flip dynamics ((2.102) and (2.114)) and Kawasaki or exchange dynamics (2.127), could be derived. A systematic approach was chosen unifying different results as special cases ad-hoc found until now.

As a first demonstrating example the Fredrickson-Andersen model - a lattice model for the description of relaxation phenomena in glasses - was extended. Cells with different densities are mapped to spin-up and spin-down states of which dynam-

ics is given by spin flip processes with restrictions. As it was shown for a variation with strong hindrance of the local dynamics, this model can also be used for the exploration of such complex system which possesses other properties as glasses. There are non-changeable segments of spins below a temperature in the one-dimensional case. Thermodynamical properties as energy, heat capacity and entropy (Fig. 3.2 and 3.3) could be exactly determined. Whereas only the equilibrium properties were computed in this case, a second study is dedicated to the exploration of the non-equilibrium behavior of the Fredrickson-Andersen model. The influence of a, to the density states added, third component (vacancies) on the temporal evolution was tested, which initiated a second relaxation process (on shorter time scales) apart from the  $\alpha$ -process (on longer time scales). It can be interpreted as  $\beta$ -process. The correlation function and the spectrum of the eigenvalues for the temperature-dependent relaxation times (Fig. 3.4-3.8) could be computed in an extended mean-field approximation. A possible scenario of the common behavior of both processes was convincingly pictured. It was shown that the correlation function (Fig. 3.9) well agrees with numerical simulations.

In a next example, an exclusion model was considered, where every particle of a many-body system performs a random walk on a lattice. The existence of one particle at one site prevents the existence of another particle there at the same time. The asymmetry follows from different transition probabilities with which a particle changes its position to the next lattice site. A possible collective motion of many particles, a shock, was firstly explored in a discrete time update in this work. A temporal evolution of such a shock distribution could exactly determined for an one-dimensional chain. Surprisingly, the resulting distribution is a shock distribution again (3.100). The distribution can be assigned to a position index, which enabled us to reduce the many-particles dynamics to a single-particle dynamics. Hence, the motion of a shock can be regarded as a random walk of only one particle. From this correspondence, it could be derived the shock velocity (3.124) and the shock diffusion coefficient (3.127), pointing to general principles of shocks independent from the detailed realization of the dynamics.

$Q$ -deformed models form the third example. They represent a new class of models, possibly relevant for the application to growth processes, logistic problems and biological systems. This type of models is an extension of flip models or birth and death models and includes the usage of  $q$ -deformed operators during its derivation.  $Q$ -deformed models interpolate between fermion systems with only two states and boson systems with an infinite number of states. A criterium was developed during the exploration that the general model, depending on a parameter, relates more to the behavior of the former or of the latter limit case. A new kind of an equilibrium distribution (3.156) could be discussed, which is similar to the Poisson distribution which becomes its limit for an infinite number of states. The general dynamical solution reveals as difficult, so that only in some special cases a solution could be computed. Aside from the two already known limit cases (boson and fermion case) a



three component system was calculated exactly (3.193) and compared with its mean-field approximation (3.191). Due to a good, qualitative agreement between both, this approximation should yield sufficient results for other cases as well. The exploration could be rounded off by a simulation and shows an exponential-like decrease or increase of the averaged occupation number (Fig. 3.19). Especially interesting are results in the mid of the range for the parameter, where the equilibrium distribution possesses two local maxima, which leads to a decrease and a subsequent increase in the temporal evolution of the averaged occupation number.

The temporal evolution of kinetic processes can be equivalently described by functional integrals. Within this work, a propagator was determined by means of the functional integral describing an evolution of a particle undergoing a force-free, but  $q$ -deformed motion. This so-called Chebyshev process (basing on the notation for the orthogonal polynomials) yields the time evolution for a pulsed oscillator as well. Both systems can be unified to a  $q$ -object of which the propagator (3.252) could be calculated. The propagator of the free particle and the harmonic oscillator was found as special cases.

Obviously, the application of the methods could be only demonstrated on a few examples. However, for other complex systems such a treatment will be possible and will lead to relevant results.

# Appendix A

## Index of all applied symbols

### A.1 Latin Constants

$a$	Lattice constant, layer difference
$D, D_0$	Diffusion constant
$D_S$	Shock diffusion constant
$d$	Spatial dimension
$h$	Energy difference between the liquid and the solid state (FAM)
$j_{s+1}$	Deformation parameter, $(s + 1)$ th simple root of unity
$\tilde{N}$	Ratio of the kinetic parameter ( $q$ -deformed model)
$n_C$	Coordination number, number of the nn
$n_R$	Restriction number (FAM)
$p_R, p_L$	Jump probabilities
$q$	General deformation parameter
$s$	Number of the highest state
$v$	Velocity of the random walk
$v_s$	Shock velocity

## A.2 Latin Temporal, Spatial and State dependent Quantities

$A_k$	Spin up (FAM)
$\hat{a}_k^\dagger, \hat{a}_k$	Raising and lowering operator of the para-statistics
$B_k$	Spin down (FAM)
$\hat{b}_{k,+}, \hat{b}_{k,-}$	Raising and lowering operator of the $q$ -statistics
$\hat{c}_{k,+}, \hat{c}_{k,-}$	General raising and lowering operator
$C(T)$	Heat capacity (FAM)
$exp_q(x)$	$Q$ -deformed exponential function (see Eq.2.34)
$E[z]$	Energy functional ( $q$ -deformed model)
$F$	Free energy (FAM)
$G$	Arbitrary (diagonal) operator
$H_k(x)$	Hermit polynomials
$\hat{i}$	Identical operator
$J_m^n$	Probability current ( $q$ -deformed model)
$K(x_1, x_2; t)$	Propagator ( $q$ -object, functional integral)
$\hat{L}$	Continuous time evolution operator
$L$	Lagrangian ( $q$ -object, functional integral)
$(M_m^n)$	Dynamical matrix of the master equation
$\hat{N}_k$	Number operator
$[\hat{N}]_k$	Deformed number operator
$  [\hat{N}]  _k$	Symmetric-deformed number operator
$ n\rangle$	General Fock state
$O$	Projector to the state $o$
$p$	Momentum ( $q$ -object, functional integral)
$p_A, p_B$	Probability of spin up/down (FAM)
$p_m^n$	Transition probability
$P(\vec{n}, t)$	Probability of a state $\vec{n}$
$P_{alt}$	Prob. site is in an alterable segment (FAM)
$\hat{Q}_k$	Density jump operator (ASEP)
$\langle r  $	Reference state with eigenvalue $r$
$R_S$	Scattering ratio (FAM)
$S(T)$	Entropy (FAM)
$S$	Action ( $q$ -object, functional integral)
$T$	Temperature ( $k_B$ is set to 1)
$\hat{T}$	Discrete time evolution operator
$\hat{T}_o, \hat{T}_e$	Parallel update operator (ASEP)
$T_P$	Period of the pulsed oscillator
$T_m(x), U_m(x)$	Chebyshev polynomials

$U(T)$	Internal energy (FAM)
$U(t)$	Transfer matrix
$V[z(r)]$	Potential ( $q$ -deformed model)
$\hat{V}$	Help matrix (ASEP)
$w_m^n$	Transition rate
$\hat{X}$	Help matrix (ASEP)
$z(r)$	Height ( $q$ -deformed model)
$\hat{Z},  \hat{Z} , z,  z $	Generalized number operators and its eigenvalues

### A.3 Greek Constant and State dependent Quantities

$\beta$	Inverse temperature
$\delta$	Delta distribution
$\hat{\Delta}_S$	Shift operator (ASEP)
$\Delta$	Vacancy energy (FAM)
$\partial$	Ordinary derivative
$\delta_{n,m}$	Kronecker's symbol
$\partial_{;q}$	Symmetric derivative with resp. to $q$
$\Theta_k$	Vacancy (FAM)
$\kappa, \lambda$	Kinetic parameters
$\mu$	Mass ( $q$ -object, functional integral)
$\mu_k$	Shock measure
$\nu$	Number of the n.n. spin ups
$\hat{\Xi}$	Reduced density operator (ASEP)
$\xi$	Reduced density (ASEP)
$ \Pi(t)\rangle$	Fock space state vector
$\pi_n$	Prob. of an alterable segment with n sites
$\pi_L, \pi_S, \pi_R$	Hopping probabilities (ASEP)
$\rho_A, \rho_B$	Sublattice densities (ASEP)
$\sigma_i$	Spin variable, $\pm 1, 0$
$\tau, \tilde{\tau}$	Relaxation time, characteristic time
$\psi(p_A, p_B)$	Help function (FAM)
$\psi_n$	State function ( $q$ -object, functional integral)
$\Omega_l$	Density exchange operator (ASEP)
$\omega$	Frequency ( $q$ -object, functional integral)

# Bibliography

- [1] C.Morgenstern, *An Kayßler* (1913)
- [2] C.W.Gardiner, *Handbook of Stochastic Methods* (Springer, Berlin, 1985)
- [3] J.Honerkamp, *Stochastische dynamische Systeme* (VCH Verlagsgesellschaft, Weinheim, 1990)
- [4] N.G.v.Kampen, *Stochastic Processes in Physics and Chemistry* (North-Holland, Amsterdam, 1992)
- [5] V.Privman, *Nonequilibrium Statistical Mechanics in One Dimension* (Cambridge University Press, Cambridge, 1997)
- [6] D.Matthis and M.L.Glasser, *Rev. Mod. Phys.* **70**, 979 (1998)
- [7] G.M.Schütz, *Exactly Solvable Models for Many-Body Systems far from Equilibrium, Phase Transitions and Critical Phenomena*, Eds. C.Domb and J.Lebowitz (Academic Press, London, 2000)
- [8] R.B.Stinchcomb, *Physica A* **224**, 248 (1996)
- [9] M.Doï, *J. Phys. A* **9**, 1465 (1976)
- [10] M.Doï, *J. Phys. A* **9**, 1479 (1976)
- [11] P.Grassberger and M.Scheunert, *Fortschritt der Physik* **28**, 547 (1980)
- [12] L.Peliti, *J. Physique* **46**, 1469 (1985)
- [13] S.Sandow and S.Trimper, *Europhys. Letter* **21**, 799 (1993)
- [14] S.Sandow, PhD Thesis, University at Halle (1993)
- [15] G.M.Schütz, *Phys. Rev. E* **47**, 4265 (1993)
- [16] S.Sandow and G.M.Schütz, *Europhys. Letter* **26**, 7 (1994)
- [17] G.M.Schütz, *J. Phys. A* **28**, 3405 (1995)

- [18] M.Schulz and S.Trimper, Phys. stat. sol. B **215**, 1119 (1999)
- [19] M.Schulz and S.Trimper, Phys. Letters A **216**, 235 (1996)
- [20] M.Schulz and S.Trimper, J. Phys. A **29**, 6543 (1996)
- [21] C.Pigorsch, M.Schulz and S.Trimper, Int. Journal of Mod. Physics B **13**, 1379 (1999)
- [22] C.Pigorsch, M.Schulz and S.Trimper, Int. Journal of Mod. Physics B **15**, 135 (2001), C.Pigorsch, diploma (1996)
- [23] M.Schulz and S.Trimper, Phys. Rev. B, **53**, 8421 (1996)
- [24] M.Schulz, S.Trimper and J.Kimball, Phys. Letters A **235**, 113 (1997)
- [25] G.Gentile, Nouvo Cimento **17**, 17 (1940)
- [26] H.S.Green, Phys. Rev. **90**, 270 (1953)
- [27] A.P.Polychronakos, *Les Houches Lectures Summer 1998*, hep-th/9902157 (1999)
- [28] B.I.Halperin, Phys. Rev. Letters **52**, 1583 (1984)
- [29] B.I.Halperin, Phys. Rev. E **39**, 2390 (1984)
- [30] M.Arik, J.Kornfilt and A.Yildiz, Phys. Letters A **235**, 318 (1997)
- [31] U.Kayserilioglu, J.Kornfilt, G.Unel and M.B.Unlu, Phys. Letters A **253**, 132 (1999)
- [32] R.B.Laughlin, Phys. Rev. Letters **60**, 2677 (1988)
- [33] G.H.Fredrickson and H.C.Andersen, Phys. Rev. Letters **53**, 1244 (1984)
- [34] G.H.Fredrickson and H.C.Andersen, J. Chem. Phys. **84**, 5822 (1985)
- [35] G.H.Fredrickson, Ann. Rev. Phys. Chem. **39**, 149 (1988)
- [36] G.H.Fredrickson and S.A. Brewer, J. Chem. Phys. **84**, 3351 (1986)
- [37] D.Chowdhury, L.Santen and A.Schadschneider, Phys. Rep. **329**, 199 (2000).
- [38] J.Kärger, G.Fleischer and U.Roland, *PFM NMR Studies of Anomalous Diffusion in Diffusion in condensed matter*, Eds. J.Kärger, P. Heitjans and R.Haberlandt (Vieweg, 1998, Braunschweig).
- [39] J.T. MacDonald, J.H.Gibbs and J.H.Pipkin, Biopolymers **6**, 1 (1968)

- [40] T.M.Liggett, *Stochastic Models of Interacting Systems: Contact, Voter and Exclusion Processes* (Springer, Berlin, 1999)
- [41] P.Nozières, in *Solids far from Equilibrium*, Ed. C.Godrèche (Cambridge University Press, Cambridge, 1992)
- [42] W.Feller, *An Introduction to Probability Theory and Its Application*, Vol. I (Wiley, New York City, 1968)
- [43] R.P.Feynman and A.R.Hibbs in *Quantum Mechanics and Pathintegrals* (McGraw-Hill, New York, 1965)
- [44] H.Kleinert, *Pfadintegrale in Quantenmechanik, Statistik und Polymerphysik* (Spektrum Akademieverlag, Heidelberg, 1993)
- [45] V.de Alfaro, S.Fububi and G.Furlan, *Nouvo Cimento* **34**, 569 (1976)
- [46] W.Jackiw, *Ann. Phys. (NY)* **129**, 183 (1980)
- [47] P.Y.Cai, A.Inomata and P.Wang, *Phys. Letters A* **91**, 331 (1982)
- [48] M.R.Kibler in *Symmetry and Structural properties of Condensed Matter*, Eds. W.Florek, D.Lipinski and T.Lulek (World Scientific, Singapore, 1993)
- [49] W.-S.Chung, *Helv. Phys. Acta* **70**, 367 (1997)
- [50] O.W.Greenberg, *Phys. Rev. Letters* **64**, 705 (1990)
- [51] O.W.Greenberg, D.M.Greenberger and T.V.Greenbergest, *(Para)Bosons, (Para)Fermions, Quons and other Beasts in the Menagerie of Particle Statistics in Quantum Coherence and Reality*, Eds. J.S.Anandan and J.L.Safko (World Scientific, Singapore, 1994)
- [52] M.Arik, N.M.Atakishiyev and K.B.Wolf, *J.Phys. A* **32**, L 371 (1999)
- [53] T. Hakioglu, *J. Phys. A* **31**, 707 (1998) and citations therein
- [54] D.Galetti, J.T.Lunardi, B.M.Pimentel and M.Ruzzi, *math.QA/0003143* (2000)
- [55] A.J.Macfarlane, *J. Phys. A* **22**, 4587 (1989)
- [56] L.C.Biedenharn, *J. Phys. A* **22**, L 873 (1989)
- [57] H.Exton, *q-hypergeometric function and application* (Ellis Horwood, Chichester, 1983)
- [58] O.W.Greenberg and A.M.L.Messiah, *J. Math. Phys.* **6**, 500 (1965)

- [59] W.Greiner, *Theoretische Physik, Band 4A:Quantentheorie, Spezielle Kapitel* (Verlag H.Deutsch Thun, Frankfurt/Main, 1989)
- [60] R.Haag, *Local Quantum Physics* (Springer, Berlin, 1992)
- [61] C.Quesne, Phys. Letters A **260**, 437 (1999)
- [62] S.Meljanac, M.Mileković and M.Stojić, J. Phys. A **32**, 1115 (1999)
- [63] A.Inomata, private communication (1999)
- [64] R.J.Glauber, J. Math. Phys. **4**, 294 (1963)
- [65] K.Kawasaki, Phys. Rev. **145**, 224 (1966)
- [66] K.Kawasaki in *Phase Transition and Critical Phenomena*, Vol.II, Eds. C.Domb and M.S.Green (Academic Press, London, 1972)
- [67] R.Leonhard, *Aeonen des Fegefeuers, Aphorismen* (Leipzig, 1917)
- [68] C.Godrèche, *Solids far from Equilibrium* (Cambridge University Press, Cambridge, 1992)
- [69] E.Bartsch, O.Belus, F.Fujara, M.Riebel, W.Petry, H.Sillescu and J.H.Magill, Physica B **180/181**, 808 (1992)
- [70] W.Götze in *Liquids, Freezing and the Glass Transition*, Eds. Hansen et al. (North Holland, Amsterdam, 1991)
- [71] W.Götze and L.Sjögren, Rep. Prog. Phys. **55**, 241 (1992)
- [72] J.Jäkle, Rep. Prog. Phys. **49**, 171 (1986)
- [73] E.Leutheusser, Phys. Rev. A **29**, 2765 (1984)
- [74] G.Adams and J.H.Gibbs, J. Chem. Phys. **43**, 139 (1965)
- [75] M.L.Williams, R. F. Landel and J.D.Ferry, J. Am. Chem. Soc. **77**, 3701 (1955)
- [76] W.Götze and L.Sjögren, Zeitschrift für Physik B Cond. Matter **65**, 415 (1987)
- [77] G.P. Johari, Ann. Phys. (NY) Acad. Sci., **171** (1976)
- [78] G.P. Johari, M.Goldstein, J. Chem. Phys. **55**, 4245 (1971)
- [79] W.Götze and L.Sjögren, J. Phys. C **21**, 3407 (1988)
- [80] T. Gleim, W.Kob and K.Binder, Phys. Rev. Letters **81**, 4404 (1998)



- [81] M.Schulz and P.Reinecker, Phys. Rev. B **48**, 9369 (1993)
- [82] M.Schulz and P.Reinecker, Phys. Rev. B **52**, 4131 (1995)
- [83] M.Schulz, P.R.S.Sharma and H.L.Frisch, Phys. Rev. B **52**, 7195 (1995)
- [84] S.Butler and P.Harrowell, J. Chem. Phys. **95**, 4454 (1991)
- [85] A.Heuer, U.Tracht and H.U.Spiess, J. Chem. Phys. **107**, 3831 (1997)
- [86] A.Krönig and J.Jäckle, J.Phys. Condensed Matter **6**, 7655 (1994)
- [87] M.Schulz and S.Trimper, J. Stat. Phys. **94**, 173 (1999)
- [88] M.Schulz and S.Trimper, Phys. Rev. E **57**, 6398 (1998)
- [89] A.C.D. van Enter, J. Stat. Phys. **48**, 943 (1988).
- [90] J. Adler and A. Aharony, J. Phys. A **21**, 1387 (1988)
- [91] J. Adler, Physica A **171**, 453 (1991)
- [92] C.Pigorsch, J.C.Kimball and H.L.Frisch, Phys. Rev. B **59**, 3196 (1999)
- [93] A.Kudlik, C.Tschirwitz, S.Benkhof, T.Blochowicz and E.Rößler, Europhys. Letters **40**, 649 (1997)
- [94] S.A.Kivelson, X.Zhao, D.Kivelson, T.M.Fisher and C. M. Knobler, J. Chem. Phys. **101**, 2391 (1994)
- [95] D.Kivelson, G.Tarjus, X. Zhao and S.A.Kivelson, Phys. Rev. E **53** 751 (1996)
- [96] M.Blume, V.J.Emery and R.B.Griffiths, Phys. Rev. A **4**, 1071 (1971)
- [97] F.J.Stickel, PhD thesis (1995)
- [98] R.Casalini, D. Fioretto, A.Livi, M.Lucchesi and P.A.Rolla, Phys. Rev. B **56**, 3016 (1997)
- [99] E.Donth, S.Kahle, J.Korus and M.Beiner, J. Phys. I France **7**, 581 (1997)
- [100] V.Popkov and G.M.Schütz, Europhys. Letters **48**, 257 (1999)
- [101] B.Derrida, Phys. Rep. **301**, 65 (1998)
- [102] A.Boldrighini, C.Cosimi, A.Frigio and M.Grasso-Nunes, J. Stat. Phys. **55**, 611 (1989)
- [103] A.B.Kolomeisky, G.M.Schütz, E.B.Kolomeisky and J.P.Straley, J. Phys. A **31**, 6911 (1998)

- [104] P.A.Ferrari and L.R.G.Fontes, *Probab. Theor. Rel. Fields* **99**, 305 (1994)
- [105] P. A. Ferrari, *Shocks in one-dimensional processes with drift* in *Probability and Phase Transition*, Ed. G.Grimmett, (Cambridge University Press, Cambridge, 1993)
- [106] V.Belitsky and G.M.Schütz, preprint (2000)
- [107] K.Krebs, PhD thesis, University at Bonn (1999)
- [108] A.Honecker and I.Peschel, *J. Stat. Phys.* **88**, 319 (1997)
- [109] C.Pigorsch and G.M.Schütz, *J. Phys. A* **33**, 7919 (2000)
- [110] R.J.Baxter, *Exactly solved models in statistical mechanics* (Academic Press, New York, 1982)
- [111] J.Fuchs, *Affine Lie-Algebras and Quantum Groups* (Cambridge University Press, Cambridge, 1992)
- [112] G. M.Schütz, *J. Stat. Phys.* **86**, 1265 (1997)
- [113] B.I.Halperin, P.C.Hohenberg and S.Ma, *Phys. Rev. B* **10**, 139 (1974)
- [114] B.I.Halperin, P.C.Hohenberg and E.D.Siggia, *Phys. Rev. B* **13**, 1299 (1976)
- [115] S.Chui and J.D.Weeks, *Phys. Rev. Letters* **40**, 733 (1978)
- [116] J.Zinn-Justin, *Quantum Field Theory and Critical Phenomena* (Clarendon Press, Oxford, 1989)
- [117] J.W.Negele and H.Orland, *Quantum Many-Particles Systems* (Addison-Wesley, Redwood City, 1988)
- [118] A.Inomata, J.C.Kimball and C.Pigorsch, *Proceedings GROUP 23, Dubna* (1999)
- [119] H.Goldstein, *Classical Mechanics*, 2nd edition (Addison-Wesley, Reading, 1980)
- [120] A.Dimakis and F.Müller-Hoissen, *Phys. Letters B* **295**, 242 (1992).
- [121] I.S.Gradshteyn and I.M. Ryzhik, *Table of Integrals, Series, and Products*, (Academic Press, London, 1965)
- [122] A.Erdélyi, *Higher Transcendental Functions*, Vol. II (McGraw-Hill, New York, 1953)
- [123] C.-H. de Saint-Simon, *Über die Reorganisation der europäischen Gesellschaft, Ausgewählte Schriften* (Berlin, 1977)

# Acknowledgment

Firstly, I will thank my advisors Prof.Dr.S.Trimper and PD Dr.M.Schulz for their help and the opportunity to work on these fields. Furthermore, there was always the possibility for the valuable discussion with both importantly contributing to this thesis and to other publications. Secondly, I cordially thanks all members of the physics department of SUNY at Albany, especially Prof.J.C.Kimball, Prof.H.L.Frisch and Prof.A.Inomata, for the warmly welcome and the wonderful time during my visit in the United States of America. Remembering many discussion and private conversations about physics and beyond this stay yields a further main contributions to this work. So I learned many things about one-dimensional system, functional integrals as well as quantum groups. Further I would like to thank PD Dr.G.Schütz for his efforts to introduce me in the topics of shocks and exclusion processes. I benefitted also from his hints for interesting literature and particular results. I want to thank all collaborators of the theoretical physics group for the pleasant time, the Deutsche Forschungsgemeinschaft to enable my work at the Sonderforschungsbereich 418, the German Academic Exchange Service for financing my stay in the United States and the FZ Jülich for supporting my research.

Last, but not least I am very grateful to my wife for her support and her understanding for my work. Her help was a very valuable contribution for the success of this thesis.



# Zusammenfassung

Dissertation

## Quantum Theoretical Methods in Application to Classical Systems

Ein bedeutender Teil der physikalischen Forschung ist dem theoretischen Studium der Dynamik komplexer Systeme gewidmet, insbesondere den Phänomenen, die weit ab vom Gleichgewicht stattfinden. Diese komplexen Vielteilchensysteme erfordern eine Vielzahl von theoretischen Zugängen und Modellen, so unter anderem auch quantentheoretische Methoden. Diese Techniken beruhen auf der strukturellen Ähnlichkeit der Mastergleichung mit der Schrödingergleichung. Die quantentheoretischen Verfahren zur ihrer Lösung können somit auch auf die Mastergleichung angewendet werden, nachdem sie dabei an die Gegebenheiten von klassischen Systemen angepaßt wurden. Diese Arbeit gibt einen weiteren Beitrag zur Erweiterung dieser Behandlungsmethoden als auch zur Vereinheitlichung verschiedener, schon bekannter Ansätze. Der methodische Teil wird um illustrierende Beispiele ergänzt, die die Anwendbarkeit auf Vielteilchensysteme unterschiedlicher Art demonstrieren sollen. Im Mittelpunkt der Betrachtungen stehen die Mastergleichung in Fock-Raum-Darstellung einschließlich zweitquantisierter Operatoren sowie das Funktionalintegral.

Um auch die zeitliche Entwicklung klassischer Systeme mit einem erweiterten Ausschließungsprinzip zu behandeln, wurden Para-Fermi- und  $q$ -deformierte Operatoren in den Fock-Raum-Formalismus der Mastergleichung erstmals eingeführt. Die in diesen Operatoren aufgestellte Mastergleichung enthält schon bekannte Fälle der boson- und fermionartigen Darstellungen der Dynamik. Dabei spielt die interpolierende Eigenschaft der neu eingeführten Operatoren zwischen beiden Grenzfällen eine wichtige Rolle. Die Vertauschungsregeln wurden entsprechend angepaßt und bilden ein wichtiges Mittel zur Berechnung, z.B. der Korrelationsfunktionen. Außerdem wurde in der Arbeit der Referenzzustand, welcher für die Berechnung der statistischen Mittelwerte von Bedeutung ist und dem bra-Vektor in den bilinearen Mittelwerten der Quantentheorie entspricht, hinsichtlich der neuen Operatoren erweitert. Neben Regeln für Erwartungswerte konnten auch allgemeine Darstellungen für zwei fundamentale dynamische Prozesse, Glauber- oder Umklapp-Dynamik und Kawasaki- oder Austausch-Dynamik abgeleitet werden. Dabei wurde ein systematischer Zugang gewählt, der viele der bisher ad-hoc gefundenen Ergebnisse als Spezialfälle enthält.

Als ein erstes Anwendungsbeispiel wurde das Fredrickson-Andersen-Modell gewählt, welches als Gittermodell wurde für die Beschreibung der Relaxationsvorgänge in Gläsern entwickelt wurde. Dabei werden unterschiedliche Dichtebereiche auf Spin-

auf und Spin-ab Zustände abgebildet, deren Dynamik durch Spin-Umklapp-Prozesse mit bestimmten Behinderungen gegeben ist. Wie für eine Variante mit starken Einschränkungen der lokalen Dynamik in dieser Arbeit gezeigt wurde, läßt es sich auch als Studienobjekt für komplexe Systeme benutzen, die über andere Eigenschaften als Gläser verfügen. Im eindimensionalen Fall existieren nicht mehr veränderbare Segmente der Spinkette unterhalb einer bestimmten Temperatur. Es konnten die thermodynamischen Eigenschaften, wie innere Energie, Wärmekapazität und Entropie exakt bestimmt werden. Während für dieses Modell nur die Betrachtung des Gleichgewichtes eine Rolle spielte, konnten durch das Hinzufügen eines zusätzlichen Zustandes neben Spin-auf und Spin-ab und einer diffusiven Dynamik neue, im ursprünglichen Modell nicht vorhandene Nichtgleichgewichtseigenschaften untersucht werden. Hierbei konnte ein zweiter Relaxationsprozeß neben dem  $\alpha$ -Prozeß (auf längeren Zeitskalen) initiiert werden, der als  $\beta$ -Prozeß (auf kürzeren Zeitskalen) gedeutet werden kann. Die Korrelationsfunktionen und das Eigenwertspektrum der Relaxationszeiten als Funktion der Temperatur wurden in einer erweiterten Molekularfeldnäherung berechnet. Dabei wurde ein mögliches Szenario des gemeinsamen Verhaltens von  $\alpha$ - und  $\beta$ -Prozeß aufgezeigt. Die Korrelationsfunktion stimmt gut mit numerischen Ergebnissen überein.

In einem weiteren Beispiel wurden ein Ausschließungsmodell betrachtet, in dem jedes einzelne Teilchen eines Vielteilchensystems einen Zufallsweg auf einem Gitter beschreibt. Dabei schließt die Existenz eines Teilchens die Existenz eines weiteren auf dem selben Gitterplatz aus. Die Asymmetrie folgt aus den unterschiedlichen Übergangswahrscheinlichkeiten, mit denen ein Teilchen auf den nächsten Gitterplatz wechselt. In dieser Dissertation wurde nun eine mögliche kollektive Bewegung vieler Teilchen, ein Schock, in einer diskreten Zeitabfolge erstmals untersucht. Es konnte die exakte Zeitentwicklung für eine Schockverteilung auf einem eindimensionalen Gitter berechnet werden. Die sich ergebende Verteilung ist dann wiederum eine Schockverteilung. Den Verteilungen kann ein Positionsindex zugeordnet werden, der es erlaubt, die Vielteilchendynamik wieder auf eine Einteilchendynamik zurückzuführen. Somit kann die Schockbewegung als Zufallsweg eines einzelnen Teilchens behandelt werden. Daraus kann man die Schockgeschwindigkeit und die -diffusionskonstante berechnen, die auf allgemeine Prinzipien unabhängig von der konkreten Realisierung der Dynamik hindeuten.

$Q$ -deformierte Modelle bilden ein weiteres System, welches umfassend in dieser Arbeit untersucht wurde. Bei  $q$ -deformierten Modellen handelt es sich um eine neue Modellklasse, welche für die Anwendung auf Wachstumsprozesse, logistische Abläufe bis hin zu biologischen Systemen interessant sein könnte. Dieser Typ von Modellen stellt eine Erweiterung der Umklapp-Modelle oder der Geburts- und Sterbemodelle dar und beinhaltet die Verwendung der  $q$ -deformierten Operatoren bei ihrer Herleitung. Diese Systeme interpolieren zwischen fermionischen Modellen mit zwei Zuständen und bosonischen Modellen mit unendlich vielen Zuständen. Im Rahmen der Untersuchungen wurde ein Kriterium entwickelt, das das System, pa-

parameterabhängig, eher dem Verhalten ersterer oder letzterer zuordnen kann. Es wurde eine neue Art von Gleichgewichtsverteilung diskutiert, die sich ähnlich einer Poisson-Verteilung verhält und im Grenzfall in diese übergeht. Die allgemeine dynamische Lösung erweist sich als ungleich schwieriger und kann nur in Spezialfällen exakt angegeben werden. Neben dem bosonischen und fermionischen Fall wurde ein Dreizustandemodell exakt gelöst und mit einer Molekularfeldnäherung verglichen. Dabei konnte eine qualitativ gute Übereinstimmung erzielt werden, so daß diese Näherung auch für andere Fälle eine hinreichende Aussage besitzen sollte. Die Untersuchungen wurden durch eine Simulation abgerundet und zeigen ein exponentielles Ansteigen oder Abklingen der mittleren Besetzungszahl. Als interessant erweisen sich die Ergebnisse in einem mittleren Parameterbereich, in dem die Gleichgewichtsverteilung zwei lokale Maxima besitzt, was zu einem zeitlichen Abfall und darauffolgenden Anstieg der mittleren Besetzungszahl führt.

Funktionalintegrale sind ein weiteres Mittel, Informationen über Statik und Dynamik von physikalischen Systemen zu erhalten. Im Rahmen dieser Dissertation wurde ein Propagator mit Hilfe eines Funktionalintegrals bestimmt, der die zeitliche Entwicklung eines Teilchens beschreibt, das einer kraftfreien, aber  $q$ -deformierten Bewegung entspricht. Der wegen der zugrundeliegenden orthogonalen Polynome so genannte Tschebyschew-Prozeß erweist sich auch als zutreffend für die Beschreibung eines gepulsten Oszillators. Beide Formen können als  $q$ -Objekt verallgemeinert werden, dessen Propagator berechnet wird. Als Spezialfälle konnten die Zeitentwicklungen des freien Teilchens als auch des harmonischen Oszillators abgeleitet werden.

Die hier angegebenen Beispiele decken nur einen kleinen Teil der Anwendungen der vorgestellten Methoden ab. Dennoch sollte damit für viele andere komplexe Systeme ebenso eine Behandlung möglich sein und zu relevanten Ergebnissen führen.





# Curriculum Vitae

## Persönliche Angaben

Name: Christian Pigorsch  
Geburtsdatum: 21.11.1971  
Geburtsort: Lutherstadt Eisleben  
Familienstand: verheiratet mit Steffi U. Pigorsch

## Private Adresse

Anschrift: Rainstraße 1, 06114-Halle  
Telephon ++49-(0)345 8045931  
FAX ++49-(0)345 8045931

## Berufliche Adresse

Anschrift: Martin-Luther-Universität Halle-Wittenberg,  
FB Physik FG Theoretische Physik, 06099 Halle/Saale  
Telephon ++49-(0)345 225459  
FAX ++49-(0)345 225446  
e-mail pigorsch@physik.uni-halle.de

## Schulbildung

1978-1988 Speziialschule mit erweitertem  
Russischunterricht in Eisleben  
1988-1990 Spezialklassen für Mathematik und Physik der  
Martin-Luther-Universität Halle-Wittenberg (Abitur 1.1)

## Zivildienst

1990-1991 Zivildienst in einem Altenpflegeheim in L. Eisleben

## Hochschulstudium

1991-1996 Physik-Studium an der Martin-Luther-Universität  
Halle-Wittenberg  
Juli 1996 Abschluß als Diplomphysiker (1.0)

## Praktikum

08-09.1994 Entwicklung eines Computer-Ultraschallsystems  
für Tumorerkennung am "Institute of Cancer Research"  
des "Royal Marsden Hospital" London, G.B.

**Berufliche Entwicklung**

- 1996-2001 Doktorand in Halle, Sonderforschungsbereich 418  
"Struktur und Dynamik nanoskopischer Inhomogenitäten  
in kondensierter Materie" Projekt B1, Gittermodelle,  
Gläser und Fock-Raum-Formalismus (mit M.Schulz und  
S.Trimper)
- 1998-1999 Forschungsaufenthalt an der SUNY at Albany, N.Y.  
U.S.A.; Forschung Glasmodelle, Pfadintegrale und  
q-Statistik (mit J.Kimball, H.L.Frisch und A. Inomata)
- 11-12/1999 Forschungsaufenthalt im FZ Jülich; Erforschung von  
& März 2000 Schocks in Ausschließungsmodellen (mit G. Schütz)

**Fremdsprachen**

Englisch (fließend)  
Französisch, Russisch, Italienisch

**Computer Kenntnisse**

Delphi, C++, Java, HTML, LaTeX, MSOffice, Mathematica

**Aktivitäten**

Mitarbeit in der Universitätssenatskommission

**Hobbies**

Genealogie, Radsport, Fußball, Wandern, Fotografie, Videobearbeitung

Halle, dem 15.Januar 2001

Christian Pigorsch

## Erklärung

Hiermit versichere ich, daß ich diese Arbeit selbständig und ohne fremde Hilfe angefertigt habe. Bei dieser Dissertation fanden nur die angegebenen Quellen und Hilfsmittel Verwendung. Die den benutzten Werken wörtlich oder inhaltlich entnommenen Stellen sind als solche kenntlich gemacht.

Christian Pigorsch

Halle/Saale, 22. Juni 2000